5-2013

THE p63 ISOFORM ΔNp63α INHIBITS EPITHELIAL – MESENCHYMAL TRANSITION BY PROMOTING THE EXPRESSION OF MIR-205 IN HUMAN BLADDER CANCER CELLS

Mai Tran

THE P63 ISOFORM ΔNp63α INHIBITS EPITHELIAL – MESENCHYMAL TRANSITION BY PROMOTING THE EXPRESSION OF MIR-205 IN HUMAN BLADDER CANCER CELLS

By

MAI NGOC-ANH TRAN, B.S.

APPROVED:

David J. McConkey, Ph.D., Chair
Supervisory Professor

Michelle C. Barton, Ph.D.

Elsa R. Flores, Ph.D.

Gary E. Gallick, Ph.D.

Sendurai Mani, Ph.D.

APPROVED:

Dean, The University of Texas
Graduate School of Biomedical Sciences

THE p63 ISOFORM ΔNp63α INHIBITS EPITHELIAL – MESENCHYMAL TRANSITION BY PROMOTING THE EXPRESSION OF MIR-205 IN HUMAN BLADDER CANCER CELLS

A

DISSERTATION

Presented to the Faculty of

The University of Texas

Health Science Center at Houston

and

The University of Texas

M.D. Anderson Cancer Center

Graduate School of Biomedical Sciences

In Partial Fulfillment

of the Requirements

for the Degree of

DOCTOR OF PHILOSOPHY

by

Mai Ngoc-Anh Tran, B.S.

Houston, Texas

May, 2013

DEDICATION

I would like to dedicate this dissertation to my parents,

Mr. Trần Phát Trường and Mrs. Nguyễn Ngọc Ánh,

who are always there for me, trust and support me

with all their unlimited love and care.

To my two brothers,

Mr. Trần Phát Minh and Mr. Trần Phát Ngọc Quang,

for the wonderful childhood memories that we have,

for their love, friendship and support for me

throughout the years from childhood to adulthood.

ACKNOWLEDGEMENTS

My great appreciation is for my mentor, Dr. David McConkey. I thank him for taking me on initially as a Vietnamese graduate student with little knowledge in the cancer biology field and molding me into the cancer biology scientist I am today. I sincerely appreciate him for his guidance, encouragement and support throughout my PhD training. I am very thankful that I had the opportunity to work with and learn from a great mentor and an honorable person like him.

I would also like to thank my advisory and supervisory committee members for their advice, suggestions and comments that helped me overcome obstacles in research and finish the study. Special thanks to Dr. Michelle Barton and members of Barton's lab for helpful advice and support. Thank you to Dr. Gary Gallick for being a great committee member and a role model for me as an educator and a scientist. I would like to acknowledge Drs. Elsa Flores and Sendurai Mani for their expertise in p63 and EMT research. Their comments and suggestions have really helped me in refining my project.

I am very thankful for the past and present members of McConkey's lab and Urology lab including Woonyoung Choi, Matthew White, Goodwin Jinesh Gerald, I-ling Lee and others for their friendship, help and support in the lab. I also appreciate members of Bar-Eli's lab including Russell Braeuer, Lily Huang, Takafumi Kamiya, Aaron Mobley and Einav Shoshan for helping me in research and making my PhD journey enjoyable. Special thanks to Dr. Santosh Chauhan for his instruction in chromatin immunoprecipitation technique.

To my wonderful friends: Rotor Le, Hanh Lam, Vy Nguyen, Phuc Le for being there for me throughout good times and bad times in my professional life as well as my personal life. I don't

think I can finish my PhD without their support. They will never know how much I appreciate them.

It is with immense gratitude that I acknowledge the Vietnam Education Foundation Fellowship program. They have provided me not only an opportunity to come to the U.S. for my PhD training but also a great fellow community with great friendship and support.

To Russell Braeuer for stepping into my life and walking with me this final part of the journey.

THE p63 ISOFORM ΔNp63α INHIBITS EPITHELIAL – MESENCHYMAL TRANSITION BY PROMOTING THE EXPRESSION OF MIR-205 IN HUMAN BLADDER CANCER CELLS

Publication No. _____

Mai Ngoc-Anh Tran, BS.

Supervisory Professor: David J. McConkey, PhD.

p63, a p53 family member, is a transcription factor that has complex roles in cancer. This study focuses on the role of the ΔNp63α isoform in bladder cancer (BC). Epithelial – mesenchymal transition (EMT) is a physiological process that plays an important part in metastasis and drug resistance. At the molecular level, EMT is characterized by the loss of the epithelial marker E-cadherin, and the acquisition of the transcriptional repressors of E-cadherin (ZEB1, ZEB2, TWIST, SNAI1 and SNAI2). Recent publications highlight the role of microRNAs belonging to the miR-200 family and miR-205 in preventing EMT through suppression of ZEB1 and ZEB2. p53, the homologue of p63, is implicated in regulating EMT by modulating the expression of miR-200c; however, the mechanisms underlying miR-205 control remain unclear. Here we show that ΔNp63α regulates the transcription of miR-205 and controls EMT in human BC cells. We observed a strong correlation between the expression of ΔNp63α, miR-205 and E-cadherin in a panel of BC cell lines (n=28) and also in bladder primary tumors from

a cohort of patients (n=98). A remarkably inverse correlation is observed between ΔNp63α and ZEB1/2 in cell lines. Stable knockdown (KD) ΔNp63α in UC6, an "epithelial" BC cell line, decreased the expression of miR-205 and induced ZEB1/2 expression, the effects that were reversed by expression of exogenous miR-205. Moreover, overexpressing ΔNp63α in UC3, a "messenchymal" BC cell line, brought about opposite results, an increase in miR-205 expression and a reduction in ZEB1/2 expression. Modulation of ΔNp63α expression resulted in a parallel change in the expression of miR-205 and miR-205 "host" gene (miR-205HG). Nuclear run-on and chromatin immunoprecipitation experiments demonstrated that ΔNp63α regulates the transcription of miR-205 through controlling the recruitment of RNA Polymerase II to the promoter of miR-205HG. Interestingly, high miR-205 expression correlated with poor clinical outcome in BC patients, consistent with our recent publication highlighting the enrichment of ΔNp63 in a lethal subset of muscle invasive BC.

In summary, our data present the important roles of ΔNp63α in preventing EMT mediated by miR-205. Our study also identifies miR-205 as a potential molecular marker to predict clinical outcome in BC patients.

TABLE OF CONTENT

LIST OF FIGURES

LIST OF TABLES

CHAPTER 1:

INTRODUCTION: BACKGROUND AND RATIONALE

1. EPITHELIAL-MESENCHYMAL TRANSITION (EMT) – MESENCHYMAL-EPITHELIAL TRANSITION (MET) – CANCER PLASTICITY

1.1. General introduction

Epithelial – mesenchymal transition (EMT) is a reversible biological process in which epithelial cells lose some of their epithelial characteristics including the apico-basolateral polarity, rigid structure, and cell-cell and cell-basement membrane adhesion, and assume properties of mesenchymal cells including flexible structure and enhanced migratory and invasive capacity. EMT involves multiple molecular processes such as down regulation of adhesion molecules via activation of an EMT-related transcription factor circuit, modulation of microRNA expression, reorganization of cytoskeletal proteins, and production of extracellular matrix (ECM) degrading enzymes (1,2). Well characterized molecules associated with the epithelial (E) and mesenchymal (M) phenotype that have been widely used as E and M markers for EMT research are listed in Fig. 1. The majority of E markers are molecules participating in maintaining the epithelial phenotype such as cell junction molecules (E-cadherin, ZO-1, desmoplakin), cytoskeletal proteins (cytokeratins), and molecules mediating cell-extracellular matrix interaction (entactin, collagen). M markers are more variable in functions but they all suppress the epithelial phenotype and promote messenchymal phenotype. Transcription factors (ZEB1, ZEB2, SNAI1, SNAI2, and TWIST) and microRNAs (miR-10b, miR-21) involved in regulating the expression of adhesion molecules are considered as M markers. Besides, cytoskeletal proteins and cell-ECM interaction proteins that are specific for mesenchymal cells are also M markers, such as vimentin, fibronectin, N-cadherin, and $\alpha 5\beta 1$ integrin.

The reverse process of EMT, mesenchymal-epithelial transition (MET), which involves the reversion of mesenchymal cells to epithelial cells, has been documented in normal

development processes such as kidney development (3,4) and hepatogenesis (5). However, information regarding MET is still limited.

1.2. Classification of EMT

EMT was discovered in three different biological settings with distinct functional consequences. Based on the biological context, EMT was classified into three subtypes. Type 1 EMT occurs in implantation, embryogenesis and organ development. The EMT happening later in life and involved in wound healing, tissue regeneration and organ fibrosis is the second type. Type 3 EMT is associated with cancer progression and metastasis (1) (Fig. 2).

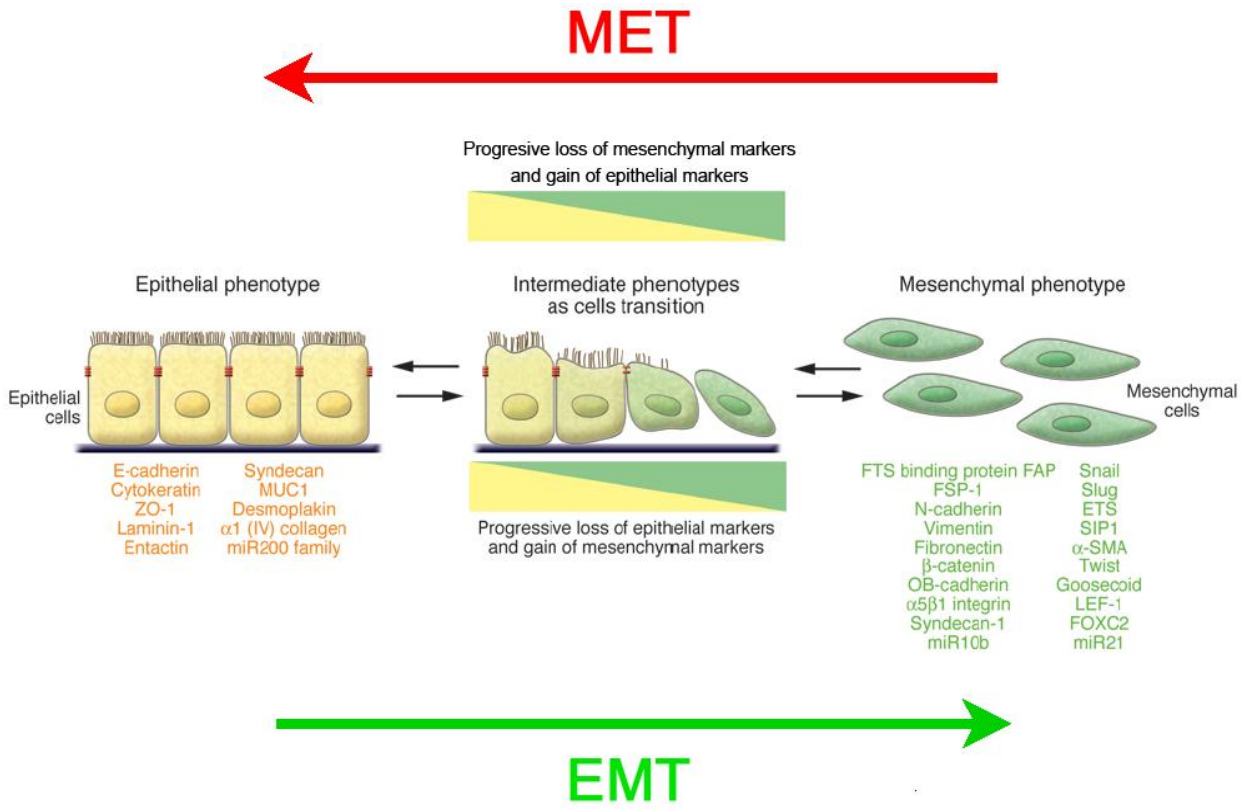

Figure 1: Epithelial-mesenchymal transition (EMT) and mesenchymal-epithelial transition (MET). Common markers for epithelial cells and mesenchymal cells are listed in orange and green, respectively. Colocalization of both epithelial and mesenchymal markers presents in cells in the transition state. This intermediate phenotype indicates that cells have passed only partly through either EMT or MET process. ZO-1, zona occludens 1; MUC1, mucin 1, cell surface associated; miR200, microRNA 200; SIP1, survival of motor neuron protein interacting protein 1; FOXC2, forkhead box C2. *Adapted from Kalluri, R. et al., J Clin Invest* ***119****, 1420-1428 (2009) with permission from Journal of Clinical Investigation.*

Type 1 EMT:

During implantation, when the blastocyst attaches to the uterine wall, the trophoblast undergoes EMT, acquiring the invasive capacity to invade through the epithelial lining of the uterus – the uterine endometrium - allowing the blastocyst to embed in the underlining tissue (6,7). Once properly localized in the endometrial stroma, the blastocyst proceeds to gastrulation to generate three germ layers: ectoderm, mesoderm and endoderm. The embryoblast has already developed into a two layer structure: a layer of columnar cells, called epiblast, lining the amniotic cavity and a layer of cells, called hypoblast, lining the primary yolk sac. Via furrowed invagination in the midline of the epiblast layer, the primitive streak is formed, marking the initial step of gastrulation. The epithelial-like epiblast cells experience molecular changes that induce expression of proteins associated with migration and differentiation to facilitate the primitive streak formation (8,9). Via EMT, epiblast cells invaginate into the space between epiblast and hypoblast and generate mesendoderm which subsequently separates to form mesoderm and endoderm by replacing hypoblast cells (10). The epiblast cells that remain in the original epiblast layer become ectoderm (Fig. 2.A).

Type 1 EMT also happens during neurulation. When the neural plate fold along its central axis, a neural groove is formed and lined on each side by a neural fold. Two neural folds fuse together in a zipper-like manner and pinch off to form neural tube. The neural crest cells, originated from the neural folds, undergo EMT and migrate throughout the embryo and differentiate into multiple cell types, among which are the melanocytes (11-13).

Type 2 EMT

Type 2 EMT occurs in adult tissue and plays a crucial role in wound healing, tissue regeneration and organ fibrosis. This type of EMT is associated with inflammation. It occurs in

response to inflammatory signal and ceases when inflammation is diminished (1). In wound healing, fibroblasts generated from the epithelial cells in the adjacent tissue via EMT migrate and proliferate across the wound site, participating in the formation of granulation tissue that continues to grow until the wound bed is covered (14,15). Fibroblasts secrete multiple components of the extracellular matrix (ECM), such as fibronectin, collagens, elastins, laminin and tenacins, to support their migration and the attachment of cells involved in inflammation, angiogenesis, and connective tissue construction (16). During the re-epithelialization step of the cutaneous wound healing process, keratinocytes lose cell-cell adhesion and gain migratory capacity via an EMT-like process to migrate across the new tissue and seal the wound (17). Once wound healing finish, inflammatory signals are attenuated, and EMT is halted.

Organ fibrosis is the formation of excess fibrous connective tissue that eventually leads to tissue destruction. Organ fibrosis is a form of wound healing that is unabated due to persistent inflammation. In the setting of organ fibrosis, inflammatory cells and fibroblasts release a variety of inflammatory signals to trigger EMT. This type of EMT was identified in fibrosis of the kidney, liver, lung and intestine (18-20). Particularly, during kidney fibrosis in mice, about 30% of fibroblasts arise from the tubular epithelial cells via EMT (21). Growth factors (TGF-β, PDGF, EGF, and FGF-2), chemokines and MMPs (MMP-2, MMP-3, MMP-9) are secreted from a various type of cells, prominently macrophages and activated resident fibroblasts, due to inflammation (22). Under the influence of these molecules, together with inflammatory cells, epithelial cells degrade the basement membrane, lose their polarity and migrate into the interstitial area following a gradient of the signals. This process, which is characterized by multiple molecular markers, happens through sequential steps in which epithelial cells gradually shed their epithelial phenotype and accumulate mesenchymal traits. Concomitant expression of epithelial markers (E-cadherin, cytokeratins) and mesenchymal

markers (vimentin, desmin, DDR-2, FSP-1 and α-SMA) are identified in cells in the transition process. These cells present the intermediate phenotypes, generating the notion of "partial EMT". Identification of such cells demonstrates that epithelial cells can advance to various extents through an EMT. Eventually, when these cells completely pass through the basement membrane and locate in the interstitium of the tissue, they shed all of their epithelial markers as well as their epithelial morphology and gain fully mesenchymal markers and fibroblast shape (23) (Fig. 2.B).

Type 3 EMT

Besides tissue fibrosis, the pathological aspect of EMT is revealed in cancer progression and metastasis. This type of EMT is classified as type 3. Uncontrolled proliferation, the capacity to evade apoptosis and angiogenesis are well characterized as some of the hallmarks of cancer cells. These characteristics provide cancer cells the growth advantage to setup the tumor bulk at the primary site (24). Subsequently, cancer cells intravasate into the blood vessels, follow the blood circulation, extravasate, form micrometastases at distant organ and finally colonization to establish macrometastases, completing the multistep process of metastasis with lethal consequence (25). Multiple studies have been focusing on the metastasis cascade and many of these studies suggest the crucial role of EMT in providing the epithelial cancer cells the invasive capacity and, to a certain extent, stem-like characteristics to survive the blood circulation and drug treatment (1,26). Cancer cells at the invasive front present mesenchymal phenotype and mesenchymal markers such as α-SMA, FSP-1, vimentin, and desmin, indicating that they have undergone EMT (1). These mesenchymal cells can enter the blood vessels and complete the metastasis cascade.

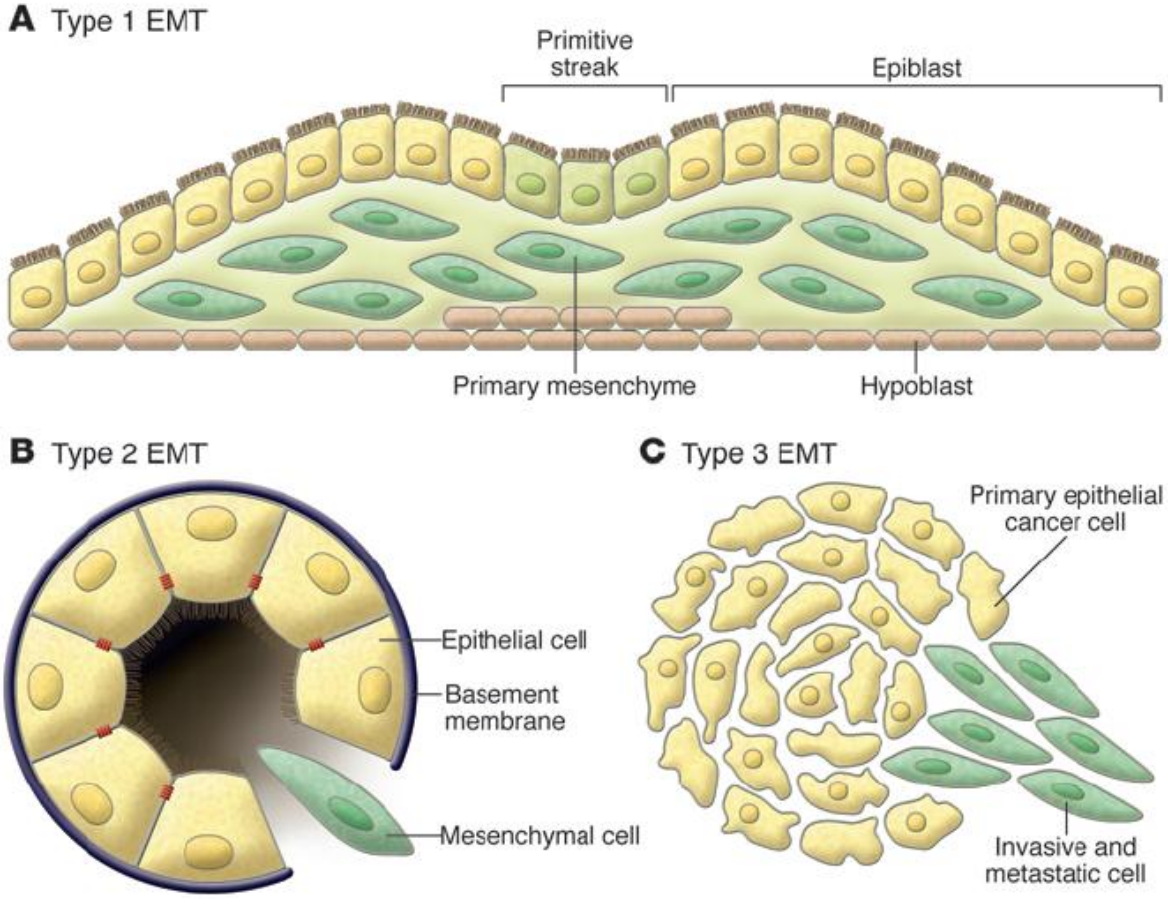

Figure 2: Three different types of EMT. (A) Type 1 EMT happens in embryonic gastrulation. Epiblast cells invaginate along the primitive streak and give rise to primary mesenchyme via EMT. **(B)** Type 2 EMT occurs in adult tissue in response to inflammation in wound healing process or in organ fibrosis. Prolonged inflammatory signals can result in organ destruction. **(C)** Type 3 EMT presents in cancer progression, providing cancer cells migratory and invasive capacity to metastasize. *Reprinted from Kalluri, R. et al., J Clin Invest **119**, 1420-1428 (2009) with permission from Journal of Clinical Investigation.*

However, it is well documented that distant metastases histopathologically resemble the primary tumors, and no longer display mesenchymal phenotype but exhibit epithelial characteristics. An explanation for this paradoxical observation is the reversibility of EMT. The absence of EMT-triggering signals in the distant organs induces disseminated cancer cell to experience MET, the reverse process of EMT, to shed their mesenchymal traits and acquire their original epithelial phenotype (27-29). These considerations emphasize the importance of EMT in tumor invasion and metastasis as well as the crucial role of MET in subsequent colonization at distant organ. Multiple studies have been designed to understand EMT and MET in tumor progression and metastasis. So far, multiple signaling pathways involved in EMT activation, EMT markers, and other aspect of EMT, such as drug resistance and "stemness", have been identified. This knowledge promises clinical implications in the near future (Fig. 2.C).

1.3. EMT in cancer

Mechanism of EMT activation

Typically, EMT is determined by the loss of the epithelial markers and the acquisition of the mesenchymal markers. Popular epithelial markers used in EMT studies are cell adhesion molecules, such as E-cadherin, plakophilins, desmoplakin, PAR6, occludin, and claudins, cytoskeletal proteins, such as CK8, CK18, and CK19 (30), and cell polarity protein (PAR6(31)). Mesenchymal markers that have been reported in EMT are the transcriptional repressors of E-cadherin (ZEB1, ZEB2, TWIST, Snail, and Slug). These repressors directly bind to E-box elements located within the proximal E-cadherin promoter and suppress E-cadherin transcription (32). MicroRNAs are also key players of EMT. Members of the miR-200

family and miR-205 inhibit EMT by binding to 3'UTRs of ZEB1/2, repressing the expression of ZEB1/2's transcripts and, as a result, induce E-cadherin expression (33-36).

Signaling pathways

EMT is generally triggered by extracellular signals secreted by the mesenchymal cells in the stroma (2). The best characterized EMT inducers are members of the transforming growth factor-β (TGF β) family. The canonical TGFβ signaling pathway starts with the formation of the heterogenic complex of type I and type II transmembrane serine-threonin kinase receptors in response to TGF-b ligand binding (37,38). Activated TGFβRII phosphorylates TGFβRI which subsequently phosphorylates Smad2 and Smad3 at their C-termini (37,38). Phosphorylated Smad2/3 partner with cytoplasmic Smad4 and translocate into the nucleus, where they regulate transcription of multiple targets among which are crucial EMT players including SNAI1/2, ZEB1/2, E12/E47, TWIST, Ids (37,38). Obstruction of TGFβ signaling at any point of the cascade blocks EMT and promotes the epithelial phenotype (37,38). TGFβ can activate EMT through a Smad independent pathway. In mammary epithelial cells, TGFβII interacts with and phosphorylates PAR6, an important regulator of cell polarity and tight junction. Phosphorylated PAR6 interacts with the E3 ubiquitin ligase Smurf1, which in turn targets RhoA, a small GTPase protein regulating the assembly of focal adhesions and actin stress fibers, leading to RhoA degradation and subsequently, loss of tight junction and apical-basal polarity (31). TGFβ also promotes EMT by cooperating with other signaling pathways such as Wnt, Notch, MAPK and integrin signaling in a cell-context dependent manner.

Wnt signaling can trigger EMT by itself or in cooperation with TGFβ signaling. In the absence of Wnt, cytoplasmic β-catenin is phosphorylated by glycogen synthase kinase - 3β

(GSK3β) at its N-terminal domain. Phosphorylated β-catenin is then rapidly ubiquitinated by an E3 ubiquitin protein complex containing F-box protein β-Trcp1 and subject to proteasome-mediated degradation. When Wnt signaling is activated, GSK3β is inhibited, leading to cytoplasmic β-catenin accumulation, allowing β-catenin to partner with TCF or LEF, two related transcription factors, and translocate to the nucleus where they regulate transcription of multiple targets among which are EMT players (39,40). β-catenin/TCF4 has been shown to directly bind to the promoter and activate the transcription of ZEB1, which induces the expression of pro-invasive markers MT1-MMP and LAMC2 in colorectal cancer (41). Wnt signaling also can activate EMT markers independent of β-catenin. Wnt/GSK3β/β-trcp1 axis blocks Snail and Slug phosphorylation, preventing their ubiquitin-dependent proteasome-mediated degradation and inducing EMT (42,43). Convergence of multiple TGFβ signaling and Wnt signaling molecule confers EMT. Snail and Slug promote the formation of β-catenin-TCF4 complexes which induce the transcription of TGFβ3. TGFβ3 in turn activates the TGFβ signaling and increases LEF1 transcription, triggering the formation of β-catenin-LEF1 complexes which are responsible for EMT initiation. TGFβ1 and TGFβ2 are also involved in signaling mechanism by up-regulating the expression of Snail and Slug (44).

Notch and Hedgehog are the two other developmental pathways involved in EMT(45). Notch is one of a few signaling pathway that acts in a localized manner. Upon contact with the ligands on the membrane of neighboring cells, the transmembrane Notch receptors are cleaved at two domains (46). The first proteolytic cleavage is at its extracellular domain by tumour necrosis factor-alpha(TNFα)-converting enzyme (TACE) - a protease of the ADAM family, and the second one is at its intracellular domain by the γ-secretase complex to release the NIC (Notch intracellular domain) (46). NIC enter the nucleus, associates with the transcription repressor complex C protein binding factor 1/Suppressor of Hairless/Lag-1 (CSL), inducing the

dislocation of co-repressors (CoRs) and recruitment of the co-activators (CoAs) such as Mastermind to activate the transcription of Notch's target genes including the *HES/HEY* family (46). The Notch pathway plays crucial roles in embryonic development. Notch is also involved in tumorigenesis, cancer progression and metastasis; however, the outcome of Notch is cell-type dependent and can either be oncogenic or tumor suppressive (45). Notch is reported to suppress E-cadherin transcription by directly activating the transcription of Snail and Slug, thus inducing EMT. Cross-talk between Notch and TGFβ signaling as well as between Notch and receptor tyrosine kinase (RTK) signaling such as FGF, PDGF to regulate EMT are also documented (47,48). Similar to Notch, Hedgehog signaling regulates important aspects of developmental biology and cancer biology. Members of Hedgehog signaling pathway are involved in proliferation, cell-fate determination, and stemness. Cooperation between Hedgehog signaling and Wnt, EGF/FGF and/or TGFβ signaling promotes EMT through E-cadherin suppression (49). As a result, it appears that signaling pathways regulating stem cell functions are also involved in EMT, suggesting an activation of a stem cell program during EMT.

Multiple RTKs plays important roles in EMT happening in embryogenesis (9,50). Mutations of RTKs have been reported in various types of cancer. Beside their impacts on all the hallmarks of cancer such as proliferation, apoptosis, angiogenesis, RTK signaling also activates EMT via enhancing expression of E-cadherin suppresors (Snail and Slug) and molecules involved in adhesion and cytoskeletal organization (Rac and Rho)(51).

Integrins are transmembrane receptors that mediate the attachment between cells and the neighboring cells or between cells and the ECM. Cell motility depends mainly on the focal adhesion formed by integrin and other cytoplasmic proteins to connect the cytoskeleton and ECM components. As a result, in addition to disrupting cell-cell adhesion, cells undergoing

EMT also regulate their interaction with ECM mediated by integrins. Integrin-link kinase (ILK), an intracellular protein that interacts with the cytoplasmic domain of integrins, is a key component of focal adhesion. ILK can downregulate E-cadherin and is involved in TGFβ-mediated EMT (9).

Hypoxia and tumor-stroma interaction

Hypoxia is one physiological condition that triggers EMT through multiple mechanisms (2,52). Hypoxia impact on cancer progression and metastasis is mediated mainly by stabilized hypoxia inducible factors (HIFs) (52). HIFs are transcription factors some of whose downstream targets are EMT markers including TWIST, Snail, Slug, ZEB1, and ZEB2. Hypoxic conditions also activate and maintains major EMT pathways such as TGFβ, Notch, and NF-κB. Coss-talk between HIF and TGFβ pathway aids in sustaining the activation status of TGFβ signaling and the stabilization of HIF, thus stabilizing the mesenchymal state of cells located at the hypoxic areas (52). In addition, hypoxia induces recruitment of inflammatory cells which secreting inflammatory cytokines such as TNFα, TGFβ, IL-1, IL-6 and IL-8. These cytokines are known as EMT inducing factors (52). Hypoxia-activated EMT provides and explanation for the well-established association between hypoxia and tumor progression and metastasis (reviewed in (52)).

Since EMT activating factors are mostly secreted by cells in the tumor surrounding stroma, increased expression of mesenchymal markers localizes at the cancer cells at the tumor-stroma interface which is also the invasive front of an aggressive tumor. This was demonstrated in many cancer types in human tumor samples as well as in animal models (53-55).

Genetic and epigenetic control

Genetic and epigenetic instabilities are well known as hall marks of cancer. Mutation and aberrant expression of crucial genes are the source of tumorigenesis, tumor progression and metastasis. Mutation and abnormal epigenetic control of *CDH1*gene leading to stable loss of E-cadherin have been reported in many tumors (56). Especially *CDH1* mutation is identified as a cause of hereditary diffuse gastric cancer (56,57). Loss of E-cahderin due to DNA hypermethylation within the promoter region of *CDH1* is more commonly found in cancer and is associated with tumor progression and metastasis (56,58). Similar to *CDH1*, genes encoding epithelial markers including miR-200 family, miR-205(59,60), and miR-34c(61) are methylated in breast and lung cancer. An alternative mechanism of EMT activation in cancer is DNA hypomethylation of genes inducing the mesenchymal phenotype. DNA methylation profiles of stem-like cells $CD44^+/CD24^-$ of breast cancer reveal a hypomethylated status of a number of genes regulating stem cell functions and EMT, leading to an enhanced expression of these genes in stem-like tumor-intitiating cell enriched $CD44^+/CD24^-$ subpopulation compared to the more differentiated $CD44^-/CD24^+$ group. These hypomethylation profiles are also associated with an increased risk of metastasis in patients (62). Interestingly, inactivation of miR-205 and miR-200 via DNA hypermethylation associated with EMT and stem-like properties are induced during malignant transformation of human lung epithelial cells in response to tobacco carcinogen exposure (59). These studies highlight the alliance between EMT and stemness in cancer.

Transcriptional control

A group of transcription factors including ZEB1, ZEB2 (also known as SIP1), SNAI1 (also known as Snail), SNAI2 (also known as Slug), TWIST, FOXC1, FOXC2, E47 (also known as E2α) are identified as EMT inducers in embryonic development and various types of cancer. All of these transcription factors directly or indirectly repress E-cadherin expression.

ZEB1/2 are two well characterized direct repressors of E-cadherin. ZEB1 (formerly known as δEF1) and ZEB2 (SIP1) belong to the ZEB transcription factor family. ZEB1/2 possess two zinc finger cluster at each ends and a homeodomain at the center. Via their zinc finger domains, ZEB1/2 bind to bipartite E-box (CACCT and CACCTG) on promoters of its target genes. Depending on the downstream targets, ZEB1/2 activates or represses transcription by recruiting the co-activators (PCAF or p300) or co-repressors (CTBP), respectively (32). ZEB1 binds to the E-box sequence on E-cadherin promoter and suppresses transcription of E-cadherin together with CtBP in breast cancer (63,64). Recently, ZEB1 has been shown to repress E-cadherin expression by recruiting the SWI/SNF chromatin remodeling protein BRG1 and inducing EMT in colorectal carcinoma (65). In response to TGFβ signals, ZEB1 and ZEB2 collaborate with each other to repress E-cadherin and promote the mesenchymal phenotype (66).

Besides E-Cadherin, the EMT promoting transcription repressors also share some common targets as well as act independently on a subset of EMT-related genes. Their targets are genes encoding cell junction proteins such as cadherins, plakoglobin (adhesion junction), claudins, occludin and ZO proteins (tight junction), integrins (cell-ECM junction), and cytoskeletal proteins such as cytokeratins. Cross talk between these EMT transcription factors generates a complex signaling network to suppress epithelial traits and maintain the mesenchymal phenotype.

microRNAs (miRNAs) in EMT

The discovery of non-coding RNAs reveals a whole new aspect of gene expression control that is implicated in all cellular process. The importance of non-coding RNAs, especially microRNAs, in EMT has been reported in many studies. The miR-200 family (miR-

200a/b/c, miR-141 and miR-429) and miR-205 are described as negative regulators of E-cadherin repressors in two independent studies in 2008 (33,35,67). These microRNAs target ZEB1/2, promote E-cadherin expression and inhibit EMT. By examining the expression of 207 miRNAs in 60 cancer cell lines from National Cancer Institute, Park *et al.* discovered the strong correlation between miR-200 family members and E-cadherin and the significant inverse correlation between miR-200 family and vimentin. In vitro experiments showed that miR-200 family represses ZEB1/2 mRNA expression, thus promoting the expression of E-cadherin and suppresses vimentin. Interestingly, introducing exogenous miR-200 or inhibiting endogenous miR-200 results in MET or EMT respectively (67). In another study, Gregory PA. *et al.* revealed that miR-200 family and miR-205 were down regulated in response to EMT induced by TGFβ and that enforced expression of miR-200 family alone can prevent TFGβ-induced EMT (33). This group described in detail the binding sites of miR-200 family and miR-205 on the 3' UTR of ZEB1/2 and demonstrated the importance of these miRNAs in ZEB1/2's 3'UTR expression by luciferase assay. Similar to the publication by Park S. *et al.*(67), they showed that miR-200 family and miR-205 maintain E-cadherin expression and the epithelial phenotype by targeting ZEB1/2. The clinical importance of this finding was illustrated in breast cancer, in which loss of the miR-200 family was identified in metaplastic regions lacking E-cadherin, indicating that downregulation of these epithelial miRNAs may participate in tumor progression (33). Recently, p53 is identified as a transcriptional regulator of miR-200c, one of the "epithelial" miRNAs (68), shedding initial light to the transcriptional control of EMT-related miRNAs. In contrast to miR-200 and miR-205, miR-10b is an inducer of invasion and metastasis in breast cancer (69). By inhibiting translation of the homeobox D10 (HOXD10) mRNA, miR-10b indirectly accelerates the expression of a well-known pro-metastatic gene *RHOC* which is represses by HOXD10 (69). Consisting with the in vitro data demonstrating

miR-10b positively regulate migration and invasion, the expression of miR-10b in primary breast cancer samples correlates with progression (69).

1.4. EMT and stemness

There are multiple evidences indicating the close relationship between EMT and stemness. The majority of the EMT activating signaling pathways such as Notch, Wnt, Hedgehog, and TGFβ are involved in regulating stem cell functions and niche-stem cells interactions. Misregulation of these EMT activating signaling pathways is found in multiple types of solid tumors. Recently, a large body of cancer research supports the "Cancer Stem Cells" hypothesis which classifies tumor cells into two groups: Cancer Stem Cells (CSCs) or tumor-initiating cells and non-CSCs. CSCs possess stem-like properties such as self-renewal and differentiation to form various types of non-CSC. CSCs are responsible for tumor initiation, drug resistance and metastasis (70). Interestingly, the emergence of CSCs is indicated as a consequence of EMT induced by signals from the tumor microenvironment (71). Mani S. et al demonstrated that EMT generates stem cell properties in normal and transformed mammary cells. EMT induction, either by over expression Snail or TWIST or TGFβ treatment in nontumorigenic, immortalized human mammary epithelial cells (HMLEs) generates mesenchymal cells with $CD44^{high}/CD24^{low}$ antigen phenotype which is well-established as neoplastic mammary stem cells markers and enhanced mammosphere formation capacity. Consistently, stem-like $CD44^{high}/CD24^{low}$ HMLEs cells, normal primary mouse mammary stem cells, primary normal and malignant human stem-like $CD44^{high}/CD24^{low}$ cells express a number of canonical EMT markers including high N-cadherin, Vimentin, Snail, Slug, TWIST, ZEB2, FOXC2 and low E-cadherin (72). In addition, an enrichment pattern of gene expression associated with embryonic stem cells was discovered in a poorly differentiated and aggressive

subset of tumors in various types of cancer (73). In summary, these publications highlight the connection between EMT, stemness and adverse clinical outcome in cancer.

1.5. Partial EMT-MET-cancer plasticity and metastasis

Since EMT and MET are reversible processes, the epithelial (E) and mesenchymal (M) phenotypes are changeable. Various intracellular signaling pathways triggered by extracellular signals are involved in EMT and MET. Cross-talk among these pathways in cancer cells generates a complex signaling networks in which a fine-tuned change in expression of critical EMT players determine the E or M phenotype (9,32). Due to the genetic and epigenetic instability of cancer, EMT as well as any other processes in cancer cells are highly dynamic, providing cancer cells the plasticity to adapt to the surrounding environment, develop and metastasize. Activation of EMT in cancer cells at the primary tumor site facilitates invasion and dissemination; once cancer cells reach the distant site, activation of MET to revert the mesenchymal metastasizing cancer cells to the epithelial phenotype is crucial for macrometastasis formation. This hypothesis was clearly attested in the skin carcinogenesis in vivo model by Tsai J. *et al* (74). They developed a transgenic mouse model carrying an inducible TWIST1 construct that is only expressed at the basal epidermal layer upon doxycycline (dox) treatment. After skin squamous cell carcinoma formation in response to 7,12-dimethylbenz[a]anthracene (DMBA) treatment followed by weekly applications of 12-O-tetradecanoylphorbol-13-acetate (TPA), TWIST1 was activated either locally at the primary tumor site by dorsal dox injection – the "reversible EMT" model - or systemically throughout the body by dox addition drinking water – the "irreversible EMT" model. Interestingly, the reversible EMT model is significantly more efficient in generating distant metastases than the irreversible EMT model. The role of EMT was also experimentally examined in each step of the metastasis process. Their results showed that EMT activation promotes tumor cell

intravasation and extravasation; however, reversion of EMT is crucial for colonization in distant sites (74). Even though circulating tumor cells (CTC) have EMT signature (low E-cadherin, high TWIST1, high Vimentin), they also express high Cytokeratins (74-76), E markers, indicating that carcinoma cells in vivo may only need to undergo "partial EMT" for dissemination. This partial EMT phenotype, which is also reported in organ fibrosis, may be sufficient to promote invasion and dissemination; moreover, it also provides the metastasizing cancer cell the ability to quickly revert to the epithelial phenotype to proliferate and develop macrometastases.

In summary, in vitro experiments demonstrating cancer cells shed their epithelial phenotype and acquire mesenchymal traits when they undergo EMT could be misleading when applied to explain metastasis in patients. The partial EMT phenotype representing the intermediate status of EMT is possibly more common in metastasizing cancer cells in patients.

2. MICRORNA

MicroRNAs (miRNAs) are small (19-23 nucleotides) non-coding RNAs involved in regulating gene expression (77). After being transcribed, the primary form of miRNAs (pri-miRs) undergoes a multistep maturation process to form precursor miRNAs (pre-miRs) and finally mature miRNA which associates with Argonaute (Ago) proteins to form the RNA-induced silencing complex (RISC), a ribonucleoprotein complex, to mediate post transcriptional gene silencing. miRNAs guide RISC to their targets by complementary base pairing to the target mRNA, promoting mRNA degradation or blocking translation. Due to its short sequence, a single miRNA can have multiple targets, highlighting the importance of miRNAs in gene regulation that affect all functional aspects of cells. Deregulation of miRNA

biogenesis leading to abnormal expression of miRNA participates in many aspects of cancer including proliferation, apoptosis, EMT, invasion and metastasis (78,79).

2.1. Transcription of pri-miRNAs

Similar to messenger RNA (mRNA), microRNAs are transcribed inside the nucleus by either RNA Polymerase II (Pol II) or RNA Polymerase III (Pol III) to form long primary transcripts (pri-miRNAs). There are evidences proving that majority of pri-miRNAs are transcribed by Pol II; for instance many pri-miRNAs are polyadenylated and capped and pri-miRNA transcription is sensitive to treatment with the Pol II inhibitor α-amanitin (80). miRNAs are classified into two types based on their genomic location: the intragenic miRNAs located within introns or exons of protein coding genes which are considered as the miRNA "host" genes, and the intergenic miRNAs located between genes. Intergenic miRNAs are generally believed to be transcribed as independent transcriptional units. Microarray profiling of 175 human miRNAs across 24 different human organs reveals a similarity in expression pattern between intragenic miRNAs and their host genes, suggesting that intragenic miRNAs are processed from the same primary transcripts as their host genes (81). In an effort to identify promoters of miRNAs, two studies using two different approaches, chromatin structure analysis and Pol II chromatin immunoprecipitation analysis, came to the same conclusion that about one third of the intragenic miRNAs have their own promoter and are transcribed independently from their host genes (82,83). Pri-miRNA transcription is also regulated by transcription factors such as c-Myc or p53 (80). For instance, p53 directly binds to the promoter of miR-200c and transactivate miR-200c, resulting in EMT inhibition and suppression of the stem-like phenotype in mammary carcinoma cells (68). Even though pri-miRNA transcription shares some similarities with mRNA transcription, a complete understanding of pri-miRNA transcription regulation is still illusive.

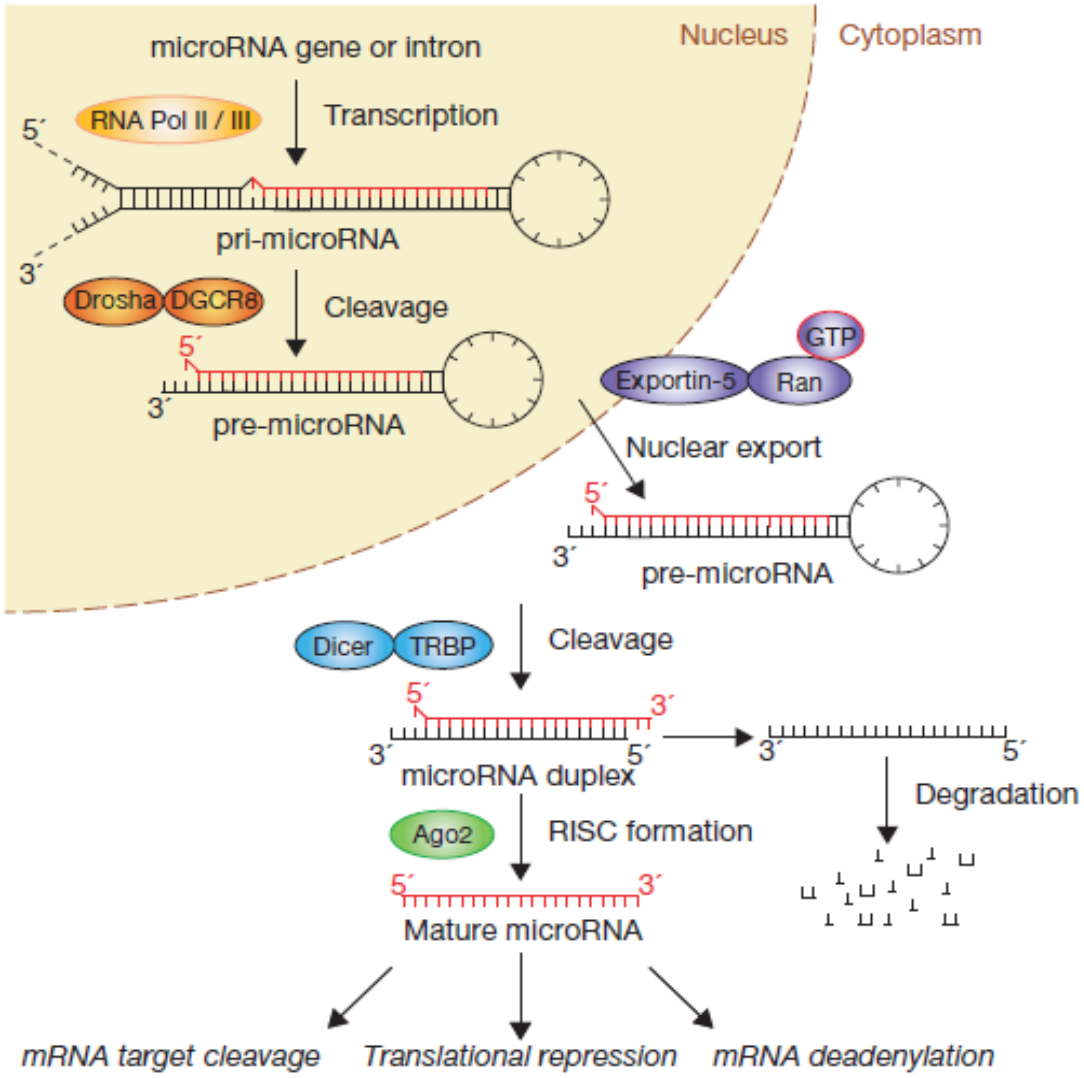

Figure 3: "The 'linear' canonical pathway of microRNA processing. The miRNA processing pathway has long been viewed as linear and universal to all mammalian miRNAs. This canonical maturation includes the production of the primary miRNA transcript (pri-miRNA) by RNA polymerase II or III and cleavage of the pri-miRNA by the microprocessor complex Drosha–DGCR8 (Pasha) in the nucleus. The resulting precursor hairpin, the pre-miRNA, is exported from the nucleus by Exportin-5–Ran-GTP. In the cytoplasm, the RNase Dicer in complex with the double-stranded RNA-binding protein TRBP cleaves the pre-miRNA hairpin to its mature length. The functional strand of the mature miRNA is loaded together with Argonaute (Ago2) proteins into the RNA-induced silencing complex (RISC), where it guides RISC to silence target mRNAs through mRNA cleavage, translational repression or deadenylation, whereas the passenger strand (black) is degraded. In this review we discuss the many branches, crossroads and detours in miRNA processing that lead to the conclusion that many different ways exist to generate a mature miRNA". *Reprinted by permission from Macmillan Publishers Ltd: Nat Cell Biol (80), copyright (2009)*

2.2. Canonical miRNA processing

MiRNA processing in the nucleus

Generation of the pre-miRNA: the long pri-miRNAs are cleaved in the nucleus by the microprocessor complex, comprised of the RNAse type III Drosha and a double-strand RNA binding protein DGCR8 to form a stem-loop-shape double-strand precursor (pre-miR). Pri-miRNA contains a double-strand hairpin stem of 33 base-pairs, a loop and two single-strand flanking regions upstream and downstream of the hairpin. The double-strand stem and the two single-strand flanking sequence are crucial for DGCR8 recognition and Drosha cleavage. Drosha cleaves the 5' and 3' arms of the pri-miRNAs at 11 base pairs away from the junction between single and double-strand RNA toward the loop (Fig. 3). Pri-miRNAs cleavage mediated by Drosha happens co-transcriptionally in both independently transcribed miRNAs and intragenic miRNAs whose transcription is host gene-dependent (80,84).

Nuclear export to the cytoplasm: correctly processed pre-miRNAs are exported into the cytoplasm by Exportin-5 (XPO5) associated with Ran-GTP (Fig. 3). Pre-miRNAs nuclear export mediated by Exportin-5 is independent of their sequence and mainly depends on the length of the double-strand stem and the 3' overhangs. As a result, only pre-miRNAs which are correctly processed can appropriately bind to Exportin-5 and be exported (80).

MiRNA processing in the cytoplasm

Generation of the mature miRNA: In the cytoplasm, pre-miRNAs are processed by the RISC loading complex (RLC) to form mature miRNA (Fig. 3). RLC is comprised of the RNAse III Dicer, the double-strand Tar RNA-binding protein (TRBP) and protein activator of PKR (PACT) and the core catalytic component Argonaute-2 (Ago2) which has endonuclease activity. TRBP and PACT may have overlapping functions and even though they both help recruiting Ago2, functional RLC and RISC can be achieved by TRBP, Dicer and Ago2 alone

(85,86). For the pre-miRNAs whose hairpin stems have a high degree of complimentary, Ago2 creates a nick in the middle of the 3' arm of the hairpin by their endonuclease capacity to generate the Ago2-cleaved precursor miRNA (ac-pre-miRNA). The cleaved strand is the potential passenger strand and this cleavage is believed to facilitate subsequent dissociation of the miRNA duplex (87). Hairpin pre-miRNAs as well as ac-pre-miRNAs are then subject to cleavage by the RNAse III Dicer to remove the loop. The miRNA duplex products contain approximately 22 nucleotides with an additional 2 nucleotides overhang at each 3' end (80).

RISC formation: After cleaving out the loop, Dicer and TRBP dissociate from the duplex. The miRNA duplex contains a functional single strand (also known as seed strand) that is incorporated into RISC and guide RISC to target mRNAs and a passenger strand that is degraded (Fig. 3). The dissociation of the functional strand and the passenger strand could be mediated by helicases; however, a universal helicase responsible for duplex unwinding is yet to be identified. Ago2, on the other hand, can facilitate duplex unwinding and RISC formation by cleaving the passenger strand, triggering its dissociation from the complex. Dissociated passenger strand is subsequently degraded. Functional strand guides active RISC to target mRNAs by complementary base-pairing with the targets. RISC inhibits protein expression by many distinct ways that result in translation inhibition, mRNA destabilization or mRNA degradation, most of which are mediated by Ago2, the main effector of RISC (80,88)

2.3. Non-canonical miRNA processing

miRNA research recently reveals several alternative miRNA biogenesis pathways. The most prominent alternative pathway is the biogenesis of intragenic miRNA located within an intron (also known as mirtrons) in which Drosha cleavage is substituted by splicing. The introns following the mirtron alternative pathway are spliced out and form lariats with the 3' branchpoint ligated to the 5' end of the intron. The spliced lariats are then subjected to

debranching by the lariat debranching enzyme (Ldbr) and fold into pre-miRNA hairpins which are subsequently exported to the cytoplasm. If the intron are long and the hairpin generating sequence locates at one side of the intron, this "tailed" mirtron undergo 5'-3' or 3'-5' trimming after being spliced and debranched (89).

2.4. miRNA degradation

In contrast to the increasing knowledge about miRNA biogenesis, little is known about miRNA degradation. miRNAs are globally stable with much longer half-life than mRNAs. As documented in Dicer-ablated mouse embryonic fibroblasts, miRNA half-lives ranged from 28 to 220 h, which is about 2- to 20-fold longer than that of mRNAs (about 10h)(90). An explanation for the stability of miRNA is the RISC complex which may shield its miRNA partner and protect it from cleavage by ribonucleases (91). Knowledge about factors involved in miRNA degradation is still limited. Enzyme involved in miRNA degradation identified so far are a family of exoribonucleases encoded by the small RNA degrading nuclease (SDN) genes in *Arabidopsis*, exoribonuclease XRN1/2 in *C. elegans*, XRN1 and PNPase PNPT1 (also known as PNPase) in human (reviewed in (91)).

3. UROTHELIAL DEVELOPMENT AND BLADDER TUMORIGENESIS: THE ROLE OF STEM CELLS

3.1. Introduction about stem cells

Stem cell is the term assigned for unspecialized cells that can unlimitedly self-renew and differentiate to generate specialized cells. Stem cells are classified into the stem cell hierarchy based on their differentiation potential as totipotent, pluripotent, multipotent, opligopotent, and unipotent (92) (Fig. 4). Cells in the higher rank are more potent and can give

rise to cells in the lower rank. Totipotent stem cells are at the top of the stem cell hierarchy. These cells can differentiate to any types of cells in the organism. In terms of human development, the zygote is the earliest totipotent stem cell which can generate cells in all three germ layers (endoderm, mesoderm and ectoderm) in the embryo as well as extraembryonic cells (92). Pluripotent stem cells are embryonic stem (ES) cells which reside in the inner cell mass of the blastocysts (93). ES cells can differentiate into all three germ cell layers; however, they cannot generate extraembryonic cells. ES cells can be maintained and expanded in undifferentiated state in vitro, providing a model for basic stem cell study as well as promising therapies based on stem cell transplantation (94). A revolution discovery in stem cell study is the generation of induced pluripotent stem (iPS) cells from mouse embryonic and adult fibroblast by introducing four transcription factors Oct3/4, Klf4, Sox-2, and c-Myc, under ES cell culture conditions (95). This study highlights the capacity of differentiated cells to dedifferentiate to acquire 'stemness'.

Right below pluripotent stem cell in the potency hierarchy is multipotent stem cell which can generate specific cell types in multilineages. Examples of multipotent stem cells are haematopoietic stem cells giving rise to cells in the myeloid lineage (thrombocytes, basophil, neutrophil, eosinophil, and macrophage) and cells in the lymphoid lineage (T cells, B cells, and Natural Killer cells), and bulge stem cells (in the skin) forming multiple lineages including cells in the epidermis, hair follicle, and sebaceous gland (Fig. 4). Multipotent stem cells are present in adult tissue; therefore, they are also referred to as adult stem (AS) cells (93). AS cells are critical for organ maintenace, tissue regeneration and wound healing. Stem cell niche is the crucial determinant of AS cell's lineage differentiation program. AS cells of a specific tissue can give rise to cell types of that tissue; however, when embedded in a different stem cell niche, AS cells can differentiate into the specialized cells of the new environment. For instance,

neural stem cells from mouse and human can produce skeletal myotube *in vitro* (by direct exposure to myoblasts) and *in vivo* (by injection into tibialis anterior), demonstrating that neural stem cells, which generate neuron, glia and blood cells, can differentiate to form skeletal muscle cells upon exposure to signals from the muscle tissue (96).

Oligopotent stem cells can produce only a few cell types within a certain lineage. A typical opligopotent stem cell is the myeloid precursor cell which differentiates to five types of blood cell: monocytes, macrophages, eosinophils, neutrophils, and erythrocytes. Unipotent cells only give rise to a single cell type, for example: mast cell progenitors in the bone marrow only produce mast cells (97).

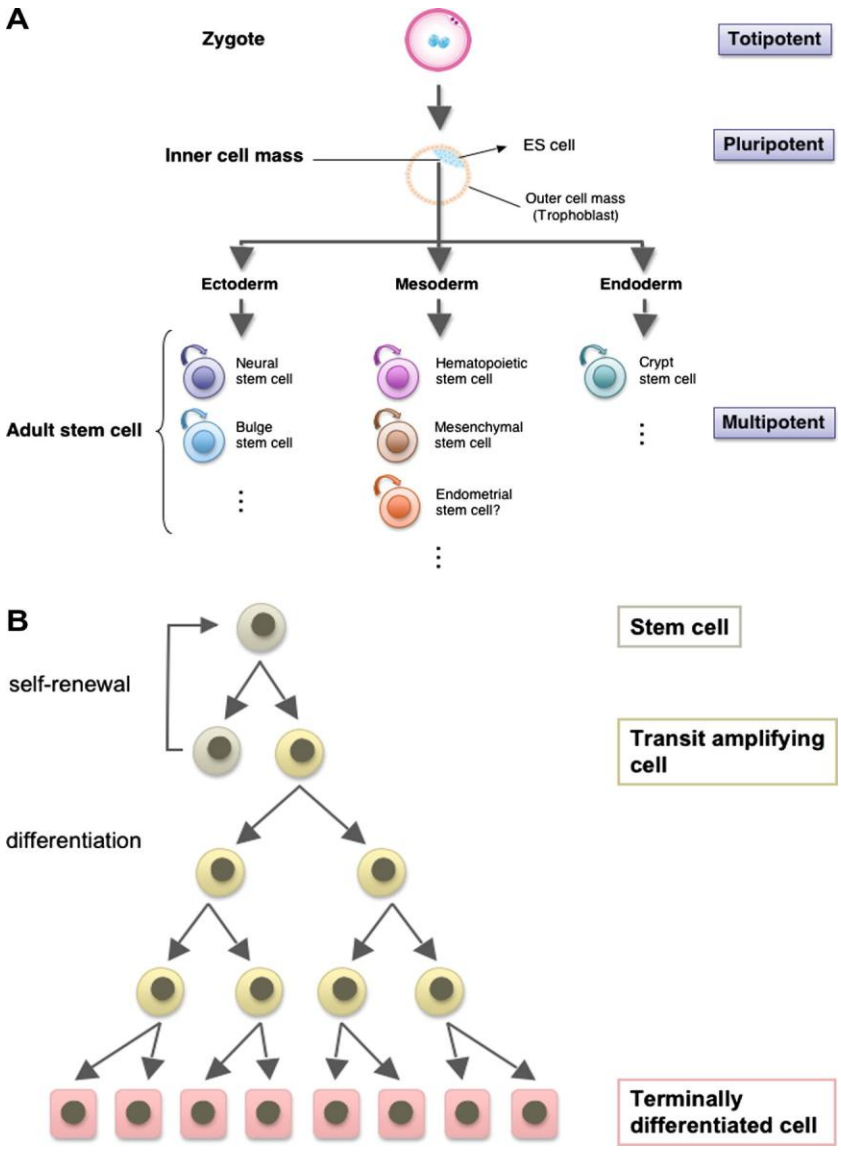

Figure 4: "Hierarchy of stem cells. (A) Developmental hierarchy. A zygote (fertilized egg) can form both embryonic and extra-embryonic tissues and is therefore at the top of the hierarchy of stem cells and is termed 'totipotent'. The inner cell mass of the blastocyst gives rise to three germ layers: mesoderm, endoderm and ectoderm as well as to germ cells. The inner cell mass and the embryonic stem (ES) cells isolated from the inner cell mass are therefore termed 'pluripotent'. An adult stem cell is an undifferentiated cell that is found among differentiated cells in a tissue, which can renew itself and can differentiate to yield some or all of the major specialized cell types of the tissue. Adult stem cells are termed 'multipotent stem cells'. (B) Hierarchy of adult stem cells. Adult stem cells in many tissues divide only rarely, but give rise to daughters that are committed to differentiation, named transit-amplifying (TA) cells, which go through a limited series of more rapid divisions before completing the differentiation process". *Reprinted from Cancer Lett, 308, Kyo, S. et al., Stem cells in endometrium and endometrial cancer: accumulating evidence and unresolved questions, 123-133 (2011), with permission from Elsevier*

3.2. Normal urothelial stem cells

The normal human bladder wall consists of four layers: the urothelium, lamina propria, muscularis mucosae, and periversical soft tissue in sequential order. Urothelium is the epithelium lining the urinary tract, forming a barrier to protect the underlining tissues from potential harm from urine. Urothelium is classified as transitional epithelium since urothelial cells are able to change their shape when the bladder tissue contracts or expands to adapt to the urine amount. Urothelium is a stratified epithelium, comprised of 3-6 layers of cells: a single basal cell layer attaching on the basement membrane, one or more intermediate cell layer(s) on top of the basal layer, and a single superficial cell layer (umbrella cell layer) exposed to the lumen (Fig. 9). Basal cells are the smallest cells of the three (10-20μm in width). They are cuboidal cells with sharply indented nuclei occupying majority of the cytoplasm (98). Intermediate cells are at the intermediate degree of location, size and shape. Similar to basal cells, intermediate cells are mononuclear (98). Superficial cells are the largest (ranging from 20-40μm in width) polygonal cells covering the inner side of the bladder wall, which is the reason why they are referred to as ‘umbrella’ cells (98). The size and shape of superficial cells largely depend on the filling state of the bladder. In unfilled bladder, superficial cells are almost cuboidal in shape; whereas in filled bladder, they stretch out to squamous morphology (99). The superficial layer directly faces the lumen and plays the critical protective role in the urothelium barrier. Superficial cells are connected by tight junctions providing an effective seal at the cell-to-cell junction. Superficial cells are mononuclear, or binuclear (98).

Under normal conditions, the urothelium turnovers every 3-6 months (99). Constant exposure to ions, solutes, and water flux, as well as potential toxic and pathogen from the urine makes superficial cells the most frequently replaced type of cells in the three. Intermediate cells and basal cells are the source of replacement of superficial cells upon pathological damage or

chemically induced injury. Monitored exposure to appropriate amount of protamine sulfate selectively damaged the superficial layer of rat bladder, resulting in necrosis and sloughing of sheets of superficial cells. To replace the damaged superficial cell layer, the underlying intermediate cells underwent rapid maturation to become functional superficial cells within 3-5 days (100). Investigation of the murine urothelium wound healing process upon superficial or full-thickness injuries revealed that the basal cells rapidly proliferate and regenerate the urothelium within 72hrs (101). These data suggest the presence of urothelial stem cells which are activated to regenerate the urothelium upon injury. In addition, the differentiation hierarchy of urothelial cells is also indicated with superficial cells being the most differentiated and the basal cells - the least differentiated cells.

The location of urothelial stem cells is a research interest for many years. Basal cells are the potential candidate of urothelial stem cells. Due to their importance in maintaining and regenerating the organ, stem cells usually locate in a protective environment, such as the intestine crypt base where the intestinal stem cells reside. The urothelial basal cell layer, which is separated from the lamina propria by the basement membrane and protected from urine by a layer of superficial cells and 1-4 layers of intermediate cells, is prominently a well protective environment for stem cells. Another feature of stem cells is their slow recycling characteristic. Stem cells of cornea (102), prostate (103) and epidermis (104) have been identified by cell labeling method to detect slow recycling cells. In label retaining assays, cells are exposed to labeled (^{3}H-thymidine) or synthetic (5-bromo-2'-deoxyuridine - BrdU) nucleosides for a specific amount of time. Proliferating cells incorporate these nucleosides into their DNA during S phase. Normal cells with rapid but limited recycling potential incorporate the label faster, mature, die and lose the label, while stem cells with self-renewing and slow-recycling cells incorporate the label and retain the label in their DNA for a long time. Thus, label-retaining

cells (LRCs) are candidates of stem cells. In one study applying the label retaining (BrdU) assay in rat bladder, LRCs were identified at the basal layer of urothelium (105). These cells retain BrdU for 1 year and account for about 9% of basal cells. In vitro characterization reveals that these cells strongly express β4 integrin and are highly clonogenic (105). Interestingly, basal cells can switch from the normal cytostatic state to highly proliferative state and regenerate all cell types in the urothelium in response to bacterial infection or chemical injury of the mouse bladder (106). In general, these data suggest that urothelial stem cells are basal cells (Fig. 5).

However, this urothelial stem cell hierarchy model starting from basal cells as urothelial stem cells, to intermediate cells and finally to superficial cells as specialized cells is challenged by studies of p63's role in urothelial development. p63 is a homolog of the transcription factor p53. p63 is highly expressed in basal/intermediate cells of the urothelium while superficial cells are negative for p63. Interestingly, $p63^{-/-}$ mice develop a bladder with abnormal urothelium, comprised of only a single layer of cells. These cells express CK18, uroplakin II (107) and uroplakin III (108), consistent with a superficial cell phenotype. These data strongly suggest that superficial cells can be generated and maintained independent of basal/intermediate cells. Moreover, by complementing p63-/- blastocysts with p63+/+ ES cells, Signoretti, S. *et al.* generated a chimeric mouse bladder comprised of both $p63^{-}$ and $p63^{+}$ cells (108). While $p63^{+}$ cells populated basal and intermediate cells, $p63^{-}$ cells did not (108). Remarkably, $p63^{+}$ cells contributed to only 0-15% of superficial cells (108). This chimeric mouse model emphasizes the presence of another pool of urothelial stem cells independent of basal cell origin (Fig. 5).

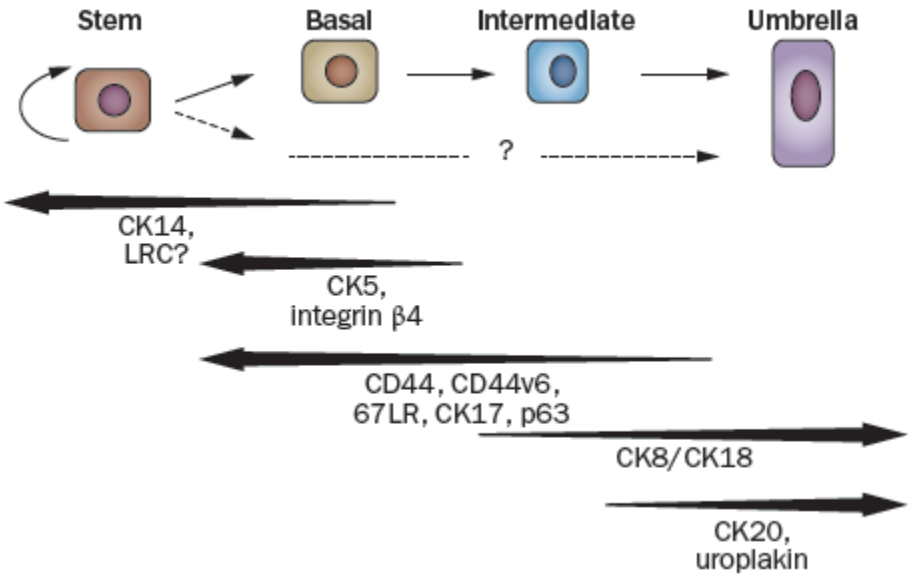

Figure 5: Urothelial stem cell hierarchy. Thin black arrows denote the sequential transition from one differentiation stage to another starting from the undifferentiated stem cells to the highly specialized umbrella cells. Dotted thin black lines demonstrate a hypothetical alternative pathway of differentiation. Markers associated with each differentiation stage are noted. Thick black arrows denote the increase in levels of expression. *Reprinted by permission from Macmillan Publishers Ltd: Nat Rev Urol (92), copyright (2012).*

3.3. 'Stemness' in bladder tumorigenesis: cancer stem cells (CSC)

Tumor heterogeneity is a hallmark of cancer. This term denotes the presence of various types of cells within a tumor, generated by random genetic and epigenetic events inside tumor cells. Cancer cells can be clustered into different subpopulations within a tumor. This feature of cancer is somewhat similar to normal tissues which also consist of different subpopulations of cells with different level of differentiation. In the case of the urothelium of the bladder, these subpopulations are basal (undifferentiated), intermediate (intermediate-differentiated) and superficial (well-differentiated) cells. As a result, the cancer stem cell (CSC) hypothesis was built upon our understanding about normal development to explain our pathological observation of intratumoral heterogeneity. CSC hypothesis postulates the presence of an intratumoral differentiation hierarchy in which a subpopulation of cells (functionally termed CSC) possesses stem cell properties including self-renewal and differentiation to generate different types of cells within the tumor bulk (70). CSCs can originate from different type of cells including normal stem cells with original stemness or transit amplifying/differentiated cells acquiring stemness via dedifferentiation during carcinogenesis process (70). Even though CSC can initiate tumor formation, the CSC term does not indicate the cancer cell of origin which is the cell initiating the original tumor (70). Since CSCs appear to be responsible for tumor initiation, tumor maintenance, drug resistance, tumor progression and metastasis, multiple research efforts have been focusing on isolating and characterizing CSC in various types of cancer including bladder cancer (BC) (92,109).

Cell surface markers are the main tools to identify and isolate viable CSCs. There are multiple markers of CSCs have been published for BC including epithelial membrane antigen (EMA), CD44v6, CD44, 67 kDa Laminin receptor (67LR), carcinoembryonic antigen-related cell adhesion molecule 6 (CEACAM6) and CD90 (Table 1). The models from which bladder

CSCs were isolated vary from cell lines to patient-derived xenografts and primary patient tumors. Since majority of cancer cell lines have been isolated out of their tumor microenvironment and cultured in plastic for a long time, they are not an ideal model for CSC research, provided that microenvironment is crucial for the maintenance of normal as well as neoplastic stem cells. Therefore, freshly isolated patient tumors or early *in vitro* passage tumor cells from patients are more reliable for CSC isolation and characterization. The critical functional characteristic of CSCs is their tumorigenicity, thus they are also referred to as tumor-initiating cells. The gold standard method to characterize CSC tumorigenicity is the *in vivo* serial transplatation with limiting dilution. Chan *et al.* successfully isolated bladder CSCs from primary human BC specimens using the cell surface marker CD44 (110). They demonstrated that $CD44^+$ tumor cells are 10-200 fold more tumorigenic than $CD44^-$ tumor cells in the *in vivo* tumor initiation assay using the immunocompromised $RAG2^{-}/\gamma c^{-}$ mouse model. Moreover, tumors formed by these $CD44^+$ cells recapitulated the tumor heterogeneity of the original tumors. As a result, $CD44^+$ cells qualify all the functional criteria of CSCs (110). Another research group also reported bladder CSC subpopulation which is positive for CD44v6, a spliced variant of CD44, and negative for EMA (111). In an effort to isolate highly tumorigenic BC cells, He *et al.* established that $67LR^+$ and $CEACAM6^-$ cells are more efficient in xenograft formation than their opposite counterpart (i.e. $67LR^-$; $CEACAM6^+$ cells) (112). Interestingly, all of the cell surface markers used to isolate bladder CSC ($CD44^+$, $CD44v6^+$, $67LR^+$, $CEACAM6^-$) are also markers of basal cells in normal urothelium (Fig. 5) (111,112), indicating the basal cell characteristics of bladder CSCs.

Study	Study design	CSC markers	Tumor cell type	Tumorgenic potential
Yang & Chang (111)	In vitro colony-forming assay	EMA^-; $CD44v6^+$	Primary patient	None reported
She *et al.*(113)	In vitro colony-forming assay	SP (DyeCycle violet staining)	SW780	>10 fold
Ning *et al.*(114)	In vitro colony-forming assay	SP (Hoechst 33342)	T24	6-fold
He *et al.*(112)	In vivo colony-forming assay and athymic nude mouse model assay	$67LR^+$; $CEACAM6^-$; $CK17^+$	SW780 and primary patient (once-passaged)	5-10 fold
Chan *et al.*(110)	In vivo colony-forming assay and in vitro $RAG2^-/\gamma c^-$ mouse model assay	$CD44^+$; $CK5^+$; $CK20^-$	Primary patient and patient-derived xenografts	10–200-fold
Su *et al.*(115)	In vivo colony-forming assay and athymic Swiss nude mouse model assay	ALDH1A1	HTB-2; HTB-9; HTB-4	100 fold
Volkmer *et al.* (116)	In vivo $RAG2^-/\gamma c^-$ mouse model assay	$CD90^+/CK14^+$	Primary patient and patient-derived xenografts	17-fold

"Abbreviations: 67LR, 67 kDa laminin receptor; ALDH1A1, aldehyde dehydrogenase 1 family, member A1 (retinal dehydrogenase 1); CD, cluster of differentiation; CEACAM6, carcinoembryonic antigen-related cell adhesion molecule 6 (non-specific cross reacting antigen); CK, cytokeratin; CSC, cancer stem cell; EMA, epithelial membrane antigen; HTB, human tumour cell bank; γc, common cytokine receptor gamma chain; RAG2, recombination activating gene 2; SP, side-population."

Table 1: Selected studies of urothelial CSC marker. *Reprinted by permission from Macmillan Publishers Ltd: Nat Rev Urol (92), copyright (2012).*

Cytokeratins are keratin-containing intermediate filaments localized in the intracytoplasmic cytoskeleton of epithelial tissues (including urothelium). The complex network formed by cytokeratin extends from the surface of the nucleus to the plasma membrane, provide the tensile strength to the cells and support the nucleus. Cytokeratins are differentially expressed during differentiation. Different cytokeratins are associated with different type of cells in the urothelium and used as markers for these cells. CK5/14/17 are strongly expressed in basal and/or intermediate cells whereas CK18/20 are expressed in intermediate and/or superficial cells (Fig. 5 and Fig. 9). Due to their intracellular location, cytokeratins are not appropriate to use as marker for the isolation of viable tumor cells by Fluorescent activated cell sorting (FACS). However, they are very informative tools to study the differentiation status of tumor cells. Interestingly, Chan *et al.* discovered that their bladder $CD44^+$ CSCs co-expressed CK5, the basal cell markers, while the $CD44^-$ non-CSCs co-expressed CK20, the superficial cell marker. In addition, the $CD44^+$ cells were relatively small, with a high nuclear: cytoplasmic ratio, a well-established phenotype of basal cells. $CD44^-$ cells, on the other hand, were heterogenously moderate or large in size, similar to the phenotype of normal differentiated urothelial cells (110). Therefore, this group of researchers categorized BC into three subpopulations based on normal differentiation markers: basal ($CK14^+CK5^+CK20^-$), intermediate ($CK14^-CK5^+CK20^-$) and differentiated ($CK14^-CK5^-CK20^-$). Analyzing these three BC subopulations using a computational algorithm known as mining developmentally regulated genes (MiDReG) revealed two other cell surface markers Thy-1(CD90) and ITGA6 (CD49f) that were up-regulated in the basal BC subpopulation and down-regulated in the differentiated BC subpopulation. The combination of the three cell surface markers CD44/90/49f classified BC cells into four subsets with predicted developmental lineage. Interestingly, xenotransplatation using subfractionated BC cells from FACS with CD44/90/49f markers in the

basal, intermediate, differentiated subpopulations showed that only the most upstream population could regenerate tumors and recapitulate all downstream population (117). An independent study by He *et al.* demonstrated that 67LR+ CSC located at the tumor-stroma interface and strongly expressed the basal cell marker CK17 while non-CSC located inside the tumor nest expressed the superficial cell marker CK20 (112). Collectively, this evidence, again, highlight the basal cell traits in bladder CSCs, indicating that bladder CSCs can either originate from normal basal cells or from dedifferentiated intermediate/superficial cells. In addition, they demonstrate the presence of differentiation hierarchy in BC and the correlation between this hierarchy with tumorigenesis. More importantly, these data suggest that the basal cell phenotype/markers can be used to identify subpopulation of bladder CSCs or used as prognostic markers in patients providing that CSCs is the 'roots' of cancer progression and lethality.

4. BLADDER CANCER

4.1. Incidence and classification of bladder cancer and treatment

Bladder cancer (BC) was ranked as the fourth leading type for estimated new cancer cases and the eighth leading type for estimated deaths in males in the United States in 2012 (118). The majority of BCs (90%) are carcinoma of the urothelium (urothelial carcinoma – UC), formerly called transitional cell carcinoma (TCC). The urothelium is the stratified transitional epithelium lining the urinary tract (National Cancer Institute, 2012). The TNM classification system is applied for pathologic staging of BC (Fig. 6). The depth of tumor penetration into the tissue of the bladder (T), the regional lymph node status (N) and the presence or absence of distant metastases (M) reflect the severity of BC in specific patients. Tumor grade reflects the microscopic histological abnormality of tumor cells, which is also very helpful for oncologists to determine treatment regimens. Bladder cancer is divided into two major phenotypic variants: 80% of the cases are low-grade papillary non-invasive tumors (termed "superficial tumors") and the rest 20% are high-grade invasive tumors (termed "muscle invasive tumors") (119). Superficial tumors arise from hyperplastic urothelium. These tumors (stage Ta and T1) tend to localize within the bladder and rarely invade into the muscle, therefore, rarely metastasize. However, their frequent recurrence after resection makes BC the most costly malignancy to healthcare systems due to the requirement of intensive surveillance and frequent tumor resections (120,121). Muscle invasive bladder cancer (MIBC) arises from severe dysplasia or carcinoma in situ (CIS). The majority of MIBC patients do not have prior history of superficial tumors. Muscle invasive tumors tend to invade into the muscle and metastasize to regional lymph nodes and distant organs. As a result MIBC is lethal and very challenging in terms of treatment. Despite multi-modal therapy including radical surgery and systemic chemotherapy, 50% of MIBC patients succumb to the disease. About 10-15% of superficial tumors progress to

muscle invasive tumors, preceded by CIS in the adjacent bladder mucosa or within the papillary tumor (122). To identify an effective therapy for MIBC as well as a recurrence prevention therapy for superficial tumor, the molecular biology underlying aggressiveness of MIBC cells, the recurrence tendency of superficial tumor and the progression from superficial to muscle invasive phenotype needs to be explored.

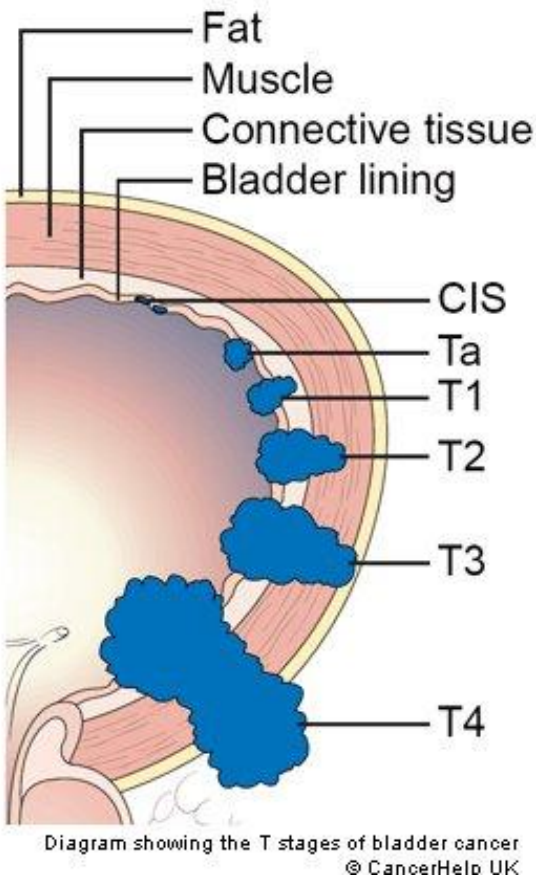

Figure 6: Bladder cancer stage. CIS (carcinoma *in situ*): small lesion in the innermost layer of the urothelium, high grade. Ta: tumors are restricted in the urothelium. T1: tumors have started to grow into the lamina propria, the connective tissue underneath the urothelium. T2: tumors have invaded into the muscle underneath the lamina propria. T3: tumors have invaded through the muscle into the fat layer. T4: the cancer has grown through the bladder wall and spread outside the bladder. *Taken from CancerHelp UK, the patient information website of Cancer Research UK: http://www.cancerresearchuk.org/cancerhelp*

4.2. Molecular pathways of BC progression

The dual-tract concept generalizes bladder carcinogenesis in two distinct but somewhat overlapping pathways: the papillary pathway accounting for superficial BC and the non-papillary pathway accounting for MIBC (Fig. 7) (119,122). These two pathways overlap at the initial step, when normal urothelium acquire genetic alterations leading to the formation of hyperplasia (also referred to as low-grade intraepithelial neoplasia – LGIN) with strong proliferation capacity determined by expression of Ki67 in the entire LGIN and the upregulation of the tumor suppressor RB also in the entire LGIN. These genetic alterations are loss of heterozygosity (LOH) and/or mutation at regions containing loci of critical genes such as p16/ARF and IFNα (9p region), and TSC1 (9q.34). Six critical regions (3q22, 5q22–23, 9q21, 10q26, 13q14, and 17p13) were identified as drivers of human BC development (122). Mutation and/or single nucleotide polymorphism (SNP) at regions surrounding Rb gene resulting in inactivation of genes located in these regions is determined as a risk factor of BC development. These genes are referred to as "forerunner genes" since their inactivation precedes inactivation of RB, a well-established critical tumor suppressor in BC (122). Aromatic amines or nitrosamines from tobacco smoke or industrial solvent are determined as a carcinogen for BC (123). Similar to its effect on other types of cancer, tobacco causes DNA alterations throughout the entire bladder, initiating bladder carcinogenesis process (122).

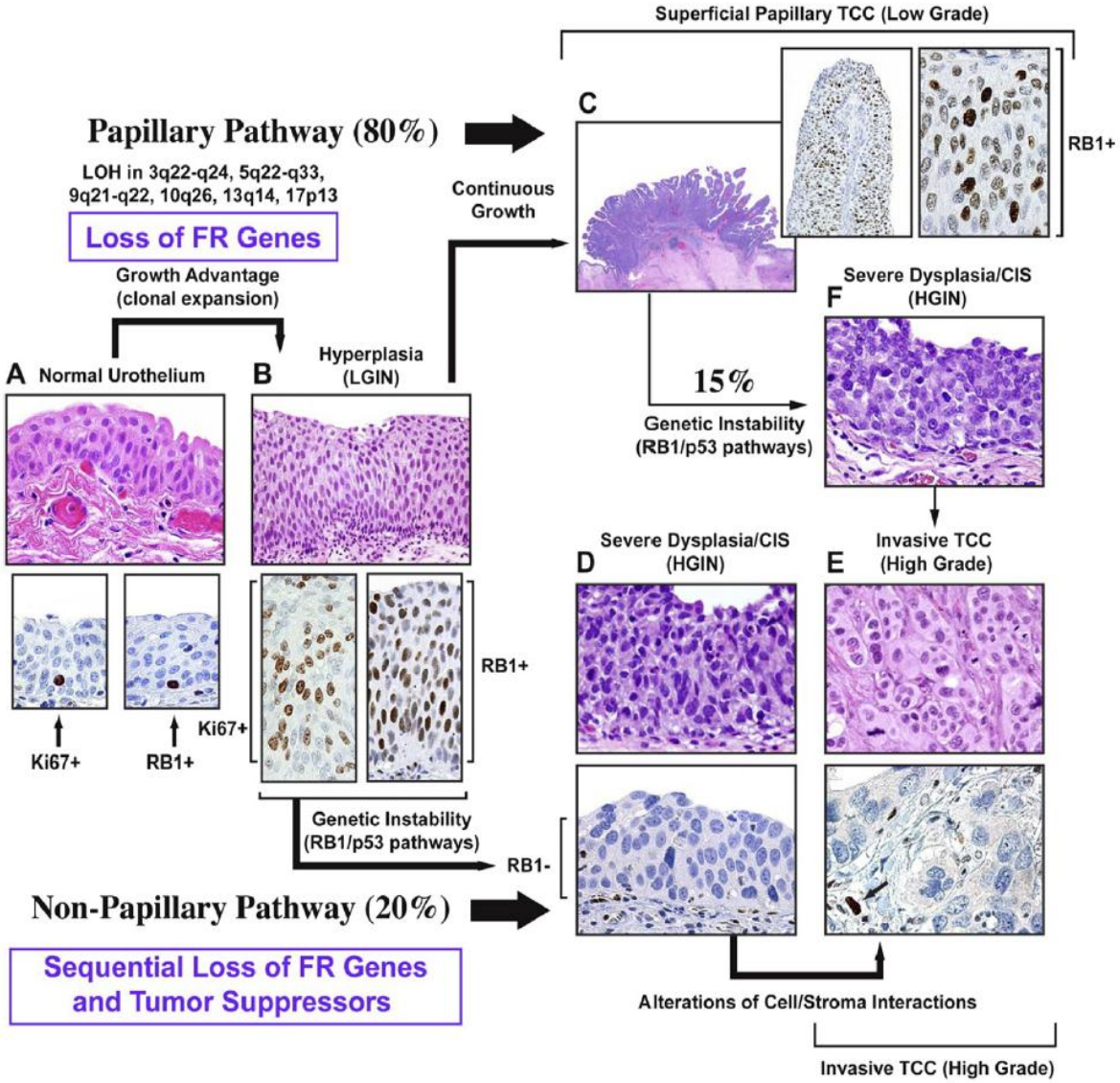

Figure 7: "Dual-track concept of bladder carcinogenesis. The expansion of a preneoplastic clone, which shows minimal phenotypic deviation from the normal urothelium, is the incipient event in bladder carcinogenesis referred to as LGIN. In this phase, the loss of FR genes function provides growth advantage associated with the expansion of proliferating compartment. The proliferating cells expressing normal RB protein are seen in the entire thickness of LGIN. In contrast, normal urothelium contains only scattered proliferating cells expressing RB protein located in its basal layer. The continuous growth of LGIN leads to the development of low grade superficial papillary TCC. In the non-papillary pathway, clonal evolution results in the establishment of a successor clone with microscopic features of HGIN, which often shows a loss of major tumor suppressors such as RB1 and has a high propensity for progression to an invasive high grade non papillary TCC. (A) Normal urothelium (upper panel). Expression of Ki67 in proliferating basal cells of normal urothelium (lower panel, left). Expression of RB protein in peribasal cells of normal urothelium (lower panel, right). (B) Urothelial hyperplasia with mild atypia referred to as LGIN (upper panel). Expression of Ki67 in the entire thickness of LGIN (lower panel, left); expression of RB protein in the entire

thickness of LGIN (lower panel, right). (C) Low-grade superficial TCC retaining normal expression of the RB protein: insets to (C) show low and high power photomicrographs illustrating the expression of normal RB protein in low grade papillary TCC. (D) Severe intraurothelial dysplasia/carcinoma in situ (HGIN) (upper panel). Loss of RB protein expression in HGIN (lower panel). (E) High-grade invasive nonpapillary carcinoma (upper panel). Loss of RB protein expression in high grade invasive nonpapillary TCC. Arrow shows expression of RB protein in endothelial cells adjacent to tumor, which serve as an internal positive control (lower panel). (F) Severe intraurothelial dysplasia/carcinoma in situ developing in bladder mucosa adjacent to a low-grade papillary tumor. It is responsible for switching the pathway and progression of some low-grade papillary tumors to high-grade invasive cancers". *Reprinted from Urol Oncol 28, McConkey, D. J., et al., Molecular genetics of bladder cancer: Emerging mechanisms of tumor initiation and progression, 429-440 (2010) with permission from Elsevier*

Studies using transgenic mouse models provide insights into the molecular mechanisms of the papillary pathway and non-papillary pathway. By using uroplakin II (UPII) promoter, Zhang *et al.* successfully generated two lines of transgenic mice closely recapitulating the two distinct types of BC in human (124,125). UPII is a member of the Uroplakins family (Ia, Ib, II, III) which are major protein components of the asymmetric unit membrane (AUM), a hallmark of urothelial differentiation (126). UPII is specifically expressed in urothelium, restricted to the umbrella cells in normal urothelium (127). Transgenic mice carrying a constitutively active *Ha-Ras* oncogene under the control of UPII promoter developed simple urothelial hyperplasia followed by superficial papillary tumors (125). In addition, mice bearing a high copy number of the *Ha-ras* transgene displayed urothelial hyperplasia and progressed to papillary tumors at much earlier age than mice carrying low copy number of the transgene, strongly suggesting that activation of Ha-ras induces the papillary pathway *in vivo*, and that urothelial hyperplasia is the precursor of superficial papillary tumors (125).

While superficial tumors retain RB expression, loss of RB and p53 is associated with MIBC. Intriguingly, when SV40T transgene under the control of UPII promoter was used to generate transgenic mice, mice carrying low copy number of the transgene developed only bladder carcinoma in situ (CIS), whereas those carrying high copy number of the transgene developed CIS as well as invasive and metastatic tumors (124). Since SV40T (SV40 large T antigen) inactivates p53 and RB tumor suppressors, the formation of CIS and muscle invasive/metastatic tumors (not the superficial tumors) in SV40T transgenic mice demonstrates that p53 and RB are responsible for the aggressive muscle-invasive type of BC. The presence of only CIS in mice sacrificed at early age and the presence of both CIS and muscle invasive lesions in the same bladder of mice sacrificed at older age, suggesting that CIS precedes muscle invasive tumors, at least in mice bearing high copy number of SV40T transgene (124). Analysis

of mice carrying low copy number of SV40T reveals that p53 was completely loss in CIS of the mouse bladder but these CIS persist for a long period of time without muscle invasion and eventually develop into high-grade papillary superficial tumors (128). Moreover, the combination of p53 inactivation and active Ha-Ras in the bladder of transgenic mice generated both low-grade and high-grade papillary tumors but did not promote muscle-invasive tumors. These data emphasize the role of p53 in bladder carcinogenesis; however, these data also suggest that the formation of MIBC requires inactivation of p53 and additional events such as RB inactivation. Another evidence supporting this possibility comes from another transgenic mice study that successfully generate muscle invasive tumors by eliminating both p53 and PTEN in the bladder urothelium while deletion of p53 or PTEN only does not have any effect on the bladder of this mouse model (129). Consistent with this result, PTEN disruption and AKT activation are associated with MIBC in patients (129). This study also reports the activation of mTOR, a component of the PTEN/PI3K/AKT/mTOR pathway, in mouse and human cancer cells, suggesting that mTOR can be a potential therapeutic target for MIBC (129). Inactivation of PTEN in the urogenital system of wild-type p53 background mice induces the formation of prostate cancer but not bladder cancer (130). As a result, abrogation of the p53 pathway is prerequisite for PTEN-dependent bladder carcinogenesis.

These mouse models successfully recapitulate superficial and MIBC in patients. Activating mutations of Ha-ras are common features of BC in which the frequency of Ha-ras mutation is associated with grade (131). However, two other studies exploiting urothelial carcinoma cell lines and primary bladder tumors fail to associate mutations in Ras family members (Ha-ras, K-ras, N-ras) with BC (132,133). The discrepancy regarding Ha-ras mutation in BC indicates that Ha-ras mutation varies significantly in different patient populations and Ha-ras mutation is not a reliable marker for BC. Interestingly, consistent with the Ha-ras

transgenic mouse model result, Ha-ras pathway is activated in superficial tumor via autocrine growth factor receptor activation. Fibroblast growth factor receptor 3 (FGFR3) is one of the growth factor receptors that harbor activating mutation associated with superficial tumors but not MIBC (134,135). Loss of p53 is prerequisite for CIS and combination of p53 and RB loss induces MIBC in preclinical mouse models. Similarly, inactivating mutations of p53, inactivation of the p53 pathway (loss of p21), and/or alteration of RB were associated with increased risk of recurrence and poor survival in both organ-confined and MIBC (136,137). Disruption of the RB pathway presenting in patient tumors as loss of RB, inactivation mutation of RB or inactivation of p16, an upstream regulator of RB correlates with tumor progression (138,139). Finally, LOH within PTEN locus in chromosome 10 leading to loss of PTEN is much more commonly detected in MIBC than superficial tumors (140,141).

The strong homology between p63, a member of the p53 family, and p53 as well as the crucial role of p63 in bladder development makes it become an interesting target for BC research. Many studies focus on p63 as a biomarker to predict tumor progression. High p63 expression is well correlated with superficial tumors whereas loss of p63 expression, especially ΔNp63, is associated with the aggressive muscle invasive phenotype (142-144). However, high ΔNp63 expression in primary muscle invasive tumors correlates with adverse clinical outcome (145,146), suggesting a complicated role of p63 in bladder cancer formation and progression. Deeper understanding of ΔNp63's functions should elucidate the biology of the most lethal subset of MIBC

5. P63

5.1. General introduction

p53, the well-known tumor suppressor protein, has been the subject of intensive research for more than three decades. Throughout the last decade, p63, a homolog of p53, has become a research interest of scientists in the fields of developmental biology and cancer biology. p63 exhibits remarkable sequence and structural homology to p53, especially in the DNA binding domain, suggesting overlaps in target recognition specificity. Indeed, p63 can bind to p53 response elements (p53REs) *in vitro* and *in vivo* (147). p53 targets that are also regulated by p63 include but are not limited to $p21^{Waf2/Cip1}$, 14-3-3σ, MDM2, Bax, PERP, NOXA (reviewed in (147)). However, p63 and/or p73, another member of p53 family, also can regulate transcription of genes p53 does not regulate, among which are genes involved in DNA repair such as *Rad51, BRCA2, mre11* and *Rad50* (148). The transcriptional targets of p53, p63 and p73 identified by microarray analysis in cells following DNA damage demonstrated that p53 family members can cooperate or act independently in transcriptional regulation (148). A large number of p63 target genes (almost 1000) were identified by chromatin immunoprecipitation (ChIP) on chip analysis, suggesting that p63 plays a key role in a broad transcription regulatory network involved in many biological processes (149).

While *TP53* only has a single promoter, the *TP63* gene possesses two promoters that produce two groups of isoforms – the full length TAp63 group containing full-length transactivation (TA) domains and the ΔNp63 group that contain truncated N-terminal domains (Fig. 8). Alternative splicing at the C termini of both groups generates three different isoforms, named α, β, γ (Fig. 1) (147,150). Only the α isoforms of p63 have the sterile alpha motif (SAM) domain, which is absent in p53. The SAM domain is responsible for protein-protein

interactions in developmental and other processes such as transcriptional activation, chromatin remodeling, and focal adhesion (reviewed in (147)). The TAp63 subfamily, with TA domains similar to the TA domain of p53, can activate multiple p53 target genes. ΔNp63, which lacks the TA domain, was originally believed to act as a dominant negative molecule toward TAp63 (150). However, the ΔNp63 isoforms are still able to transactivate p53 targets due to a second transactivation domain located in their N-termini (151,152). Six p63 isoforms with overlapping and independent targets cooperate/antagonize and independently regulate transcription, creating the complexity of the p63 transcriptional network (148,153). As a result, mechanistic interpretation of the biological effect of p63 family is impossible without knowledge of individual p63 isoforms.

5.2. p63 in development

p63 first attracted research interest for its crucial role in epithelial development. Two different groups produced the first p63-deficient mice, but the different targeting constructs they used produced slightly different effects on p63 expression that had important consequences for the phenotypes that resulted from them. Even though the developmental abnormalities were identical in p63 knockout mice generated by two independent groups of scientists, the groups' interpretations regarding the role of p63 in embryonic development were distinct. While p53 knockout mice survive and develop normally but are prone to cancer (154), p63 knockout mice lacking all p63 isoforms die one day after birth and have severe defects in limb, craniofacial and epithelial development. Developmentally abnormal epithelial tissues in p63 null mice include the skin, prostate, mammary gland and urothelium (155,156). Since the p63 null mice generated by Mill *et al* have an unstratified single cell layer epithelium that covers the body surface, tongue, and oral cavity where differentiation markers are absent, they

concluded that p63 is essential for lineage commitment and differentiation (155). However, Yang *et al.* observed clumps of differentiated cells in the epidermis, suggesting that p63 is crucial for maintaining the stem/progenitor cell population in the epithelium (156). Subsequent reconstitution studies shed light on the specific roles of p63 isoforms in development. Transgenic mice expressing either ΔNp63α or TAp63α under the control of K5 promoter were bred onto a p63 null background to generate mice expressing ΔNp63α and/or TAp63α in the epidermis. Only $p63^{-/-}$;ΔNp63α mice significantly developed an epidermal basal layer, whereas the $p63^{-/-}$;TAp63α's phenotype was similar to the p63 null mice. Co-expression of ΔNp63α and TAp63α rescued the epidermis, further, resulting in the formation of larger patches of differentiated skin. These data demonstrate that ΔNp63α is crucial for retaining the precursor/progenitor cell population in the basal layer whereas TAp63α acts synergistically or subsequently to control epithelial development. Consistently, ΔNp63α regulates expression of basal epidermal genes such as K14; whereas TAp63α controls expression of differentiation markers within the upper layer of the skin such as Ets1, K1, transglutaminases, and involucrin (157). During development, ΔNp63 isoforms are expressed shortly after gastrulation and remain restricted to the basal layer of the epidermis, since the epidermis at this stage (prior to the epidermal stratification) is only a single layer of ectodermal cells. On the other hand, TAp63 isoforms are only weakly expressed, and only in suprabasal cells (158). A recent study investigating Δ*Np63*-null mice further illustrates the critical role of ΔNp63 in epithelial development and differentiation (159). Δ*Np63*-null mice die shortly after birth and exhibit a developmental defective phenotype strongly similar to the phenotype of *p63*-null mice in which all of p63 isoforms are deleted (159). Interestingly, keratinocytes from Δ*Np63*-null mice formed a basal cell layer and patches of them stratified and committed to differentiation, which appeared to be unbalanced and accelerated, because it was associated with the premature

expression of terminal differentiation markers (159). These data highlight the indispensable role of the ΔNp63 isoforms in epithelial development, specifically in proliferation of basal keratinocytes in embryonic epidermis and proper differentiation (159). Unlike Δ*Np63*-null mice, *TAp63*$^{-/-}$ mice survived after birth and had median lifespans of 333 days (160). However, *TAp63*$^{-/-}$ mice exhibited multiple signs of premature aging and developed blisters, ulcerated wounds in the skin, and senescence of hair follicle-associated dermal and epidermal cells, potentially due to the crucial role of TAp63 in the maintenance of dermal and epidermal precursors (160). Analysis of *TAp63*$^{-/-}$ mice revealed that TAp63 participates in maintaining adult skin stem cells by regulating cellular senescence and genomic stability (160). Studies from the Δ*Np63*$^{-/-}$ and the *TAp63*$^{-/-}$ mouse models suggest that the ΔNp63 isoforms are important in maintaining the proliferation capacity of basal keratinocytes in embryogenesis whereas the TAp63 isoforms regulates proliferation of epidermal and dermal precursor cells post embryogenesis. These studies also emphasize the essential of both ΔN- and TA- isoforms in regulating proper differentiation of skin stem cells.

Similar to other stratified epithelia, bladder urothelium development is severely impaired in p63 null mice. In normal urothelium, cells in the basal and intermediate layers express p63 while the terminally differentiated umbrella cells do not (146). The bladders of p63 null mice have the phenotype of bladder extrophy, characterized by loss of the abdominal and ventral bladder wall. The ventral bladder of p63$^{-/-}$ mice is covered with a thin membrane comprised of a single layer of cells positive for K18 (also known as CK18), a marker of intermediate (transit amplifying) and terminally differentiated umbrella cells, and negative for Uroplakin III (UPIII), which is also a marker of umbrella cells. During bladder development in p63$^{+/+}$ mice, whereas the TAp63 isoform is only transiently expressed, ΔNp63 isoforms (ΔNp63β, ΔNp63γ) are the predominant isoforms expressed, especially at the ventral bladder

area where they function as anti-apoptotic factors to maintain the stem cell population by, potentially, suppressing the expression of the apoptotic mediators *Bax* and *Apaf1*(161). In contrast, in a recent publication, Karni-Schmidt *et al.* reported that the urothelium in p63-null embryos contains a single layer of cells positive for both CK18 and UPII, which are markers of umbrella cells, the most differentiated cells in urothelium. By using newly generated ΔNp63, p63α, and p63α/β antibodies, as well as commercially available p63 antibodies, they demonstrated that TAp63α is the first isoform detected in $p63^{+/+}$ urothelium, as early as E16.5, whereas the ΔNp63 isoform is only detected after birth (146). The discrepancies in the results from these two groups are potentially due to the use of different p63 antibodies, and further efforts are required to conclusively resolve the issue.

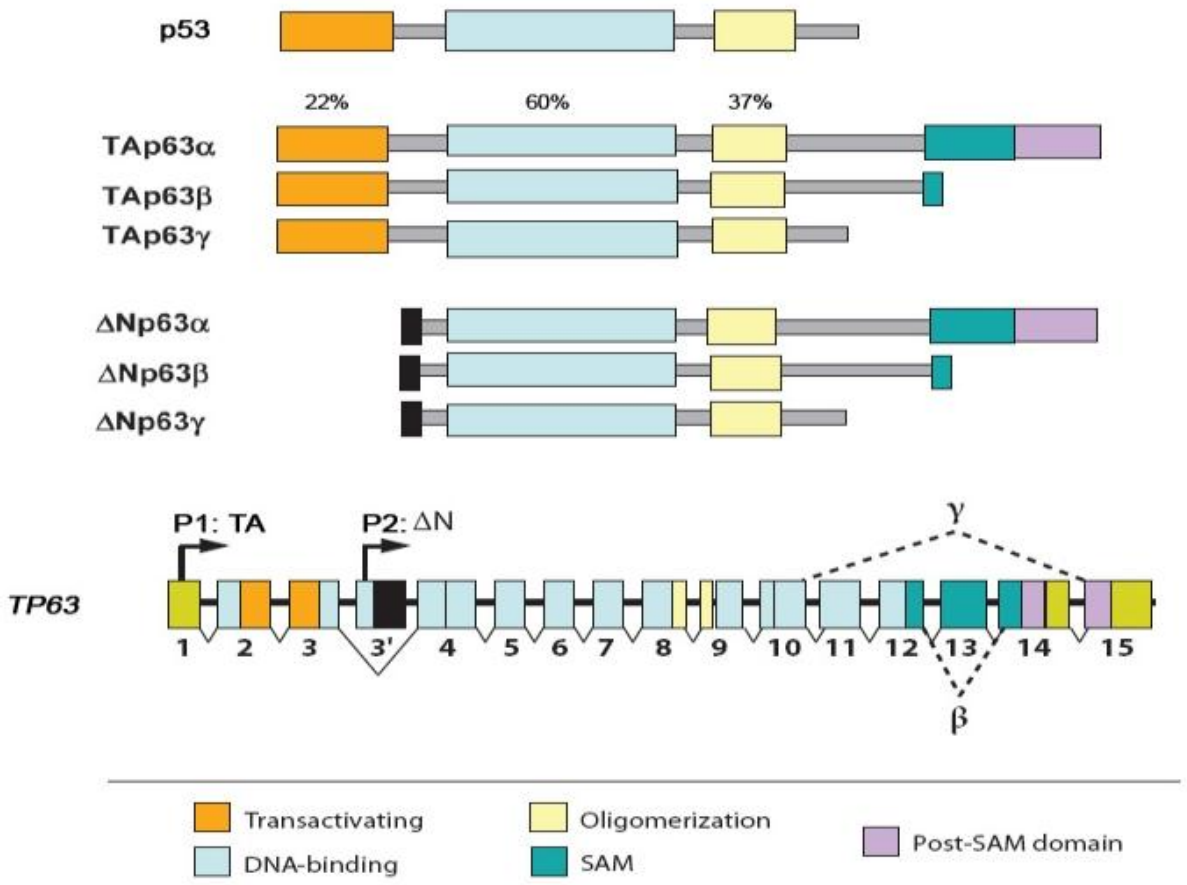

Figure 8: Schematic illustration of *TP63* gene and its six protein isoforms. *TP63* gene has two promoters (P1 and P2) resulting in two groups of isoforms one with the transactivation domain (TAp63) and without the TA domain at the N-terminus (ΔNp63). Alternative splicing at the C-terminus generates the α, β, γ isoforms in each group. The DNA-binding domains of p63 isoforms are strongly homologous to DNA-binding domain of p53. SAM, sterile alpha motif; TA, transactivating isoform; TP, tumor protein. *Republished with permission of Annual review of pathology, from "p63 in epithelial survival, germ cell surveillance, and neoplasia", Crum C. et al., 5, 2010; permission conveyed through C opyright C learance C enter, Inc.*

5.3. p63 in normal tissues and tumors

In normal tissue, p63 is highly expressed in the basal and suprabasal cells of stratified and glandular epithelia including the epithelium of foreskin, tonsil, breast, cervix, vaginal epithelium, esophagus, prostate, and urothelium. p63 expression decreases with differentiation, and terminally differentiated cells are negative for p63 (150,162,163). The p63 4A4 antibody that detects all p63 isoforms is the most widely used antibody to examine p63 protein expression in tissues. This antibody confirms the presence of p63 in the basal and intermediate cell layers and the absence of p63 in the umbrella cell layer in urothelium (143,146) (Fig. 9). Since p63 isoforms may function differently, recent research has focused on specific p63 isoform expression. RT-PCR using p63 isoform specific primers is a sensitive and specific method for p63 isoform detection. Antibodies specific for TAp63, ΔNp63, p63α, p63α/β are commercially available, however, the sensitivity and specificity of these antibodies are still controversial. For example, ΔNp63 is the predominant isoform detected in basal and intermediate cells of normal human urothelium by both RT-PCR and immunoblotting (143). On the contrary, Karni-Schmidt *et al.* reported that ΔNp63 protein expression is undetectable in normal human urothelium even though they confirmed the presence of ΔNp63 protein in normal mouse urothelium (146).

Unlike p53 whose tumor suppressive functions in cancer are well established, whether p63 is an oncogene or a tumor suppressor has been a topic of controversy (164). $p63^{-/-}$ mice display severe developmental defects and die shortly after birth; therefore, it is impossible to study the effect of germline p63 deficiency on tumorgenesis (155,156). Two independent studies of p63+/- mice provide opposite results, one suggests that p63 is a tumor suppressor (165), and the other indicates that p63 is not a tumor suppressor and that reducing p63 content may even protect cells from tumorgenesis (166). The $p63^{+/-}$ mice from the study of Flores *et al.*

developed tumors starting at 12 months of age. The tumor spectrum of $p63^{+/-}$ mice (histiocytic sarcoma, squamous cell carcinoma, lung adenoma) was different from that of $p53^{+/-}$ mice (thymic lyphoma, histiocytic sarcoma, rhabdomyosarcoma, osteosarcoma, hemangiosarcoma). Interestingly, the wild type *p63* allele was lost in tumors from $p63^{+/-}$ mice as the result of loss of heterozygosity (LOH). Mice heterozygous for both p53 and p63 ($p53^{+/-}$;$p63^{+/-}$) demonstrated a more aggressive tumor type with increased tumor burden and metastatic disease compared to the $p53^{+/-}$ and $p63^{+/-}$ mice. Their data strongly support an important role for p63 in suppressing tumor initiation, progression and metastasis (165). One year after the publication from Flores *et al*., Keyes *et al.* reported a completely different result using the same approach. Only 13% of their $p63^{+/-}$ mice developed tumors compared to 38% of $p63^{+/+}$ mice that developed tumors at 28 months of age, suggesting that the $p63^{+/-}$ mice are not tumor prone. Combination of heterozygosity in p63 and p53 ($p53^{+/-}$;$p63^{+/-}$) significantly reduced the rate of tumor incidence observed in the $p53^{+/-}$ mice. Moreover, expression of both TAp63 and ΔNp63 isoforms was maintained in tumors from $p63^{+/-}$ mice (166). The discrepancy between the two studies appears to result from the fact that the $p63^{+/-}$ mice used in the two studies were heterozygous for distinct p63 alleles (155,156). In addition, it has been reported that the null allele in the $p63^{+/-}$ mice from Keyes *et al*. might still produce some isoforms of p63 (167)(reviewed in (168)). This complicates the interpretation of the phenotypes of $p53^{+/-}$;$p63^{+/-}$ and $p63^{+/-}$ mice generated from this group since the remaining p63 isoforms may exert tumor resistance effects (168).

Studies in human malignancies also reveal differences between p53 and p63. While p53 is frequently mutated and mainly functions as a tumor suppressor, p63 remains intact in many cancer types and the role of p63 is tumor type-specific (169). For example, ΔNp63 is highly expressed in squamous cell carcinoma of esophagus, and overexpression of p63 induces tumorgenesis in non-small cell lung cancer; however, loss of p63 has been associated with

tumor progression and poor prognosis in bladder cancer (164). The lack of antibodies that are sensitive and specific for detection of p63 isoforms brings difficulties and controversies to p63 studies in human tumors. Recent discoveries in the p63 field suggest that TAp63 functions as a tumor suppressor and ΔNp63 functions as an oncogene (170). In 2010, Su *et al.* reported that $TAp63^{+/-}$ and $TAp63^{-/-}$ mice developed metastatic tumors (171). Combination of TAp63 and p53 mutation remarkably enhanced metastatic tumors in mice. $TAp63^{+/-}$;$p53^{+/-}$ and $TAp63^{-/-}$;$p53^{+/-}$ mice developed more metastatic carcinomas and sarcomas than $p53^{+/-}$ mice. Similar results were observed when $TAp63^{+/-}$;$p53^{-/-}$ and $TAp63^{-/-}$;$p53^{-/-}$ mice were compared to $p53^{-/-}$ mice. This group also determined that TAp63 suppresses metastasis by directly activating transcription of Dicer and miR-130b (171). Another study from Guo *et al.* using a TAp63-specific conditional mouse model demonstrated the crucial role of TAp63 in inducing senescence and inhibiting tumorigenesis via a p53-independent pathway (172). ΔNp63, on the other hand, is the predominant isoform and is overexpressed in squamous cell carcinomas of the lung and head and neck, potentially functioning by inactivating p53 (173-175). Without a full-length transactivation (TA) domain at its N-terminus, ΔNp63 can act as a dominant negative to p53, TAp63 and TAp73 to inhibit transcription and apoptosis (150,176,177). ΔNp63α has been shown to suppress p73-dependent apoptosis, promote proliferation, and facilitate tumorigenesis (178-180).

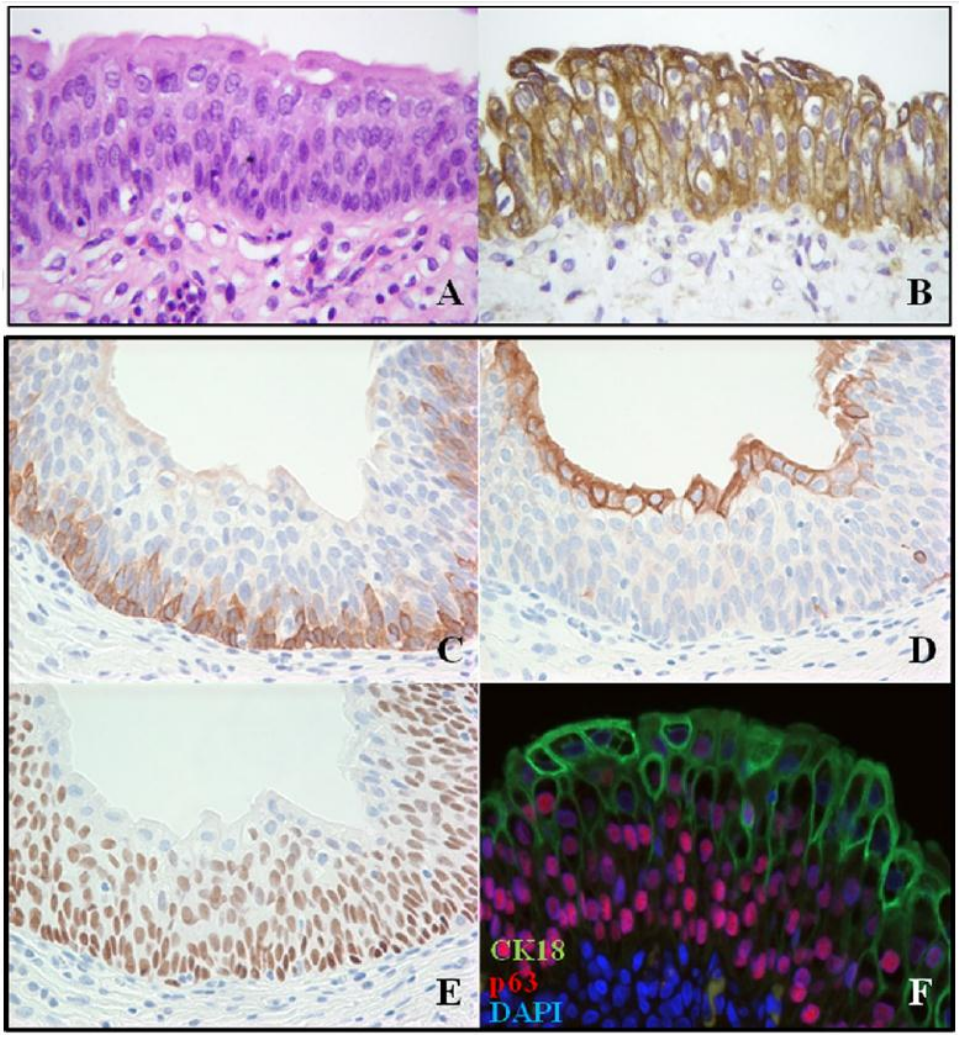

Figure 9. "Morphologic and immunohistochemical characterization of human normal urothelium. (A) Hematoxylin and eosin staining of normal human urothelium; (B) CK7 expression, as revealed by immunohistochemistry (IHC), is observed in all urothelial layers; (C)–(F) immunophenotypic characterization of urothelial cells by expression patterns of cytokeratins and p63: Basal/intermediate cells are characterized by the expression of high molecular weight cytokeratin (C) and a p63-positive phenotype (E), (F), while CK18 is expressed only by "umbrella" cells (D), (F); All microphotographs were taken at 400_ magnification." *"Reprinted from Urol Oncol 28, Molecular pathways of urothelial development and bladder tumorigenesis, 401-408(2010) with permission from Elsevier*

6. RATIONALE OF THE STUDY

Cancer statistics highlight the lethality as well as the prevalence of bladder cancer in the United States in 2013 (181). Understanding the biology of bladder cancer progression and metastasis as well as identifying critical markers of survival is very important for the long term purpose of discovering a cure for this disease. Given the crucial role of p63 in maintaining stemness during epithelial development, we undertook the present study to explore the role of p63 in bladder cancer. Bladder cancer is a very intriguing case in p63 research. Loss of p63 protein expression, especially the ΔNp63α isoform, has been implicated in tumor progression in patients. A majority of low-grade papillary non-invasive tumors express high p63 levels whereas a subset of high-grade muscle invasive tumors expresses low p63 levels (144,182). It has also been reported that EMT is involved in stemness, tumor progression and metastasis in multiple types of cancer, yet p63 expression correlated inversely with EMT markers (ZEB1, ZEB2) in human bladder cancer cell lines. We were therefore also interested in studying the relationship between p63 and EMT in bladder cancer.

CHAPTER 2:

MATERIALS AND METHODS

1. Cell culture

SW780, RT4, T24, J82, Scaber, TCCSUP, 5637, 1A6, 253J-P and UM-UC3 were purchased from American Type Culture Collection (ATCC) (Manassas, VA). BV was generated by recycling 253J-P cell line five times in the orthotopic mouse model (183). All other cell lines in the UM-UC series are provided by Dr. H. Barton Grossman (Department of Urology, MD Anderson Cancer Center). The identities of cell lines were confirmed by DNA fingerprinting using AmpFlSTR® Identifiler® Amplification (Applied Biosystems/Life Techonologies, Grand Island, NY) or AmpFlSTR® Profiler® PCR Amplification (Applied Biosystems/Life Techonologies) in the MD Anderson Characterized Cell Line Core facility or by ourselves, respectively. In this study, UM-UC cells are referred to as UC cells. All the cell lines were cultured in Minimum Essential Medium Eagle (MEM) (Life Technologies, Grand Island, NY) supplemented with 10% fetal bovine serum (FBS) and 1% each of MEM vitamin solution (Life Technologies), sodium pyruvate, L-glutamine (BioWhitaker/Fisher Scientific, Pittsburgh, PA), L-glutamine, penicillin/streptomycin solution and nonessential amino acids (Life Technologies). Cultured cells were kept at 37^0C in a standard 5% CO_2 incubator.

2. RNA isolation and Real-time Reverse Transcription PCR (qRT-PCR) analysis

The mirVana™ miRNA Isolation Kit (Ambion/Life Techonologies) was used to isolate RNA from samples. This kit combines the advantages of two traditional methods of RNA extraction - chemical extraction and solid-phase extraction - to provide high yields of pure RNA and prevents loss of small RNAs such as microRNA during the extraction procedure. Chemical extraction method uses chaotropic salts in combination with acid phenol-chloroform solution to inactivate RNAse and separate RNA from other biomolecules. This method can

provide pure RNA but usually results in low yield of RNA due to the loss during extraction steps, especially the loss of very small RNAs. Solid-phase extraction method uses salt or alcohol to increase the affinity of RNA to the solid support which is glass (silica). This method also does not effectively recover small RNAs. The mirVana miRNA isolation process comprises of four steps: sample disruption in the denaturing Lysis/Binding buffer which stabilizes RNA and inactivates RNAse, RNA separation using Acid phenol:chloroform 1:1 to collect RNA in the aqueous phase, RNA purification using glass-fiber filter and wash solutions formulated specifically for miRNA retention to avoid the loss of small RNAs, and finally RNA elution to collect high quality RNA from the filter cartridge. Pre-warmed DNAse/RNAse free H_2O was used to elute RNA. ND-1000 Spectrophotometer (NanoDrop, Wilmington, DE) was used to determine the quality and quantity of RNA. Total RNA collected was then used immediately or stored at -80^0C.

For regular mRNA Realtime reverse transcription analysis, the The AgPath-ID One-Step RT-PCR Kit (Applied Biosystems/Life Techonology) was used following the manufacturer's protocol.

For miRNA quantification, two-step Realtime RT-PCR was performed. The Taqman microRNA Reverse Transcription Kit (Applied Biosystems/Life Techonologies) was used to reverse transcribe target miRNA in 10ng of total RNA to cDNA. The primers used for this reverse transcription step contain a stem-loop sequence and a small sequence complementary to the small single strand mature miRNA. After reverse transcription, Realtime PCR was performed to quantify miRNA originated cDNA.

Name	Assay ID/Sequence
panp63	Hs00978343_m1
ZEB1	Hs00232783_m1
ZEB2	Hs00207691_m1
Cyclophylin A	Hs99999904_m1
Dicer	Hs00229023_m1
Pri-miR205	Hs03302942_pri
miR205	000509
U6 snRNA	001973
LOC642587	Hs03405498_m1
SNAI2	Hs00161904_m1
CDH2	Hs00169953_m1
KRT5	Hs00361185_m1
KRT14	Hs03044364_m1
Pri1 forward primer	5’ AAGCAATTGCAGAACACCTG 3’
Pri1 reverse primer	5’ CACCCTCTCCCTTTGTCTAGG 3’
GAPDH forward primer	5’ ACCCAGAAGACTGTGGATGG 3’
GAPDH reverse primer	5’ GAGGCAGGGATGATGTTCTG 3’
P1 forward primer	5’ GCCTGCAGAAAGACCTCTCCAT 3’
P1 reverse primer	5’ GCACCTCTCAGCAAAGCTTCAG 3’
P2 forward primer	5’ TCCAGCCTGCATGTTGGTGCT 3’
P2 reverse primer	5’ CTGTTGCTGCTCTGGCCTCT 3’
P5 forward primer	5’ CCTCAGGTCTATGGTAGATGCCCAGG 3’
P5 reverse primer	5’ GCCACATGGTCTCTCAGATATTGCCAGC 3’

Table 2: Information of primers used in the study

RNA expression is calculated by comparative ΔΔCt method and displayed as relative quantity (RQ) ± RQ max and RQ min. Regarding endogenous control, Cyclophilin A was used for mRNA expression and U6snRNA was used for miRNA expression. All Taqman primers and probes were purchased from Applied Biosystems/Life Techonologies. The catalog numbers are listed in Table 1. All PCR reactions were performed using either the ABI PRISM 7500 or the StepOne Plus PCR systems (ABI).

3. Invasion assay

BD Biocoat™ Matrigel™ Invasion Chambers (BD Biosciences, San Jose, CA, 354480) were used to access the invasive capacity of cells *in vitro*. This assay was developed based on the classical Boyden chamber assay introduced by Boyden for the analysis of leukocyte chemotaxis in 1962 (184). The invasion chambers consist of a companion plate and a cell culture insert. The bottom of the insert is a 8-micron pore size PET membrane with a thin layer of MATRIGEL Basement Membrane Matrix. Matrigel is the sterile extract of the EHS tumor that share great similarity with the basement membrane in components and structure. The discovery of matrigel dates back in 1970s when a group of scientists were studying the components of the abundant extracellular matrix (ECM) formed by EHS (Engelbreth-Holm-Swam) tumors, a benign mouse chrondosarcoma. They discovered that EHS tumors provide a large amount of basement membrane components including collagen type IV, perlecan, laminin, entactin and growth factors. Therefore, extract of EHS tumors which is cell-free and sterile – Matrigel – has been applied widely as a reconstituted form of basement membrane in vitro (185). Matrigel provides a barrier for non-invasive cells while presenting an appropriate material for invasive cells to penetrate in before passing through the membrane. This in vitro

setup mimics the real situation in bladder tumors where tumor cells need to degrade the basement membrane components to penetrate into the muscle.

Cells in serum-free medium were seeded into invasion inserts (UC6: $25x10^3$ cells/insert, UC3: $15x10^3$ cells/insert) in triplicate. 3T3 conditioned medium was added in each well. This conditioned medium served as the chemoattractant to attract cells in the inserts. The chambers were incubated at 37 °C in a 5% CO_2 incubator for 48 hrs. After incubation, the membrane surfaces facing the chemoattractant were fixed in 1% glutaraldehyde, and stained with gentian violet. Micrographs of the whole membranes were captured using an inverted microscope. Invaded cells stained in violet were counted using ImageJ software (Bethesda, MD).

4. Protein overexpression and gene knockdown

Transient KD of ΔNp63: The ΔNp63 specific siRNA (5' ACAAUGCCCAGACUCAAUU 3') was designed based on a previous publication (186) and was synthesized by Dhramacon/Thermo Scientific. The non-targeting siRNA was also from Dhramacon (D-001810-10-20). Lipofectamine RNAiMAX (Invitrogen/Life Techonologies, 13778-075) was used to transfect siRNAs into cells. Transfection procedure is following the manufacturer's instruction. Similar to transient overexpression experiment, after 48-72 hours, cells were harvested for RNA and protein extraction

Stable KD by virus infection: The panp63 lentiviral shRNA construct (V3LHS_397885) that targets all p63 isoforms and the pGIPZ empty vector (RHS4339) were purchased from Open Biosystems. To generate virus containing shRNA constructs, we transfected the constructs into 293T cells together with the packaging plasmid and the envelop plasmid. After 48 hours, the shRNA constructs were packaged completely into infectious but replication

competent viral particles that escape into the 293T culture medium. 293T culture medium was collected and filtered to avoid any 293T cell residues. Virus concentrated from 293T medium was added on BC cells together with polybrene to increase the efficiency of infection. After 48 hours, infected cells were ready for puromycin selection. Since the backbone of the two constructs contains puromycin resistant sequence, infected cells can survive in medium supplemented with puromycin. Besides, the green fluorescent protein (GFP) encoded sequence in the backbone also helps in sorting out the infected cells by fluorescence-activated cell sorting (FACS) ARIA flow cytometer (BD Biosciences). Cells containing the NT- or p63shRNA construct were enriched in the pooled population based on their high expression of green fluorescence protein (top 30%). After sorted, infected cells were maintained in medium supplemented with puromycin (4μg/ml). 24 hours before using cells for experiments, puromycin containing medium were replaced by regular medium free of puromycin.

Transient overexpression: Lipofectamine 2000 (Invitrogen/Life Techonologies, 11668-019) was used to transfect TAp63α (Open Biosystems/Thermo Scientific, Lafayette, CO, EHS1001-7380111) and ΔNp63α (GeneCopoeia, Rockville, MD, EX-Z5740-M02) into cells following the instructions provided by the manufacturer. After 48-72 hours, cells were harvested for RNA and protein extraction.

Stable overexpression by virus infection: The ΔNp63α sequence was cut out from the ΔNp63α-pReceiver-M02 expression vector (Genecopoeia, EX-Z5740-M02) and cloned into pCDH-CMV-MCS-EF1-puromycine backbone (System Biosciences). Pre-miR-205 vector was from System Bioscience (Mountain View, CA, CD511B-1). Virus packaging and infection were performed as described. The backbones of these two constructs contain puromycin resistant sequence. As a result, infected cells were selected in puromycin-supplemented medium.

Virus production, virus infection were performed in the MD Anderson Vector Core. Cell sorting was performed at MD Anderson FACS Core.

5. Immunoblotting (IB)

After washed once with PBS, cells were scraped out of 10-cm dishes and centrifuged to collect cell pellets. Whole cell lysis buffer (50 mM Tris-HCl, pH 7.4, 150 mM NaCl, 5 mM EDTA, 25 mM NaF, 1% Triton-X 100, 1% Nonidet P-40, 0.1 mM Na_3VO_4, 12.5 mM β-glycerophosphate, 1 mM PMSF, and complete protease inhibitors) were added to the cell pellets. Cell lysis were proceeded on and end-to-end rotator at 4^0C in 1 hour. Whole cell lysates were clarified at 13,000 rpm for 5 min before resolved on SDS-PAGE gels. Gel concentration depends on the molecular weight of target proteins. 6% SDS-PAGE gels were used for ZEB1 (200 kDa), 8% SDS-PAGE gels were for N-Cadherin (135 kDa), 10% SDS- polyacrylamide gel electrophoresis (PAGE) gels were for p63, and 12% SDS-PAGE gels were for Slug (34 kDa). Proteins were transferred onto nitrocellular membranes at 100 Volt in 1.5-2 hours. Primary antibody incubation was performed at 4^0C on the shaker overnight. Secondary antibody incubation was at room temperature on the shaker for 1 hour. Antibodies used for IB were anti-panp63 (clone 4A4, Santa Cruz Biotechnology, Santa Cruz, CA), anti-ZEB1 (Cell Signaling, Boston, MA), anti-N-cadherin (Life Technologies), and anti-Slug (Santa Cruz Biotechnology). Detailed information about the antibodies used in this study is in Table 3.

6. Flow cytometry

Since the targets for cell surface staining flow cytometry are two adhesion molecules: N-cadherin and P-cadherin, 100mM EDTA was used to detach cells instead of Trypsin, which

can cleave adhesion molecules on the cell surface. Cells were washed once with PBS and then blocked in incubation buffer containing 0.5% bovine serum albumin – BSA. For N-cadherin detection, a direct staining method was employed using an allophycocyanin (APC)-conjugated anti-human N-cadherin antibody (R&D Systems, Minneapolis, MN, FAB6426A) following the company's protocol in which cells were incubated with the APC-conjugated antibody for 1 hour at room temperature, washed twice with PBS, resuspended in PBS and then analyzed by flow cytometer. Negative control for N-cadherin staining is APC-conjugated sheep IgG. For P-cadherin detection, indirect staining was performed using a polyclonal rabbit anti-P-cadherin antibody (Cell Signaling, Boston, MA, 2130) and Alexa Fluor 594-conjugated goat anti-rabbit IgG (H+L) (Invitrogen/Life Technology, A11037). Cells were incubated with the primary antibody for 1 hour at room temperature, washed twice with PBS, incubated with secondary antibody 30 minutes at room temperature, washed and resuspended in PBS, and then analyzed by flow cytometer. Negative control samples were stained with the secondary antibody alone.

Antibodies	Indication	Condition	Company	Catalog number
panp63 (4A4)	IB	1:1000 in 5% milk	Santa Cruz Biotechnology, Santa Cruz, CA	sc-8431
ZEB1	IB	1:1000 in 5% BSA	Cell Signaling, Boston, MA	3396
N-cadherin	IB	1:1000 in 5% milk	Invitrogen/Life Technologies, Grand Island, NY	33-3900
Slug	IB	1:1000 in 5% milk	Santa Cruz Biotechnology, Santa Cruz, CA	sc-15391
p53	ChIP	2ug	Millipore, Billirica, MA	17-613
Pol II	ChIP	1ug	Millipore, Billirica, MA	17-620
Normal mouse IgG	ChIP	1ug	Millipore, Billirica, MA	12-371B

Table 3: Information of antibodies used in the study

7. Chromatin-Immunoprecipitation (ChIP) Assay

The ChIP-IT-Express kit from Active Motif (Carlsbad, CA, 53009) was used to for the ChIP assay. Cells were grown in 15-cm dishes until 80% - 90% confluent. Cell fixation step

were performed in media containing 1% formaldehyde for 10 minutes at room temperature. This step allowed DNA cross-link to proteins such as histones, transcription factors and other DNA-associated proteins. The fixation step was stopped by adding the stop-fix solution containing Glycine. Cells were then scraped from the dishes and pelleted by centrifugation for 10 minutes at 2,500 rpm at 4^0C. Cell lysis buffer supplemented with protease inhibitor cocktail and PMSF was used to lyse cells for 1 hour on ice. Douncing on ice with 50 strokes using a dounce homogenizer was applied to aid in nuclei releases. Chromatin in nuclei pellet was then subjected to enzymatic fragmentation. The enzymatic shearing cocktail (200 U/ml) was added to the pre-warmed nuclei in digestion buffer, followed by 20 minutes incubation at 37^0C. Shearing reaction was stopped by adding ice-cold 05M EDTA. Shearing efficiency was examined by DNA gel electrophoresis. Optimized shearing reaction will yield bands between 200-1500 bp. Appropriately sheared chromatin were subjected to immunoprecipitation using antibodies of interest and magnetic beads. Detailed information regarding antibodies used for ChIP is listed in Table 3. For each ChIP reaction, 1-8 µg of antibody was used. Chromatin were the eluted from the magnetic bead – antibody – protein complex and DNA fragments was released after reverse cross-linked at 65^0C for 4 hours. Proteinase K was used to eliminate protein in the final products. Precipitated DNA was quantified and normalized to DNA input by quantitative real-time PCR with SYBR green qPCR master mix (Applied Biosytems/Life Techonologies). Sequence of primers used for ChIP was listed in Table. The relative enrichment of target sequences precipitated by antibody bound magnetic beads is demonstrated as RQ value ($RQ = 2^{-\Delta Ct}x100$; $\Delta Ct = Ct(ChIP) - Ct(Input)$). Real-time-PCR reactions were performed in triplicate and the results are presented as mean ± SD for the triplicate samples. Data are representative of two to three independent experiments.

8. Nuclear run-on

Nuclear run-on experiments were proceeded as described in the short technical report (187) with minor modification. Briefly in this experiment, cellular nuclei were isolated and induced for transcription to happen, nascent transcribed RNA was isolated and analyzed. To collect nuclei, cell pellets was lysed in mild lysis buffer (10mM Tris-HCl, pH 7.4, 3mM $MgCl_2$, 10mM NaCl, 150mM sucrose and 0.5% Nonidet P-40) to break the cell membrane but leave the nuclear membrane intact. Nuclei were collected by centrifugation and in vitro RNA synthesis was performed at 29^0C for 30 minutes in the transcription buffer (100mM KCl, 20mM Tris-HCl, pH 8.0, 5mM $MgCl_2$, 4mM dithiothreitol (DTT), 200mM sucrose and 20% glycerol). Materials for RNA synthesis including rATP, rGTP and rCTP (Epicenter Biotechnologies, Madison, WI, RN02825) were also added to the transcription buffer. Especially, instead of using regular rUTP, biotin-16-UTP (Epicenter Biotechnologies, BU6105H) was provided in the transcription buffer. Reactions were then halted by adding a "stop" buffer containing 250mM CaCl2, and 10 units/µl DNase I (Roche Applied Science, Indianapolis, IN) which aids in eliminating DNA in the reaction. Nuclei were then lysed and RNA was extracted using mirVana™ miRNA Isolation Kit (Ambion/Life Techonologies). Biotin labeled nascent transcribed RNA was precipitated using magnetic beads coated with streptavidin (Dynabeads® M-280 Streptavidin, Invitrogen/Life Techonologies, 112.05D). Reverse transcription was performed using the high capacity cDNA reverse transcription kits (Applied Biosystems/Life Techonologies) to generate cDNA from the precipitated RNA. Fast SYBR Green master mix (Applied Biosystems/Life Techonologies) was used for qPCR analysis. Primers for the nuclear run-on experiment are described in Table 1.

9. Human specimens

Flash frozen tissue from 98 patients was obtained from the MD Anderson Genitourinary Cancer tissue bank. Samples were collected by microdissection focusing on areas with at least 80% tumor concentration to enrich the tumor content in the samples. All samples were examined by a pathologist to ensure the tumor enrichment. All patients whose samples were used in this study had previously been signed informed consent allowing collection of their tissue and clinical data in our genitourinary research database. Patients were classified as muscle-invasive if their tumors had grown into the muscularis propria (stage ≥T2); otherwise, they were classified as superficial (non muscle-invasive) (stage Ta or T1). mirVana™ miRNA Isolation Kit (Ambion/Life Techonologies) was used to extract total RNA from all the samples

10. Statistical Methods

mRNA expression data from qRT-PCR were used to analyze the correlations between p63 and mir205 and to evaluate the association between mir205 and overall survival (OS) and disease-specific survival (DSS). Spearman's rho coefficient analysis was used to determine the correlations among expression of markers. The cutoff point to classify high and low mir205 was defined by regression tree analysis. The Kaplan-Meier curves were generated to demonstrate the survival distribution of patients based on their mir205 expression characterized as high and low. We used the log-rank test to compare survival distributions between groups. The Cox proportional hazards model was used to assess the effects of multiple markers on DSS and OS, adjusting for other important covariates. All p-values presented are 2-sided. p-values less than 0.05 were considered to be statistically significant. Statistical analyses were performed using Splus 7 (Insightful Corp, Seattle, WA).

CHAPTER 3:

RESULTS

1. ΔNp63α is the most abundant isoform in human bladder cancer (BC) cell lines

p63 is a transcription factor with multiple downstream targets. Six isoforms of p63 can have the same or different targets and the effects that these isoforms have on their downstream targets can be additive or opposite. As a result, we first characterized the p63 isoforms in a panel of human bladder cancer cell lines (n=28) using quantitative real time PCR (qRT-PCR) with the panp63 primer that recognize all 6 isoforms as well as the ΔN- and TA- primers that are specific for the ΔN- and the TA- isoforms, respectively. Interestingly, the expression pattern of ΔNp63 and panp63 in all the cell lines tested (Fig. 10A a and b) are very similar, while the expression pattern of TAp63 (Fig. 10A c) is not very much similar to that of ΔN- and panp63. We also compare the expression of TA- and ΔNp63 in each cell lines. Provided that primer efficiency affect the sensitivity of PCR reactions, we characterized the efficiency of the TA- and ΔNp63 primer as described in (reference) and calculated the relative quantity (RQ) value based on normalized primer efficiency. PCR results show that the expression of ΔNp63 (black bar) is substantially higher than that of TAp63 (empty bars) in majority of the cell lines (Fig. 10A d). Moreover, panp63 and ΔNp63 cluster together while TAp63 is separated from the other two in the heatmap generated from the PCR data (Fig. 10B). All of these data clearly show that ΔNp63 is the most abundant isoform group on BC cell lines.

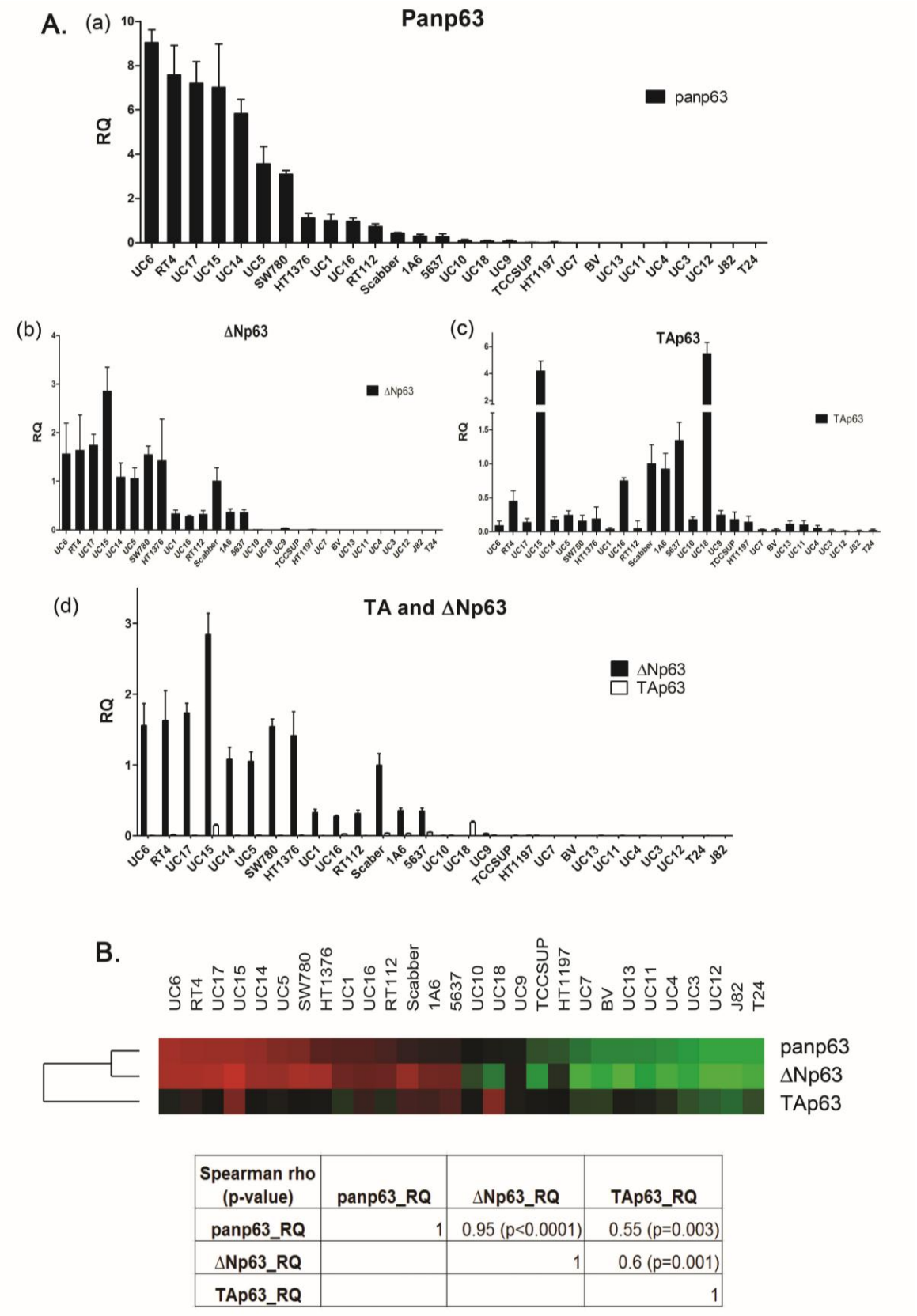

Spearman rho (p-value)	panp63_RQ	ΔNp63_RQ	TAp63_RQ
panp63_RQ	1	0.95 (p<0.0001)	0.55 (p=0.003)
ΔNp63_RQ		1	0.6 (p=0.001)
TAp63_RQ			1

Figure 10: ΔNp63 is the predominant isoform group in BC. (A) qRT-PCR quantification of panp63 (a), ΔNp63 (b), TAp63 (c), and TA-and ΔNp63 (d) in BC cell lines (n=28). Bars display the relative quantities (RQ) of gene expression ± RQ max and RQ min. (B) Heatmap generated from the RQ value of panp63, ΔNp63, TAp63 mRNA expression measured by qRT-PCR. Spearman correlation coefficient analysis results demonstrate the strong correlation between panp63 and ΔNp63. The correlation between panp63 and TAp63, ΔNp63 and TAp63 are statistical significant. However, the correlation between panp63 and ΔNp63 is the strongest.

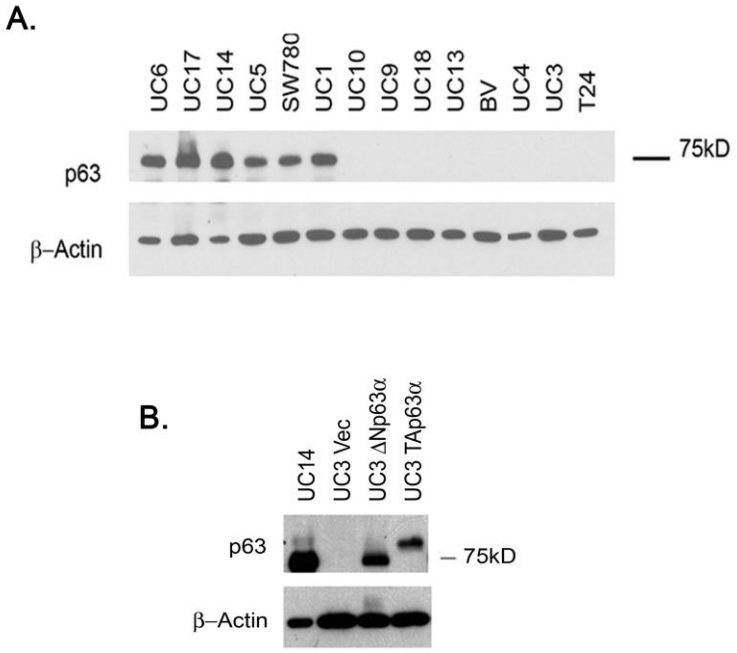

Figure 11: ΔNp63α is most abundant isoform in BC. (A) IB for p63 expression in BC cell lines (n=14). The 4A4 p63 antibody recognizes all p63 isoforms. (B) Molecular weight of ΔNp63α and TAp63α isoform. P63 protein in UC14 cell line migrates to the same position with ΔNp63α isoform.

To confirm the expression of p63 at the protein level, the monoclonal mouse anti-p63 antibody (clone 4A4) was used to detect the protein expression of all six p63 isoforms in 14 representative cell lines. Consistent with mRNA expression data, cell lines with high p63 mRNA show high p63 protein level identified by a strong band migrating at 75kDa whereas cell lines with low p63 mRNA show low or undetected p63 protein level (Fig. 11A). Among six p63 isoforms, the molecular weight of ΔNp63α, TAp63α and TAp63β are approximately 75kDa (188). Since ΔNp63 is the most abundant group of isoforms in BC cell lines, we expect thatΔNp63α is the isoform responsible for the 75kDa band. To test this idea more directly, we overexpressed TAp63α and ΔNp63α in UC3, a cell line with very low endogenous p63 expression, and examined p63 expression by the 4A4 antibody (Fig. 11B). The Western blot (WB) result clearly verify that the 75kDa band is ΔNp63α.

In summary, mRNA and protein expression analysis demonstrate that ΔNp63α is the most abundant isoform in BC cell lines.

2. ΔNp63α inhibits epithelial-mesenchymal transition (EMT)

Our previous publications reveal a correlation between ΔNp63 and E-cadherin in BC cell lines (n=15) as well as in human primary tumors (145,189), suggesting that ΔNp63 associates with the epithelial phenotype. In addition, p63 is well known for its role in epithelial stem cell homeostasis (190,191). Interestingly, stem cell properties are identified in cells that have undergone EMT (72), indicating that messenchymal cells possess stemness. As a result, the role of p63 in EMT becomes an attractive topic to explore. Our first step to learn about p63 and EMT was to characterize the expression of p63 and crucial EMT players (E-cadherin, ZEB1 and ZEB2) in our panel of 28 BC cell lines. Consistent with our previously published data, panp63, ΔNp63 and E-cadherin (CDH1) clustered together while ZEB1 and ZEB2 clustered together, demonstrating the close correlation between molecules in each cluster as well as the inverse correlation between the two clusters (Fig. 12).

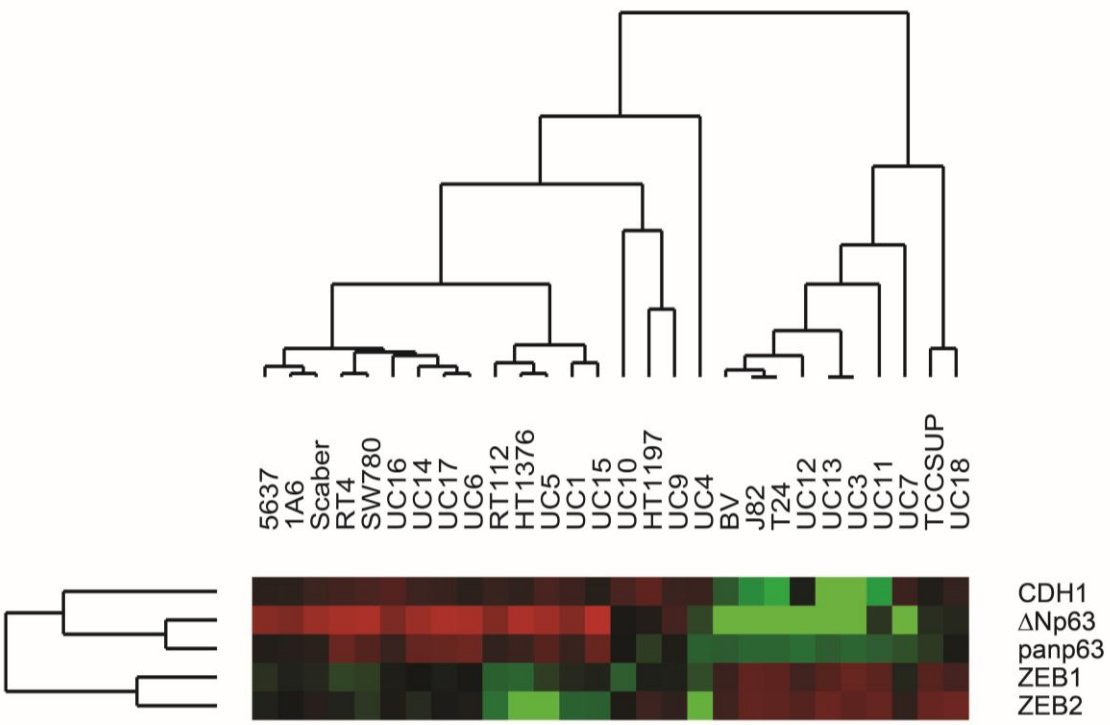

Spearman rho (p-value)	CDH1_RQ	panp63_RQ	ΔNp63_RQ	Zeb1_RQ	Zeb2_RQ
CDH1_RQ	1	0.54 (p<0.01)	0.48 (p<0.01)	-0.64 (p<0.001)	-0.52 (p<0.01)
panp63_RQ		1	0.93 (p<0.00001)	-0.54 (p<0.01)	-0.64 (p<0.001)
ΔNp63_RQ			1	-0.59 (p<0.001)	-0.7 (p<0.0001)
Zeb1_RQ				1	0.84 (p<0.00001)
Zeb2_RQ					1

Figure 12: Correlation between ZEB1and ZEB2; CDH1, ΔNp63 and panp63. Heatmap generated from the RQ value of CDH1, panp63, ΔNp63, ZEB1 and ZEB2 mRNA expression measured by qRT-PCR. Spearman correlation coefficient analysis results demonstrate the statistical significant correlation between CDH1, panp63 and ΔNp63; and between ZEB1 and ZEB2. There is no correlation between CDH1/panp63/ΔNp63 and ZEB1/2.

In order to study the functions of p63, we stably knocked down (KD) panp63 in an "epithelial" cell line (UC6) using a shRNA construct that targets all the p63 isoforms. As we had determined in Figs. 10 and 11 that ΔNp63α is the most abundant isoform of p63 in BC cells, we concluded that the shRNA construct mainly targets ΔNp63α. We also stably overexpressed ΔNp63α in a "mesenchymal" cell line, UC3, which has very low endogenous p63 expression. Strikingly, UC6 ΔNp63αKD cells acquired mesenchymal properties while UC3 ΔNp63α overexpressing cells gained epithelial traits. Regarding the morphology, UC6 ΔNp63αKD cells changed from the typical epithelial polygonal shape to elongated fibroblast-like shape. While wild-type (WT) and non-targeting (NT – cells infected with the empty vector) UC6 cells grew in discrete groups of cells, UC6 ΔNp63αKD cells tended to spread out and grow as individual cells. UC3 ΔNp63α overexpressing cells, on the other hand, obtained a morphology resembling "epithelial" cells (Fig. 13A). Regarding functional changes of cells undergoing EMT, an increase in invasion capacity is common. The loss of cell-cell and cell-basement membrane contact, the change in morphology to become more fibroblast-like, the loss of polarity, and the ability to degrade the extracellular matrix provide the cancer cells that have undergone EMT with the ability to invade through the basement membrane into the muscle and finally extravasate into the circulation. Therefore, we performed invasion assays to examine the invasive capacities of the ΔNp63α KD and overexpressing cells. In line with the effects of ΔNp63α modulation on morphology, the UC6 ΔNp63αKD cells exhibited an increase in their ability to invade through the matrigel membrane compared to the NT and the WT cells, whereas UC3 ΔNp63α overexpressing cells show a significant decrease in invasion compared to the empty-vector-infected (Vec) and the WT counterparts (Fig 13B).

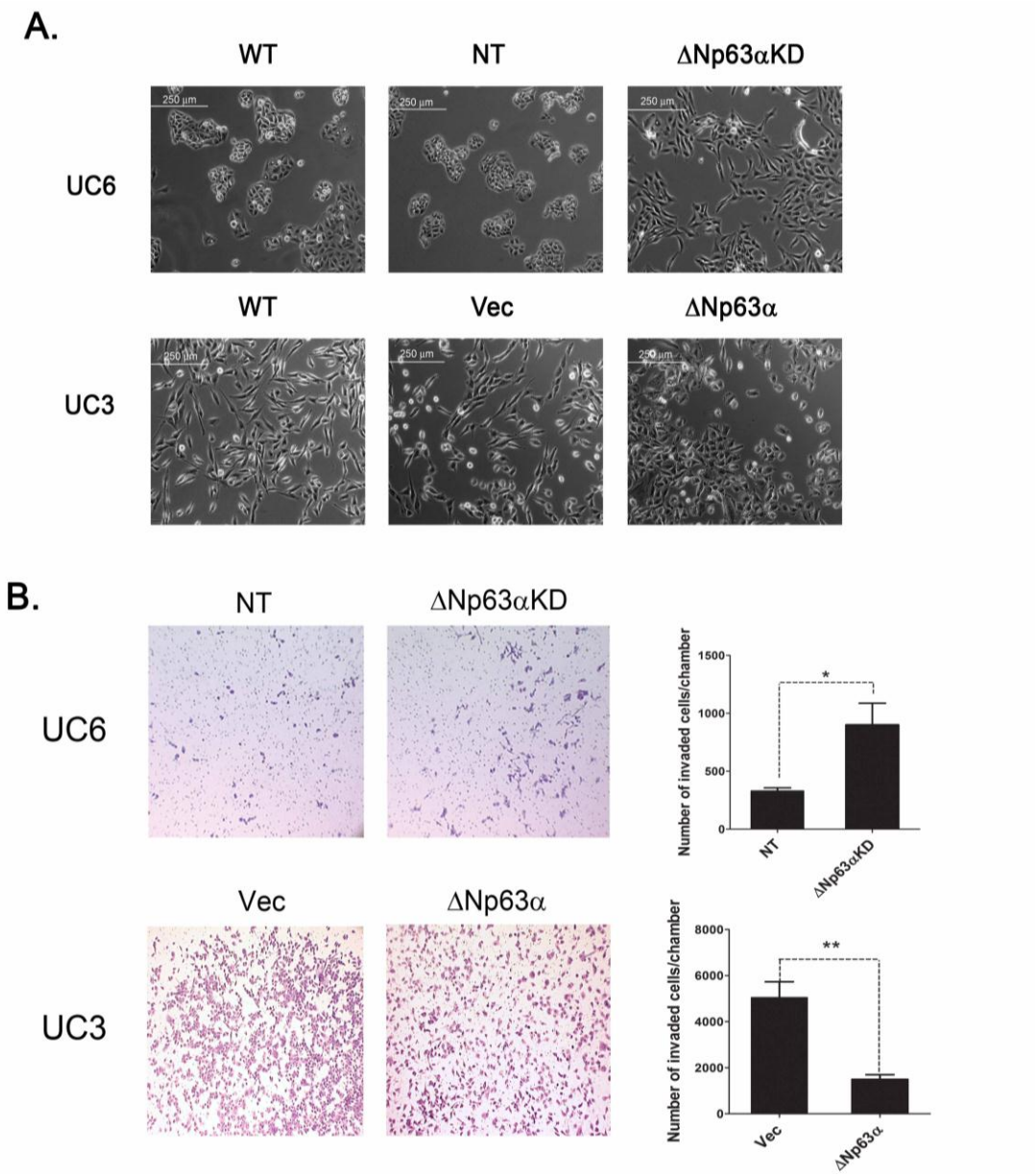

Figure 13: Modulation of ΔNp63α expression alters the morphology and the invasive capacity of BC cells. (A) Cell morphology observed under bright field microscope. ΔNp63αKD UC6 cells have mesenchymal morphology while ΔNp63α overexpressing UC3 have epithelial morphology. (B) Invasion assay demonstrating the effect of ΔNp63α modulation in the invasive capacity of cells. Pictures show cells that have invaded through the matrigel membrane of the invasion chamber. Quantification of invaded cells was demonstrated in the graph. Bars represent mean ± SEM from triplicate wells, Student t test, *$p<0.05$ and **$p<0.01$

At the molecular lever, EMT is usually characterized by the gain in the expression of messenchymal markers and the loss of epithelial markers. We examined the effect of modulating ΔNp63α on the expression of the epithelial markers CK-5 and CK-14, as well as the mesenchymal markers ZEB1/2, N-cadherin, and Slug in UC6 and UC3. Both qRT-PCR and immunoblotting revealed down-regulation of the epithelial markers (CK-5/14) and up-regulation of mesenchymal markers (ZEB1/2 and N-cadherin) in the UC6 ΔNp63α KD cells (expression reduced 80-90%). The opposite effects were observed in UC3 cells with enforced ΔNp63α expression (Fig. 14).

Cadherins are a family of calcium dependent transmembrane glycoproteins mediating cell-cell and cell-ECM adhesion. As major adhesion molecules, cadherins play crucial roles in development and carcinogenesis (192). P-cadherin specifically localize to the basal cells of normal bladder and normal prostate tissue (193,194). Therefore, P-cadherin is considered as a basal cell-specific epithelial marker, at least in the bladder and the prostate. N-cadherin, on the other hand, is a well-characterized mesenchymal marker. Increased expression of N-cadherin is commonly used as a marker of EMT (195). Interestingly, N-cadherin is not expressed in normal bladder urothelium but abnormally present in bladder tumors (193). To determine if ΔNp63α modulation affects EMT, we measured the presence of P-cadherin and/or N-cadherin protein on the surface of ΔNp63αKD UC6 cells by two-color cell surface staining and flow cytometry (FACS). UC6NT cells were double-positive for P- and N-cadherin, indicating an intermediate phenotype of cells partially undergoing EMT (1,196). ΔNp63α knockdown reduced the cell surface expression of P-cadherin and increased the surface expression of N-cadherin (Fig. 15A), generating a new population of cells that was negative for P-cadherin and positive of N-cadherin (Fig. 15B). These results demonstrate that ΔNp63α knockdown functionally

modulates the pool of P- and N-cadherin across the entire population of UC6 cells, promoting the mesenchymal phenotype.

Slug (SNAI2) is the only mesenchymal marker that did not conform to the pattern. Slug expression decreased in ΔNp63KD cells and increased in ΔNp63 overexpressing cells, indicating a hint of a pro-EMT effect of ΔNp63α (Fig. 14). We confirmed the effect of ΔNp63α in 4 other "epithelial" BC cells: UC14, UC17, UC5, and SW780. With 70-80% KD efficiency, a decrease in ΔNp63α also resulted in a decrease in Slug expression (Fig. 16). The effect of ΔNp63α on Slug expression suggests that ΔNp63α can facilitate the mesenchymal phenotype, which was reported in a recent publication (197). This observation helps explain the intermediate EMT phenotype of UC6 NT cells which strongly express ΔNp63α (Fig. 15). However, the overall impact of ΔNp63α on the morphology, invasion, and the majority of the epithelial and mesenchymal markers we tested clearly demonstrates that ΔNp63α suppresses EMT in BC cells.

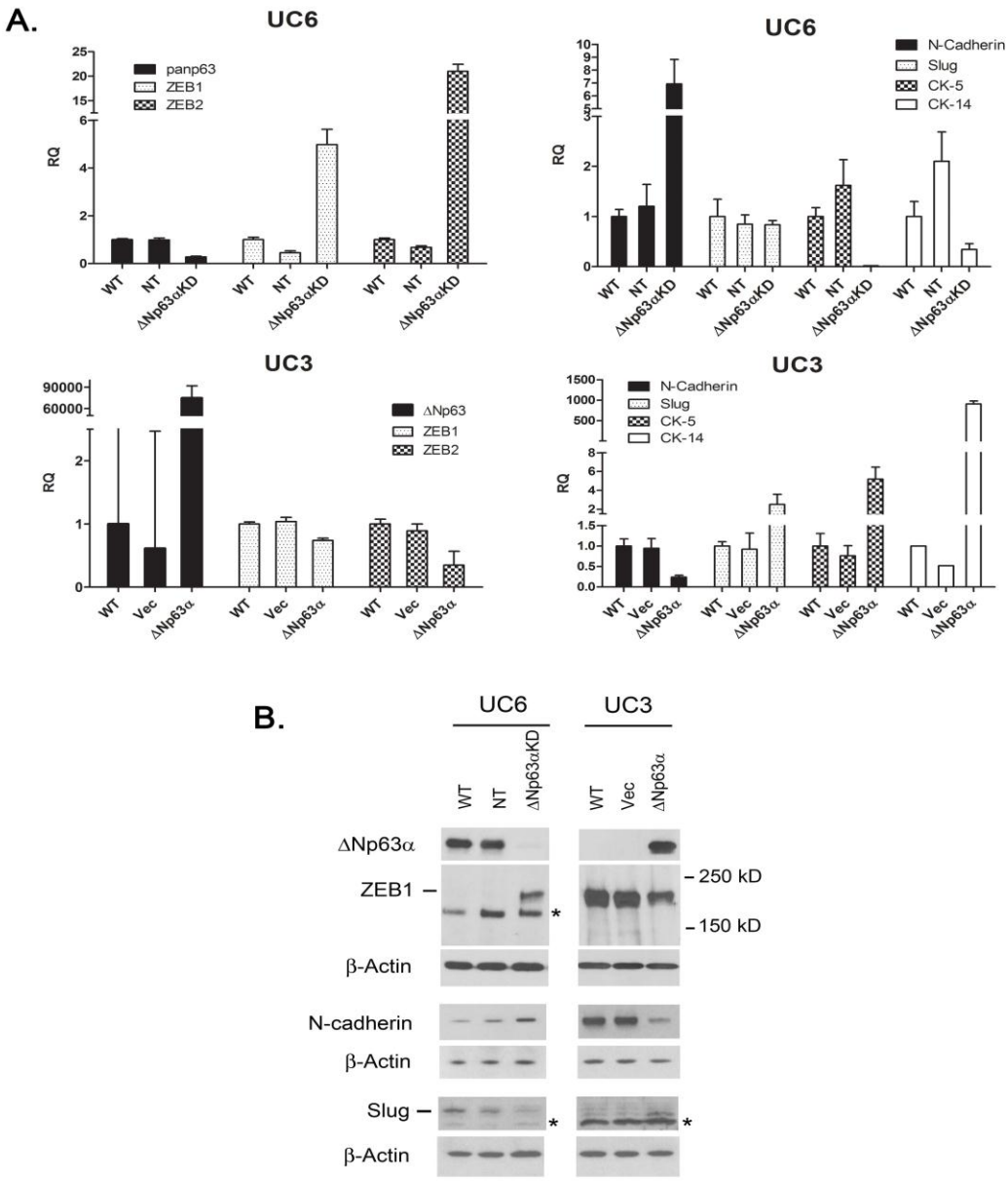

Figure 14: ΔNp63α modulation alters expression of multiple epithelial and mesenchymal markers. (A) qRT-PCR result showing mRNA expression of the epithelial markers (CK-5, CK14) and the mesenchymal markers (ZEB1/2, Slug, N-cadherin) as well as panp63 in ΔNp63α knockdown UC6 (ΔNp63αKD) and ΔNp63α overexpressing UC3 cells. Bars show the RQ of gene expression ± RQ max and RQ min. (B) IB showing protein expression of the mesenchymal markers (ZEB1, N-cadherin and Slug) and ΔNp63α in ΔNp63α knockdown UC6 (ΔNp63αKD) and ΔNp63α overexpressing UC3 cells. * denotes non-specific bands.

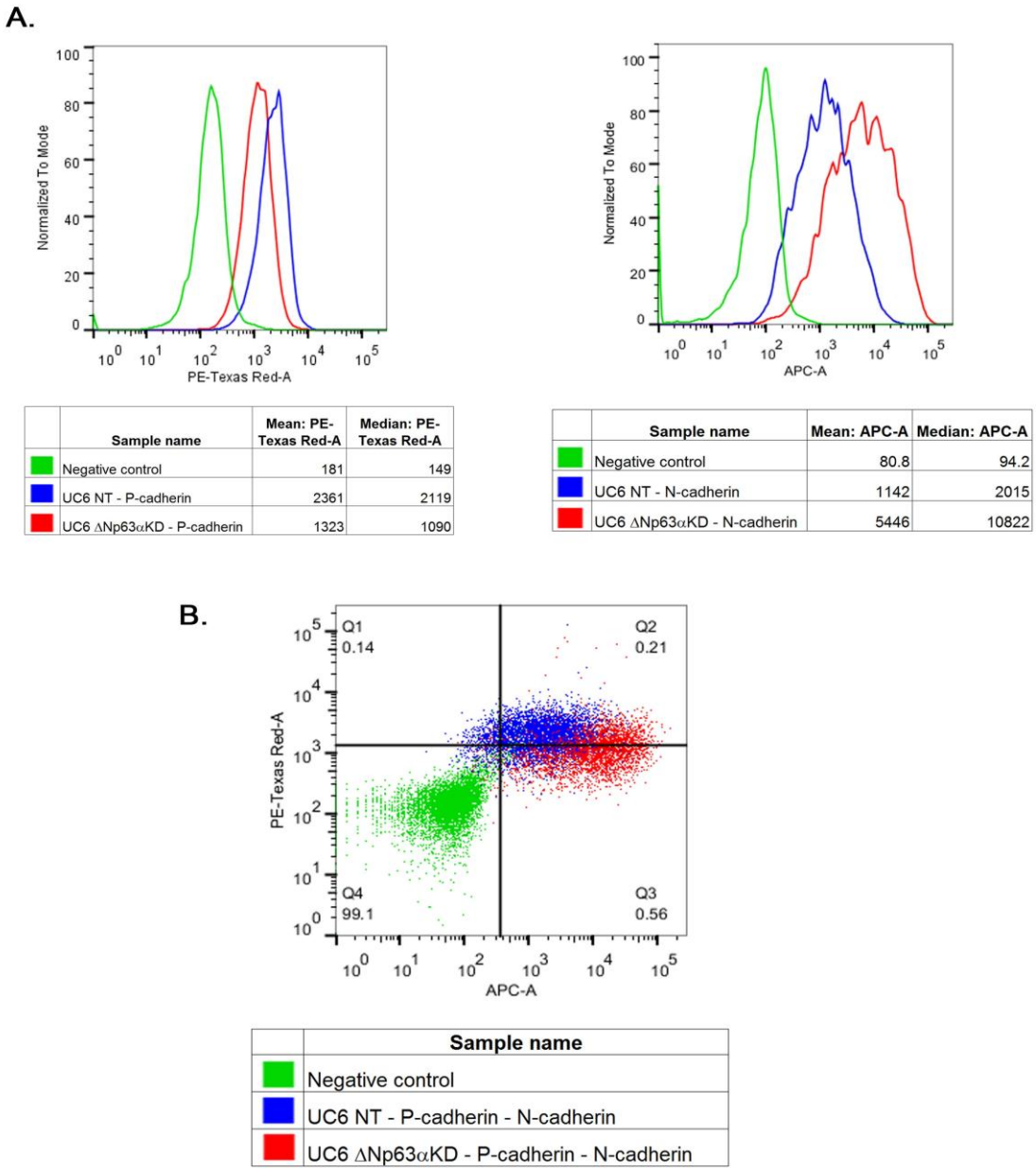

	Sample name	Mean: PE-Texas Red-A	Median: PE-Texas Red-A
	Negative control	181	149
	UC6 NT - P-cadherin	2361	2119
	UC6 ΔNp63αKD - P-cadherin	1323	1090

	Sample name	Mean: APC-A	Median: APC-A
	Negative control	80.8	94.2
	UC6 NT - N-cadherin	1142	2015
	UC6 ΔNp63αKD - N-cadherin	5446	10822

	Sample name
	Negative control
	UC6 NT - P-cadherin - N-cadherin
	UC6 ΔNp63αKD - P-cadherin - N-cadherin

Figure 15: ΔNp63α knock down reduces P-cadherin and induces N-cadherin on the cell surface. (A) cell surface P-cadherin (left) and N-cadherin (right) measured by flow cytometry. P-cadherin was labeled with Alexa Fluor 594 and N-cadherin was labeled with allophycocyanin (APC). Statistical analysis shows the differences in surface protein expression by mean and median fluorescence intensity. (B) Dual color staining for both P- and N-cadherin in the same samples. The negative control was used to set the gate for each target protein.

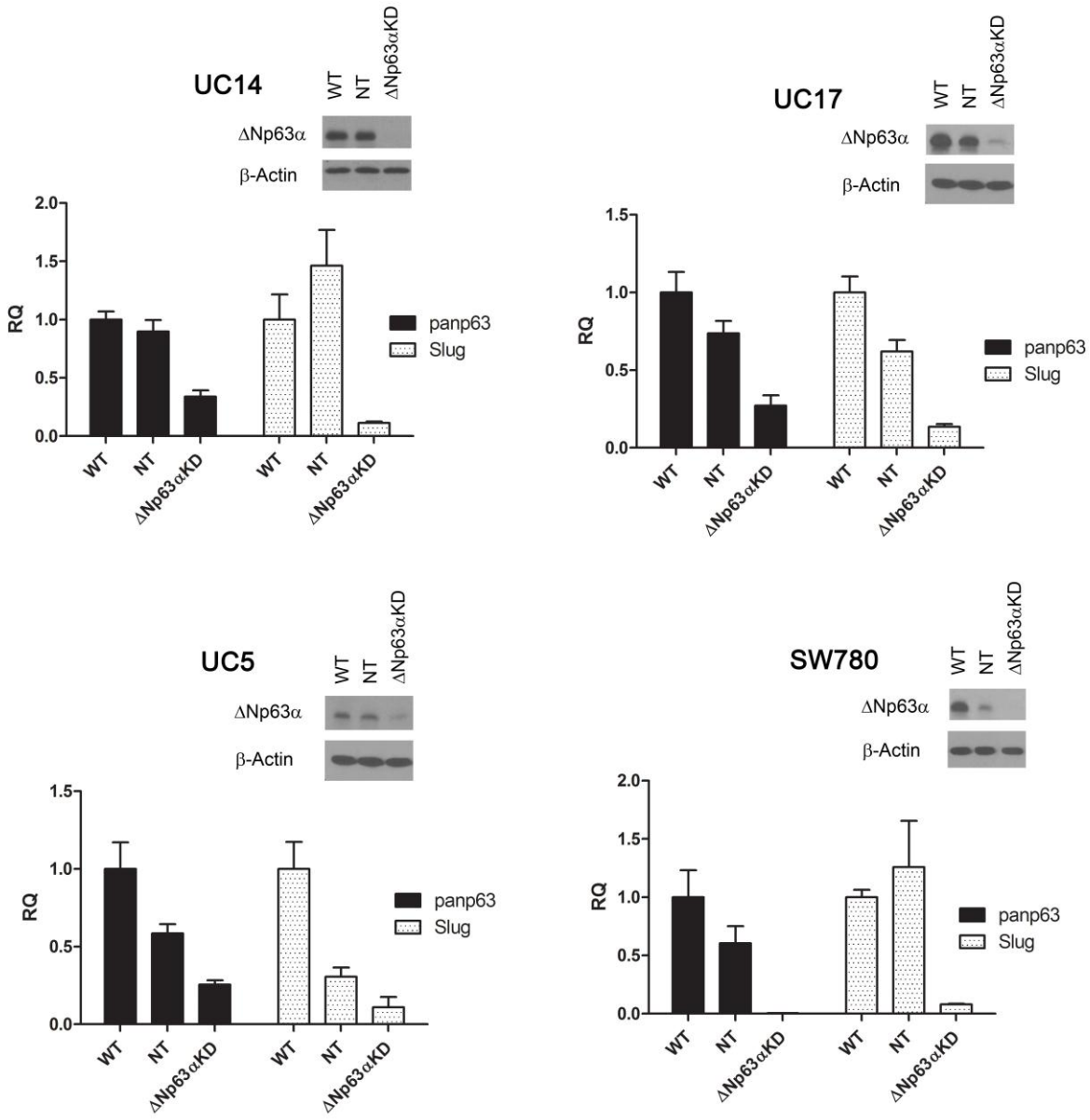

Figure 16: ΔNp63α knockdown results in downregulation of Slug. qRT-PCR results demonstrating down regulation of Slug mRNA expression in four ΔNp63αKD BC cell lines. The bars show the RQ of gene expression ± RQ max and RQ min.

3. ΔNp63α expression strongly correlates with the expression of the primary and mature forms of miR-205 in BC cell lines and primary tumors

The observation that ΔNp63α suppressed ZEB1/2 expression encouraged us to explore the relationship between these molecules. Since p63 can bind to p53 response elements (p53REs) to regulate the expression of its downstream targets, we first searched for p53REs on the promoter regions of ZEB1/2 but failed to find any, indicating that p63 may indirectly regulate the expression of ZEB1/2. It is now well known that the mir200 family functions as suppressors of ZEB1/2. In 2010, Mien-Chie Hung's group reported that p53 regulates EMT by inducing miR200c (68). We therefore measured the expression of mir200 family members in the UC6 and UC14 ΔNp63αKD cells but did not observe downregulation of miR200c or any other miR200 family members in either of the cell lines. Therefore, we carefully examined gene expression profiling data (Illumina HT12V4 chips) obtained from the WT, NT and ΔNp63KD UC6 and UC14 cells to look for changes in molecules potentially involved in EMT regulation. Interestingly, we found out that the primary form of miR-205 was down regulated in both ΔNp63KD cell lines. Because miR-205 is similar to the miR200 family in terms of its ability to bind to the ZEB1/2 mRNAs and inhibit their expression (33,35), we decided to focus our research on defining the relationships among p63, miR-205 and ZEB1/2.

Strikingly, gene expression profiling data of our BC cell lines panel revealed a strong correlation between the expression of p63 and the primary form of miR-205. By performing qRT-PCR using panp63, ΔNp63 primers and the primers specific for the primary (pri-) and the mature forms of miR-205, we confirmed the strong correlation among these molecules. A heatmap generated using the relative quantity (RQ) values of gene expression clearly showed the correlation in the expression patterns of these molecules in BC cell lines. Statistical analysis using Spearman's rho coefficients showed the significance in the correlation among these

molecules (Spearman rho>0.8, p<0.0001) (Fig. 17A). In general, after being transcribed by RNA Polymerase II to generate the primary form, microRNAs go through multiple steps of the microRNA processing to become mature microRNA. Any dysregulation of microRNA processing can result in abnormal expression of mature microRNAs. The similarity in expression patterns of the primary and mature forms of miR-205 suggests that this microRNA is regulated mainly at the transcription step rather than the processing steps (Fig. 17B).

The similarity in expression patterns of p63 and miR-205 was also observed in primary bladder tumors. Specimens from 98 patients including both superficial (n=32) and muscle invasive (n=66) bladder tumors were examined for expression of panp63 and mature miR-205 by qRT-PCR. Statistical significant correlation (Spearman rho=0.44, p<0.00001) was detected (Fig. 18), suggesting the co-expression of p63 and miR-205 in the tumors.

The correlation in p63 and miR-205 expression in BC cell lines and primary bladder tumors, identified by gene expression profiling and qRT-PCR, strongly implicates p63 in transcriptional regulation of miR-205. As determined in Fig. 10, Fig. 11 and previous publications (143,145) that established that ΔNp63α is the major isoform expressed in BC cell lines and primary tumors, we hypothesized that ΔNp63α is the isoform involved in transcriptional control of miR-205.

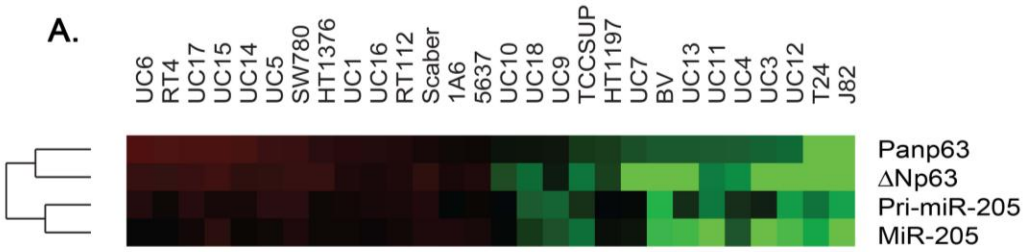

Spearman rho (p-value)	panp63_RQ	DNp63_RQ	Pri-miR205_RQ	miR205_RQ
panp63_RQ	1	0.95 (p<0.0001)	0.85 (p<0.0001)	0.79 (p<0.0001)
DNp63_RQ		1	0.81 (p<0.0001)	0.83 (p<0.0001)
Pri-miR205_RQ			1	0.82 (p<0.0001)
miR205_RQ				1

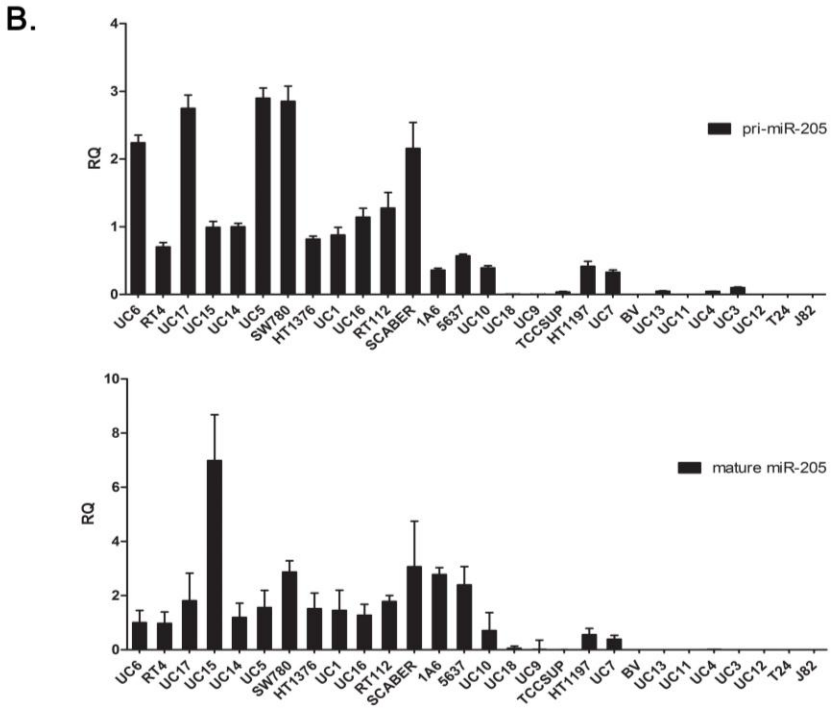

Figure 17: Correlation between p63 and pri-/mature miR-205. (A) Heatmap generated from qRT-PCR data showing the strong correlation among panp63, ΔNp63, pri-miR-205 and mature miR-205 in BC cell lines (n=28). Statistical analysis using Spearman method confirms the statistical significant of the correlation. (B) qRT-PCR data in bar graph demonstrating the strong correlation between the primary form and the mature form on miR-205. Bars show the RQ of gene expression ± RQ max and RQ min.

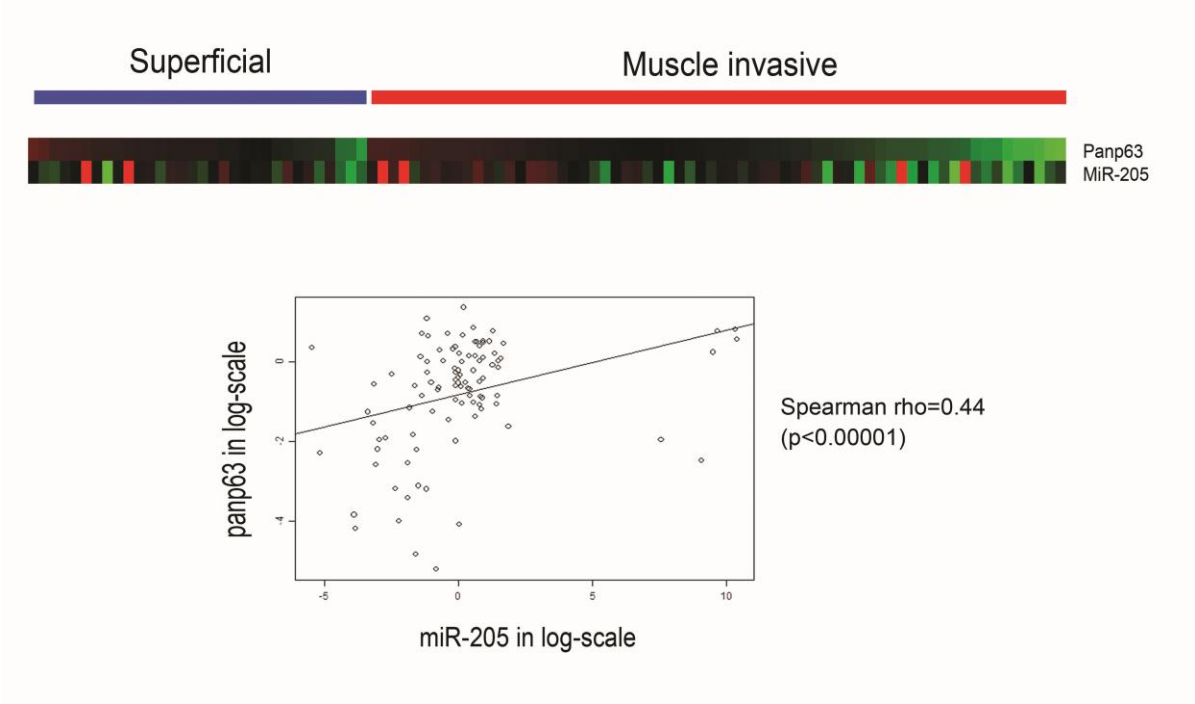

Figure 18: Correlation between p63 and miR-205 in patients. Heatmap generated from qRT-PCR data showing the correlation among panp63 and mature miR-205 in BC patient samples (n=98). Statistical analysis using Spearman method confirms the statistical significance of the correlation.

4. ΔNp63α regulates ZEB1/2 expression by through modulation of miR-205

Since ΔNp63α modulation resulted in inverse changes in ZEB1/2 and ΔNp63α expression correlated with miR-205, a negative regulator of ZEB1/2, we examined the expression of miR-205 in ΔNp63αKD and overexpressing cells. As we expected, mRNA expression of primary and mature forms of miR-205 decreased in ΔNp63αKD UC6 and increased in ΔNp63α overexpressing UC3 cells (Fig. 19A). This qRT-PCR result is consistent with the gene expression profiling data we had obtained with the UC6 ΔNp63αKD cells. We also checked miR-205 (primary and mature) expression in 4 other ΔNp63αKD cell lines (UC14, UC17, UC5 and SW780) and the obtained the same result, that down regulation of ΔNp63α decreased miR-205 expression (Fig. 19B).

Prolonged down-regulation of a gene by shRNA infection may have off-target effects. To validate the effect of ΔNp63αKD on mir-205, we transiently knocked down ΔNp63 in the UC6 cells using a ΔNp63-specific siRNA. The specificity and efficiency of the ΔNp63 specific siRNA was demonstrated by 70% decrease in ΔNp63 expression and no significant change in TAp63 expression. Similar to the effect of ΔNp63α stable KD, ΔNp63 transient KD also resulted in decreased expression of miR-205, demonstrating that miR-205 is indeed a downstream target of ΔNp63α (Fig. 20)

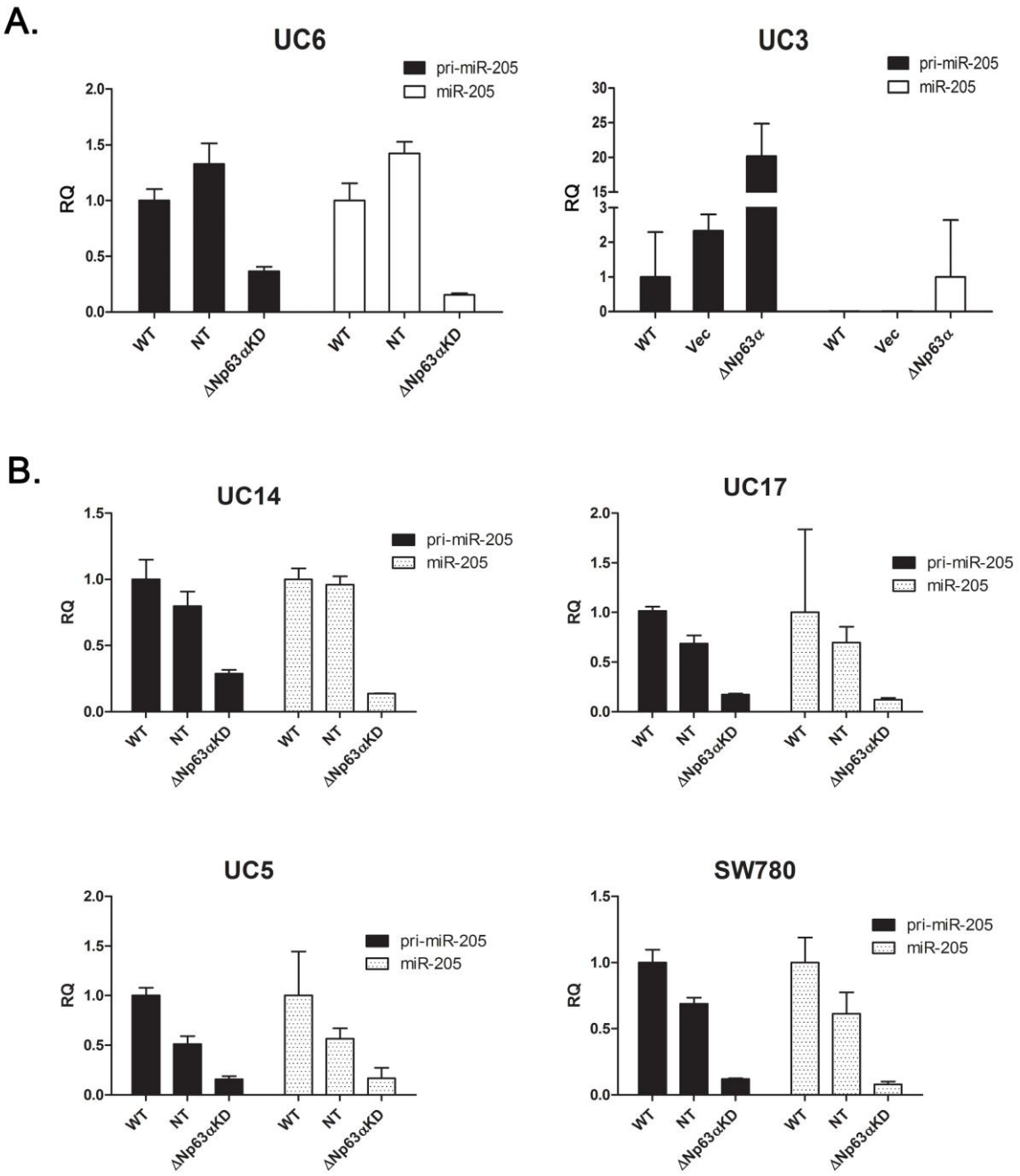

Figure 19: Expression of the primary and the mature form of miR-205 change in parallel with ΔNp63α alteration. (A) qRT-PCR results showing pri- and mature miR-205 are down-regulated or up-regulated in ΔNp63αKD UC6 or ΔNp63α overexpressed UC3, respectively. (B) Down-regulation of pri- and mature miR-205 when ΔNp63α is knocked down in four BC cell lines. Bars show the RQ of gene expression ± RQ max and RQ min.

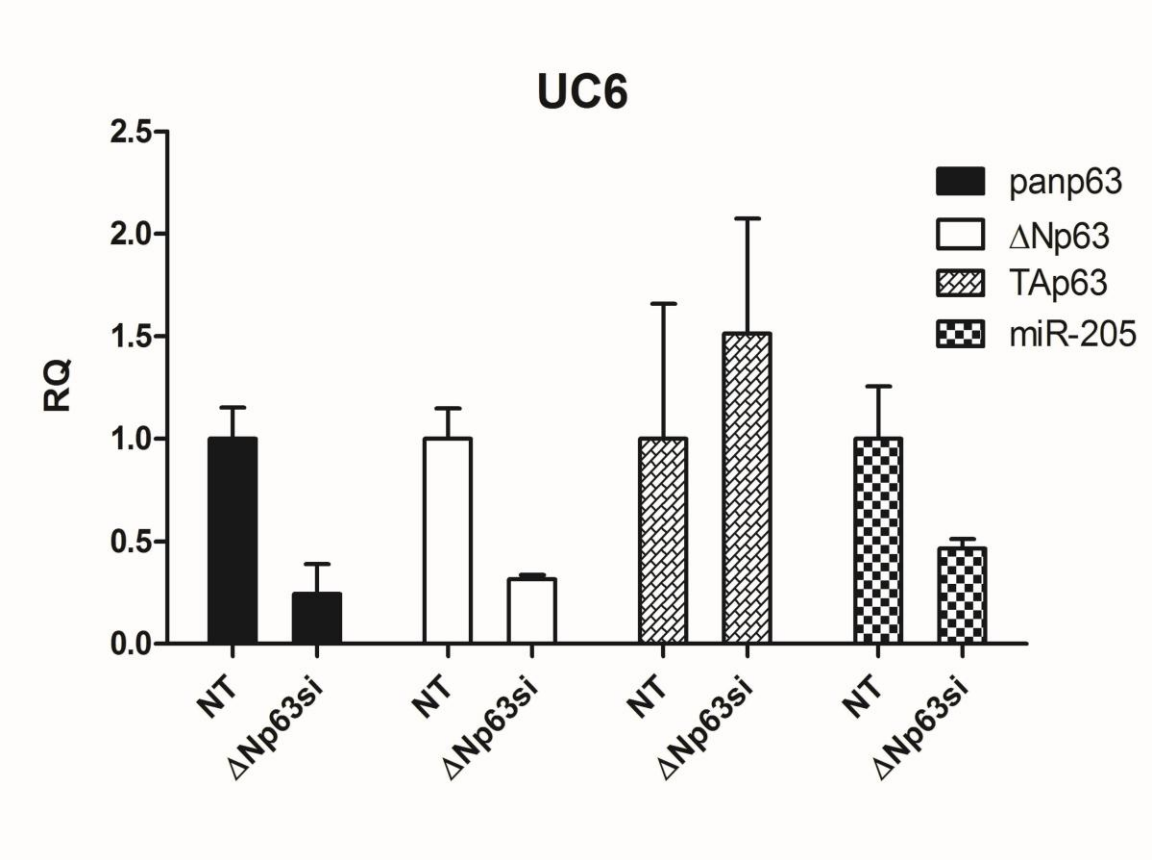

Figure 20: Down regulation of miR-205 in UC6 cells, in which ΔNp63 is transiently knocked down. qRT-PCR data show that the ΔNp63 transient knockdown is specific and that miR-205 expression is reduced in the KD cells compared to the cells transfected with the control siRNA. Bars show the RQ of gene expression ± RQ max and RQ min.

Even though miR-205 is known as a negative regulator of ZEB1/2, there is no report regarding this effect of miR-205 in BC. Therefore, we overexpressed the precursor form of miR-205 in ΔNp63αKD UC6 cells and examined the expression of ZEB1/2 to determine if decreased miR-205 mediates the effect of ΔNp63αKD on ZEB1/2 expression. The infection of virus carrying miR-205 precursor construct induced miR-205 expression in the UC6 ΔNp63αKD cells to 5 fold higher than the UC6 WT cells while the virus carrying the empty vector control did not affect miR-205 expression. p63 expression in the ΔNp63αKD UC6 cells infected with either empty vector or miR-205 virus remained lower than in the WT and NT cells (Fig. 21A). As we expected, overexpression of exogenous miR-205 largely reversed the induction of ZEB1/2 generated by ΔNp63αKD at both RNA and protein level (Fig. 21B). As ZEB1/2 are the two canonical EMT regulators, this result clearly proves the important role of miR-205 in mediating the effects of ΔNp63αKD on EMT. The relationship between ΔNp63α and EMT is generalized in Fig. 22

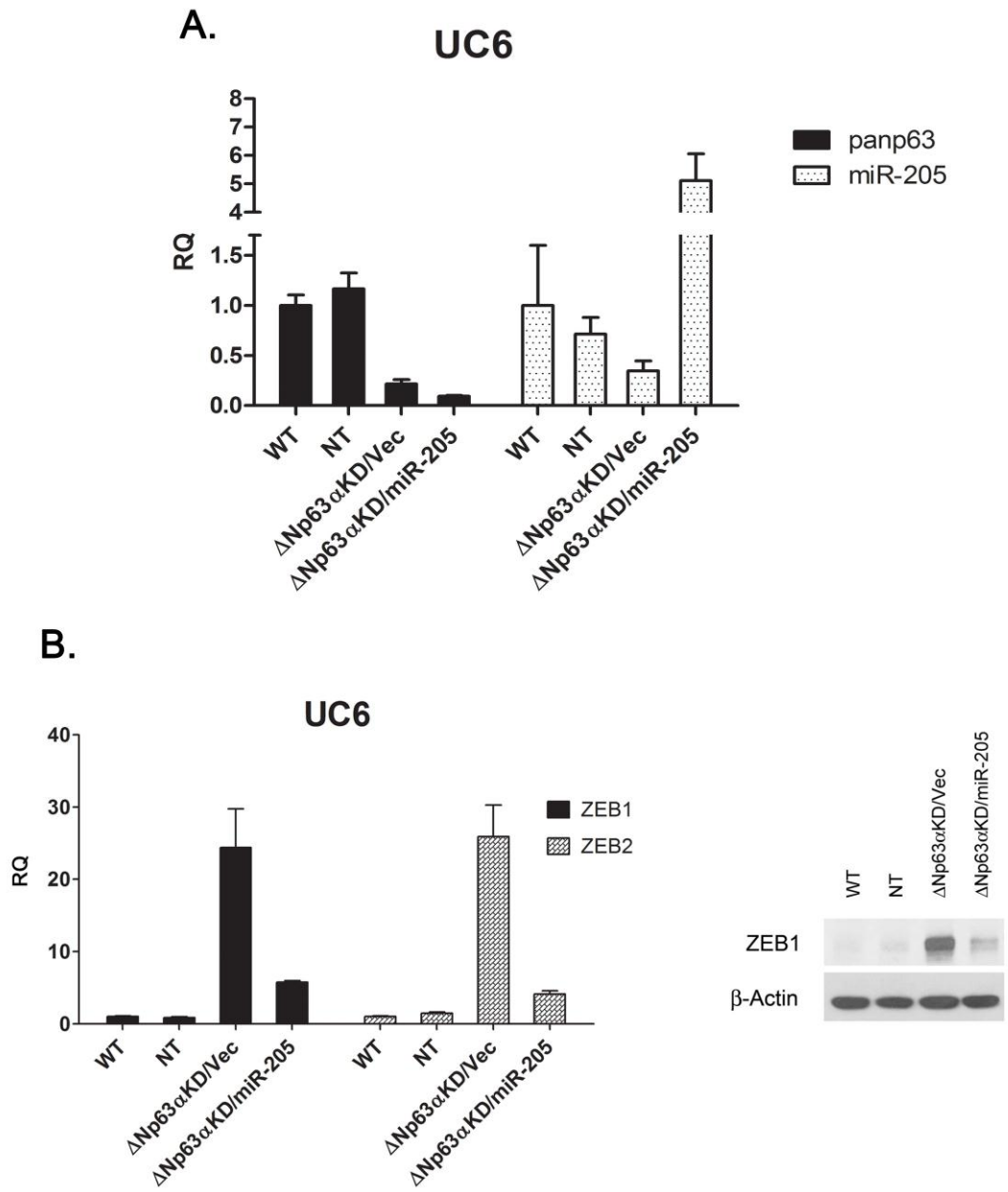

Figure 21: ΔNp63α regulates ZEB1/2 via miR-205. (A) qRT-PCR results showing that expression of panp63 remained unchanged while miR-205 expression was strongly enhanced in miR-205 overexpressing ΔNp63KD UC6 cells. (B) miR-205 overexpression reversed the effect of ΔNp63αKD on ZEB1/2. qRT-PCR and IB data demonstrate that the induction ZEB1/2 mRNA and protein by ΔNp63αKD was abrogated by miR-205 overexpression.

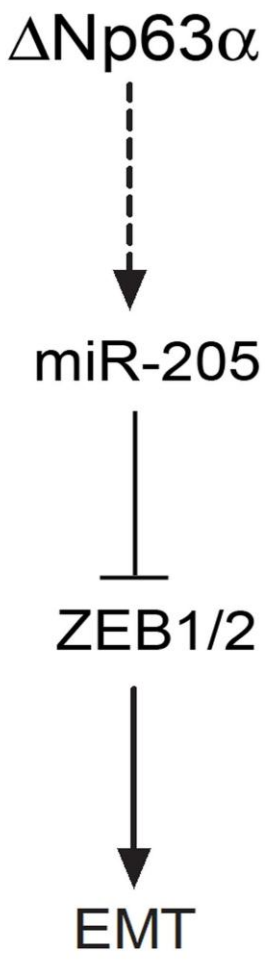

Figure 22: Schematic illustration of the relationship between ΔNp63α, miR-205, ZEB1/2 and EMT

5. ΔNp63α regulates miR-205 via miR-205HG

Since they were discovered in 1993 in *C.elegans* (198), miRNAs have become more and more attractive to scientists for their multiple impacts in all aspects of cell biology. miRNA processing from pri-miRNAs to pre-miRNAs and finally to mature miRNAs has been explored in detail in multiple cell models. However, little is known about the transcription process to generate pri-miRNAs. Based on genomic loci, miRNAs can be classified into two groups: intergenic miRNAs and intragenic miRNAs. Intergenic miRNAs are those located in between genes and are controlled as independent transcriptional units. On the other hand, intragenic miRNAs reside within protein coding genes that are referred to as the "host" genes for the miRNAs (199). The similarity in the expression patterns of miRNAs and their "host" genes indicates that this class of miRNAs is transcribed along with their "host" genes (81,200). MiR-205 is an intragenic miRNA. Its genomic location overlaps the junction between the last intron and the last exon of a poorly characterized protein-coding gene (Fig. 23). This protein- coding gene, formerly known as LOC642587, has been termed miR-205 "host" gene (miR-205HG). Since miR-205 is potentially transcribed along with miR-205HG, we performed qRT-PCR to examine the expression of miR-205HG in ΔNp63α-modulated cells using primers spanning the exon 2 and 3 junction. Interestingly, miR-205HG expression decreased in all five ΔNp63α KD cells and increased in UC3 ΔNp63α overexpressed cells (Fig. 24). These data confirm the connection between miR-205 and miR-205HG in RNA expression and the important role of ΔNp63α in their mutual regulation.

Figure 23: Genomic location of miR-205 is inside miR-205HG

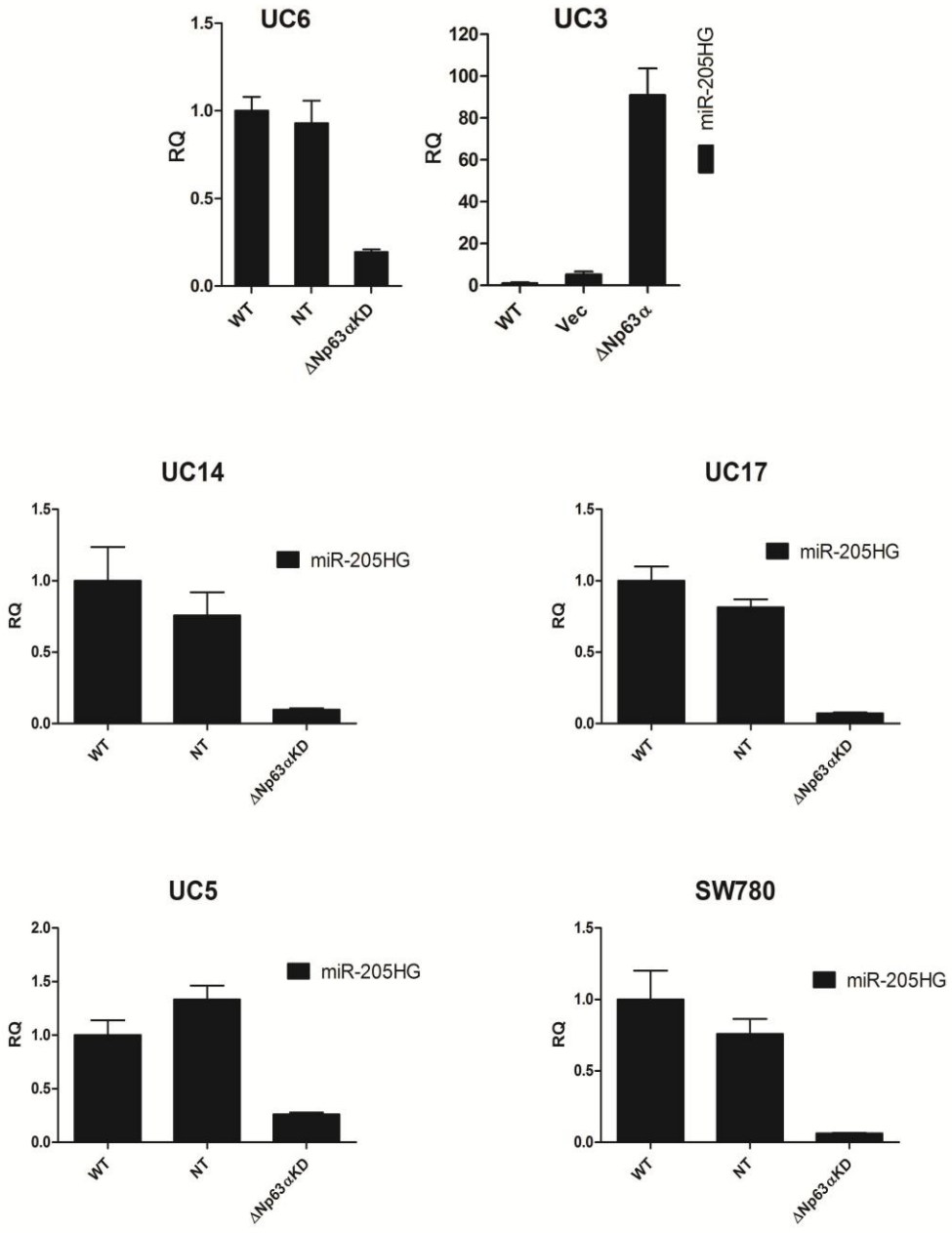

Figure 24: Expression of the miR-205 host gene (miR-205HG) changes in parallel with ΔNp63α alteration. qRT-PCR results showing miR-205HG mRNA levels were down-regulated and upregulated in ΔNp63αKD or ΔNp63α overexpressed cells, respectively. The Taqman probe for miR-205HG spans the junction of exon 2 and 3. Bars show the RQ of gene expression ± RQ max and RQ min.

The steady state of mRNA/pri-miRNA detected by qRT-PCR is the balance between the generation of new mRNA/pri-RNA and mRNA/pri-RNA degradation. To determine if ΔNp63α is involved in the transcription of miR-205 and miR-205HG *per se*, we performed nuclear run-on experiments, which allowed us to compare the quantities of nascent transcripts. In this experiment, short-time transcription induction *in vitro* allowed endogenous RNA Poll II to complete the elongation step of transcription without any *de novo* transcription initiation. Therefore, the quantity of nascent transcripts is proportional to the number of Pol II molecules that are bound to the gene of interest. By replacing rUTP with biotinylated-rUTP, this method enabled us to pull down the nascent transcript using streptavidin coated magnetic beads. Subsequent reverse transcription and real time PCR provided us quantifiable comparisons between the transcription rates of samples. The nuclear run-on results showed decreases in the miR-205HG and pri-miR-205 transcription rates in UC6 ΔNp63α KD cells, demonstrating the crucial role of ΔNp63α in the transcription of miR-205HG and pri-miR-205 (Fig. 25).

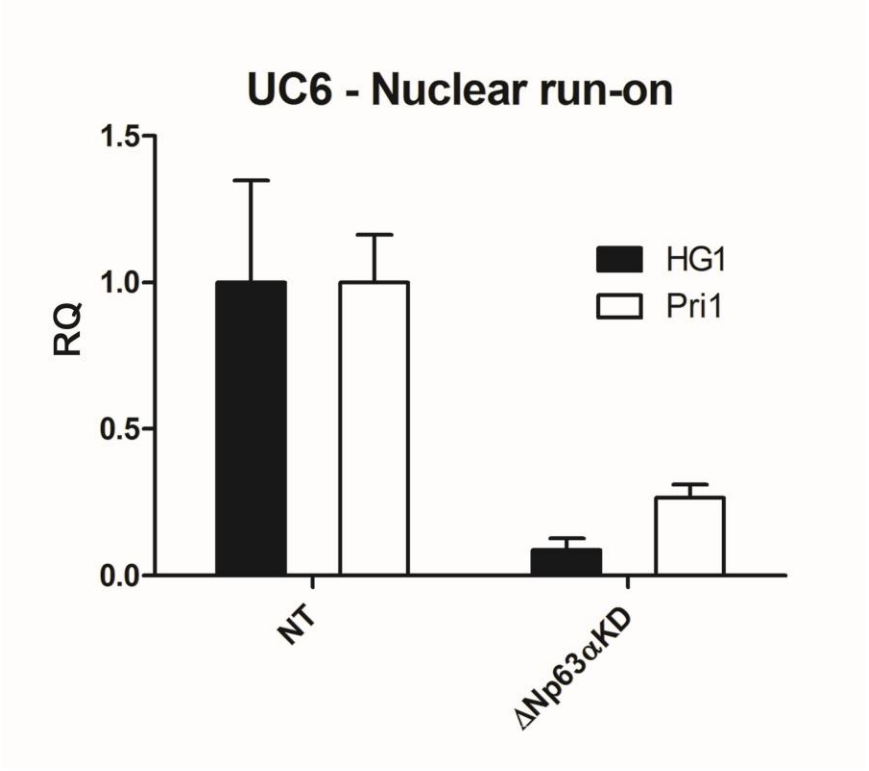

Figure 25: The transcription of miR-205HG and miR-205 is suppressed in ΔNp63kd cells. Real time PCR data show the expression of miR-205HG and pri-miR-205 in nuclear run-on experiments measuring the nascent transcripts generated from miR-205HG and miR-205. HG1 primers were designed within exon 1 of miR-205HG. Pri1 primers were designed to detect the same amplicon with the pri-miR-205 primers from ABI. GAPDH expression was used as an endogenous control

Even though intragenic miRNAs are thought to be transcribed together with their "host" genes, some recent publications reveal that intragenic miRNAs have their own promoters and transcription start sites (TSS) and can be transcribed independently of their "host" genes (82,83). In most of the cases, miRNAs are transcribed by RNA Pol II (except for some miRNA transcribed by RNA Pol III (201)). We used an anti-RNA Pol II antibody and chromatin immunoprecipitation (ChIP) to determine whether miR-205 is transcribed with miR-205HG. We designed three primer sets, one in Region 1 encompassing 1kb upstream of the miR-205HG TSS, one in Region 2 encompassing 1kb upstream of the miR-205 start site and the last one in Region 5 located 5kb away from miR-205HG (Fig. 26A). Primers for the promoter of GAPDH were used as a positive control, and primers for Region 5 were use as a negative control. As RNA polymerase pausing happens at the transcription initiation step to facilitate the time-consuming assembly of the transcription initiation complex at the promoters of genes, RNA Pol II is bound to the promoters of gene tested in this assay. The ChIP results showed an enrichment of Pol II at Region 1 comparable to Pol II enrichment at GAPDH promoter while Pol II enrichment at Regions 2 and 3 was minimal (Fig. 26B), suggesting that Region 1 is the promoter of both miR-205HG and miR-205. Therefore, we conclude that miR-205 is transcribed along with its "host" gene.

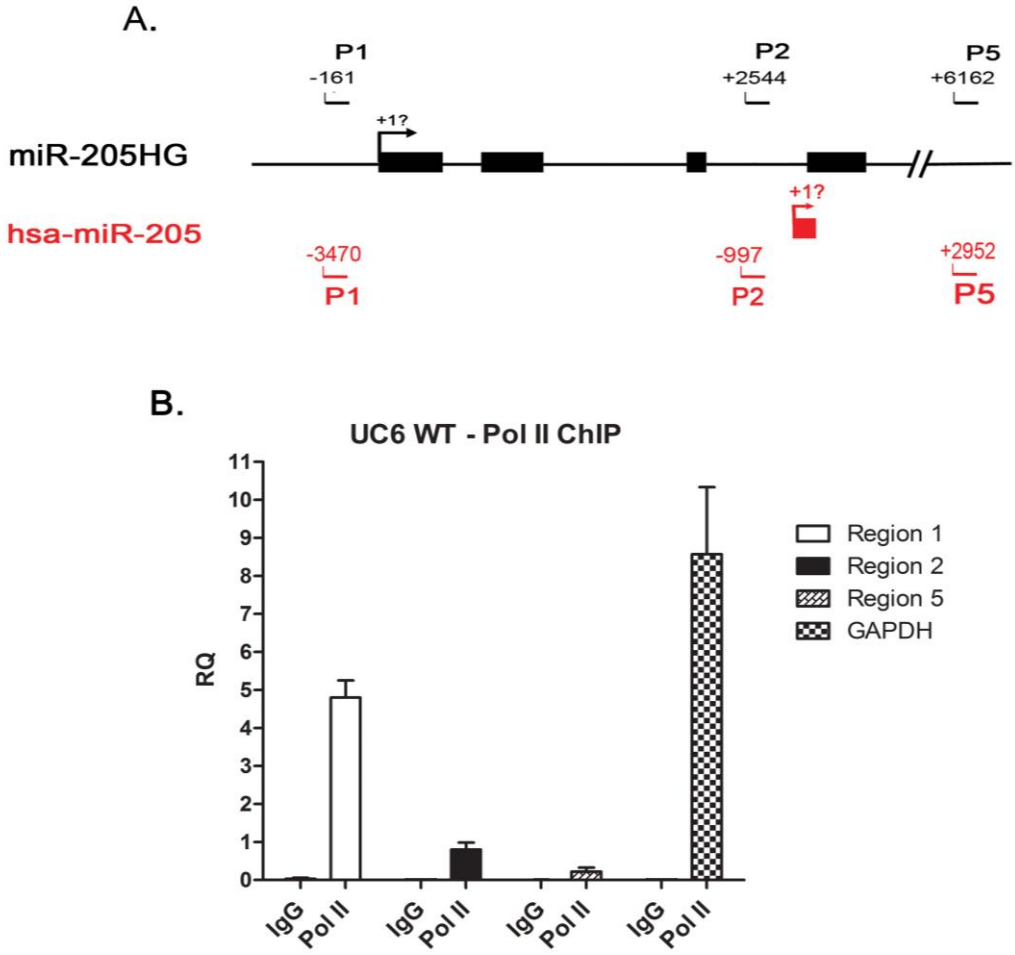

Figure 26: The promoter of miR-205HG is also the promoter of miR-205. (A) Map showing the genomic positions of miR-205 and miR-205HG in detail. Location of primers designed for ChIP experiment (P1, P2, and P5) is illustrated. The positions were numbered based on the potential transcription start site (TSS) directly 5' of miR-205 (in red, below) or based on the TSS of the miR-205 host gene (miR-205HG, in black, above). (B) Pol II binds to region 1 which is the promoter of miR-205HG. Real time PCR data show Chromatin Immunoprecipitation (ChIP) results. Primers detecting the promoter of GAPDH are used as positive control. IgG is the negative control. Bars represent mean ± SD of normalized RQ values in triplicate samples.

When analyzing the sequence of miR-205HG and its surrounding areas using the University of California Santa Cruz (UCSC) genome browser (*www.genome.ucsc.edu*), I discovered that Region 2 is highly conserved across 46 vertebrate species and hypersensitive to DNAse, similar to Region 1, which is the promoter of miR-205HG (Fig. 27B). Due to their important roles in regulating gene expression, regulatory regions such as promoters and enhancers are highly conserved during evolution. Regulatory regions are also usually in an "open" state with minimal contacts with the histones to facilitate the access of the bulky transcriptional machinery to chromatin. Therefore, these regions are hypersensitive to DNAse treatment. The conservation and DNAse sensitivity of Region 2 indicates its likely role as a regulatory region for miR-205 and miR-205HG. Interestingly, I also identified a p53 response element (p53RE) in Region 2 by the Genome Browser and Genomatix. A canonical p53RE consists of a tandem repeats of a 10bp consensus binding motifs 5' PuPuPuC(A/T)(A/T)GPyPyPy 3', separated by a 0-13bp spacer (202). Each binding motif is a half-site of a whole-site p53RE. The three purines and three pyrimidines flanking the half-site are flanking sequences. C(A/T)(A/T)G is the core sequence of the motif. The p53RE I identified in Region 2 of miR-205HG is a whole-site p53RE strongly homologous to the canonical sequence with only one nucleotide mismatch at the flanking sequence (Fig. 27A). As a member of the p53 family, p63 exhibits remarkable sequence and structural homology to p53, especially in the DNA binding domain, suggesting overlaps in target recognition specificity. Indeed, p63 can bind to p53 response elements (p53REs) *in vitro* and *in vivo* (147). I performed ChIP using the 4A4 antibody and discovered that ΔNp63α binds to Region 2 of miR-205HG (Fig. 28A). The enrichment of ΔNp63α at Region 2 is significantly reduced in ΔNp63αKD cells, suggesting that this binding is specific (Fig. 28B). As a result, Region 2 appears to be a very important regulatory region of miR-205 and miR-205HG that is bound by ΔNp63α.

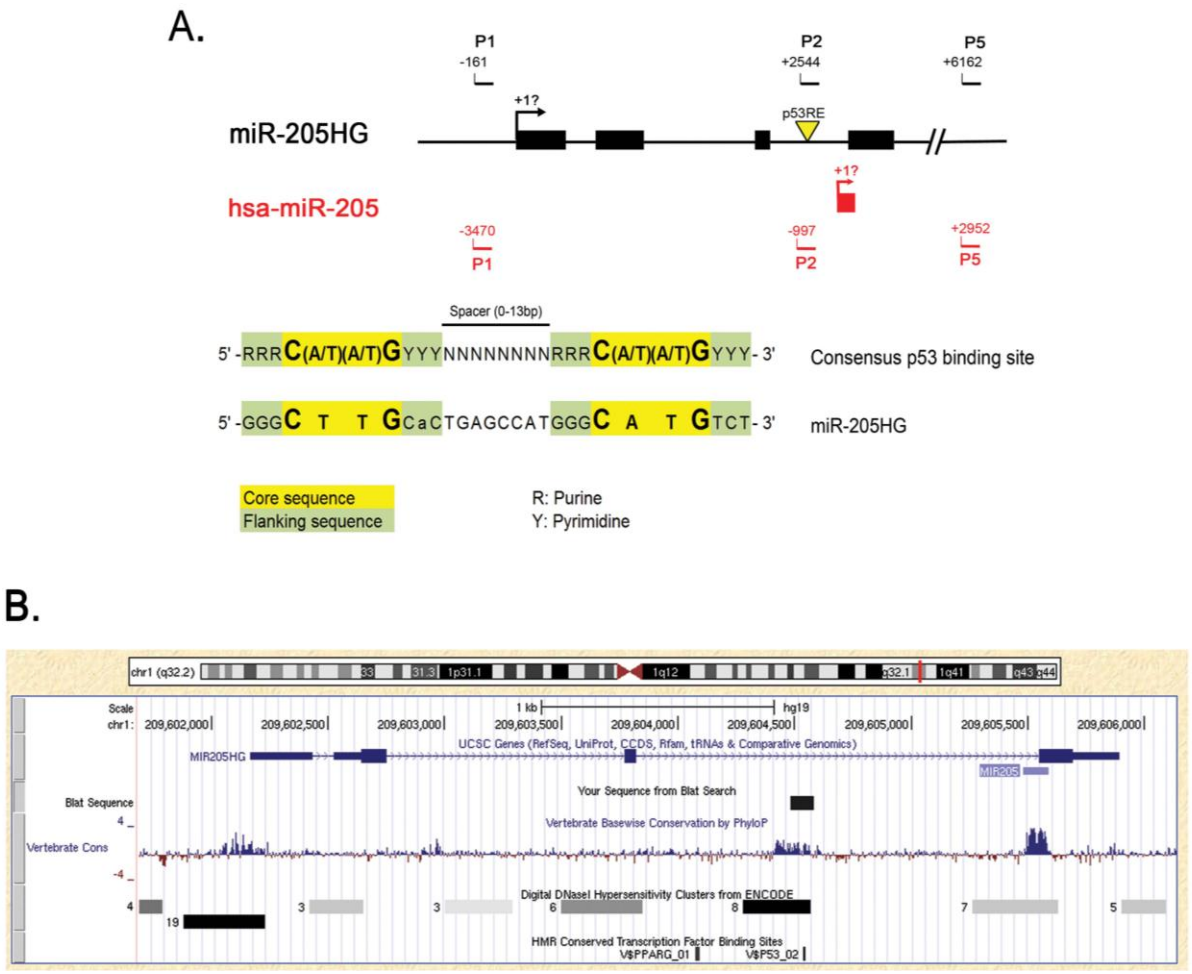

Figure 27: Region 2 containing a whole-site p53 response element (p53RE) is a regulatory region. (A) Detailed information regarding the p53RE in region 2. Comparison between the consensus p53 binding site and the p53RE in region 2 reveals only one mismatch (in lower case) in the second flanking sequence. (B) Region 2 is highly conserved and hypersensitive to DNAse. Sequence of Region 2 is blatted in UCSC Genome Browser. Evolutionary conservation among 46 vertebrate species is measure by the *PhyloP* method. Positive scores (in blue) are assigned to conserved sties, while negative scores (in red) are assigned to fast-evolving sites. DNAse hypersensitive regions tested in a large number of cell lines are shown in the DNAse hypersensitivity tract. The intensity of shading in the grey boxes represents the extent of DNAse hypersensitivity of specific regions (proportional to the signal strength) in the cell lines tested. The number on the left side of the box is the number of cell lines tested. The transcription factor binding site tract (TFBS) shows the sites that are conserved in human, mouse, and rat.

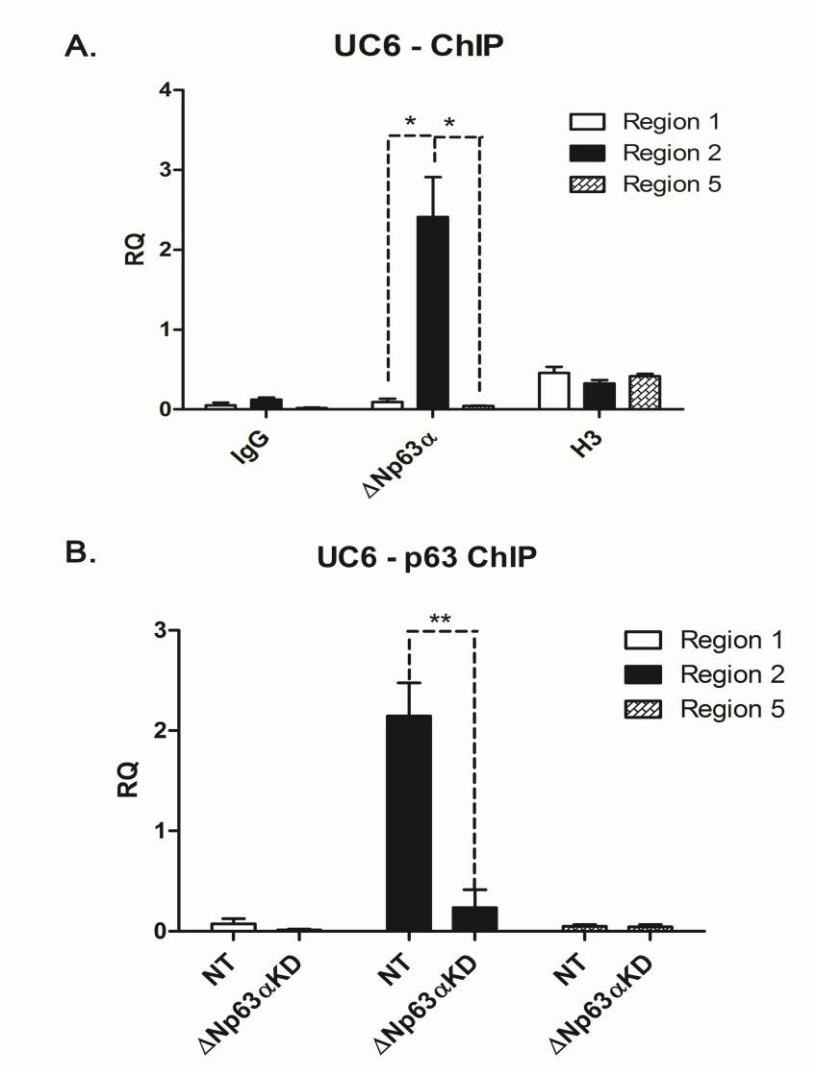

Figure 28: ΔNp63α binds to region 2. (A) Real time PCR data from ChIP experiments showing that ΔNp63α binds to region 2. Histone H3 antibody was used as a positive control. IgG was used as a negative control. (B) Decreased binding of ΔNp63α to region 2 in ΔNp63α KD cells. Bars represent mean ± SD of RQ values for target proteins (IgG, ΔNp63α, and H3) in triplicate samples. Data are representative of two to three independent experiments. A two-tailed, unpaired Student t-test was used to analyze the significance of the difference, *P<0.050, **P<0.01, ***P<0.001.

As shown in Fig. 25 and Fig. 26, miR-205 is transcribed along with miR-205HG and their transcription is reduced in the absence of ΔNp63α. We were interested in defining the mechanism of this transcriptional reduction. Since Pol II binds to Region 1 and potentially drives the transcription of miR-205HG and miR-205, we compared the binding efficiency of Pol II to Region 1,2 and 5 in the presence and absence of ΔNp63α. Consistent with the reduction in transcription determined by the nuclear run-on experiment, the binding of Pol II to Regions 1 and 2 significantly decreased in the absence of ΔNp63α (Fig. 29). We conclude that ΔNp63α plays an important role in recruiting Pol II to the promoter of miR-205HG to initiate transcription.

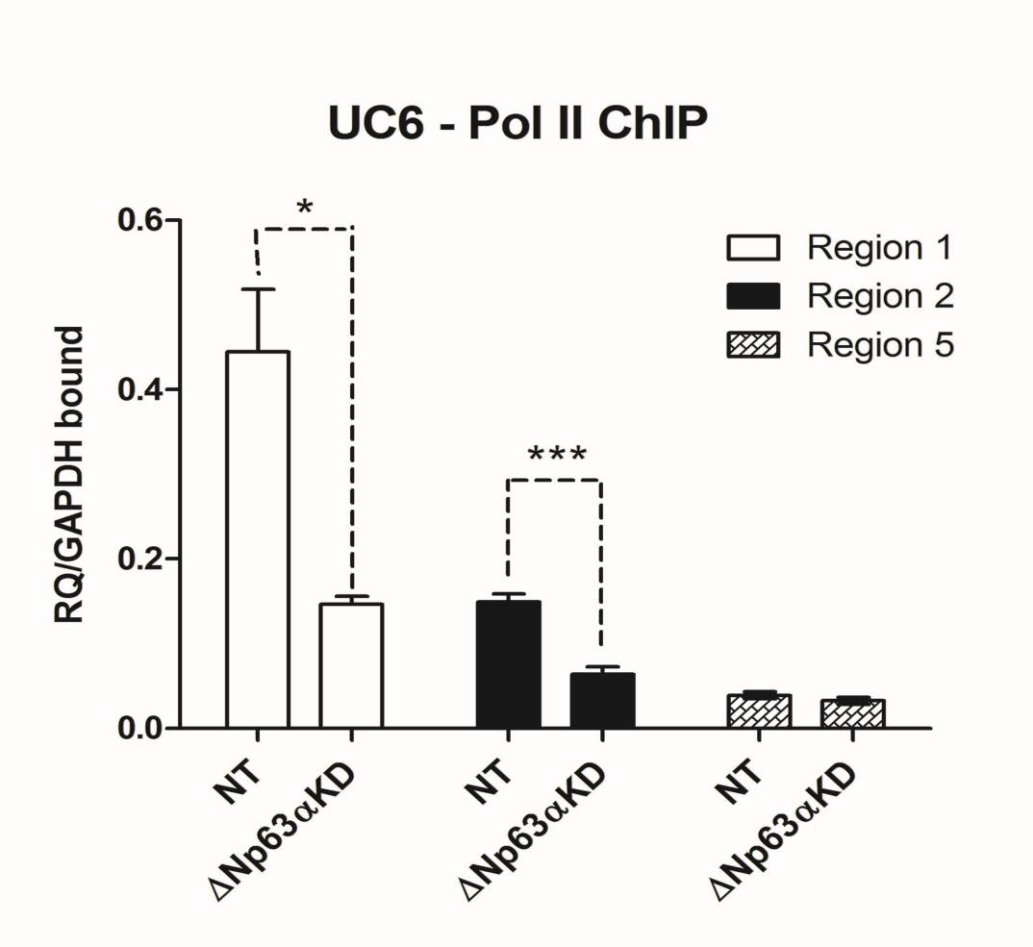

Figure 29: Pol II binding to miR-205HG is abrogated in ΔNp63α KD cells. Real time PCR results of ChIP experiments demonstrate the reduction of Pol II binding to both region 1 (promoter region) and region 2 (regulatory region) of miR-205HG and miR-205. RQ values of Pol II binding to regions 1, 2 and 5 were normalized to RQ values of Pol II binding to the GAPDH promoter. Bars represent mean ± SD of normalized RQ values in triplicate samples. A two-tailed, unpaired Student t-test was used to analyze the significance of the differences, *P<0.050, **P<0.01, ***P<0.001.

6. High miR-205 expression correlates with adverse clinical outcome

The ultimate goal of translational cancer research is to benefit cancer patients by increasing survival and eliminating recurrence. Besides searching for a way to enhance the efficiency of current therapy, identifying new markers to facilitate diagnosis and new targets for new therapy is also an important aspect of cancer research. We reported that ΔNp63α is a marker of poor prognosis in MIBC in a previous publication (145). We were also eager to know the relationship between miR-205 expression and survival given that the data demonstrated that miR-205 is a downstream target of ΔNp63α. Using the qRT-PCR results obtained previously (Fig. 16), we compared the miR-205 expression of the 98 BC patients with their survival. Samples from this cohort of patients had been used in our previous study (145). Follow up data on survival of patients were classified into overall survival (OS) which is the percentage of patients who are still alive for a certain period of time after diagnosed with BC and disease specific survival (DSS) which is the percentage of patients who have not died from BC in a certain period of time. Regression tree analyses were performed by a professional statistician to determine the cutoff point of miR-205 expression as 1.76. Kaplan Meier curves were generated to examine the relationship between miR-205 expression and survival rates. In the whole cohort of patients (n=98, superficial plus muscle invasive), low miR-205 expression ($\leq$1.76) correlated with media DSS of 140+ months and median OS of 69.1 months, whereas high miR-205 expression ($\geq$1.76) was associated with significantly worse DSS and OS, with a median DSS of 13.4 months and a median OS of 12 months ($p<0.0001$ for DSS and $p=0.0004$ for OS) (Fig. 30A). We also characterized the relationship in the MIBC subset of patients (n=66) and observed an even more remarkably result. MIBC patients with low miR-205 expression had the median DSS of 140+ months and OS of 69.1 months while those with high miR-205 expression had a median DSS and OS of only 8.11 months ($p<0.0001$ for DSS and

p<0.0001 for OS) (Fig. 30B). These data prove the substantially significant correlation between high miR-205 expression and adverse clinical outcomes, especially for the MIBC subset Therefore, like ΔNp63, high miR-205 expression identifies the lethal BC subset.

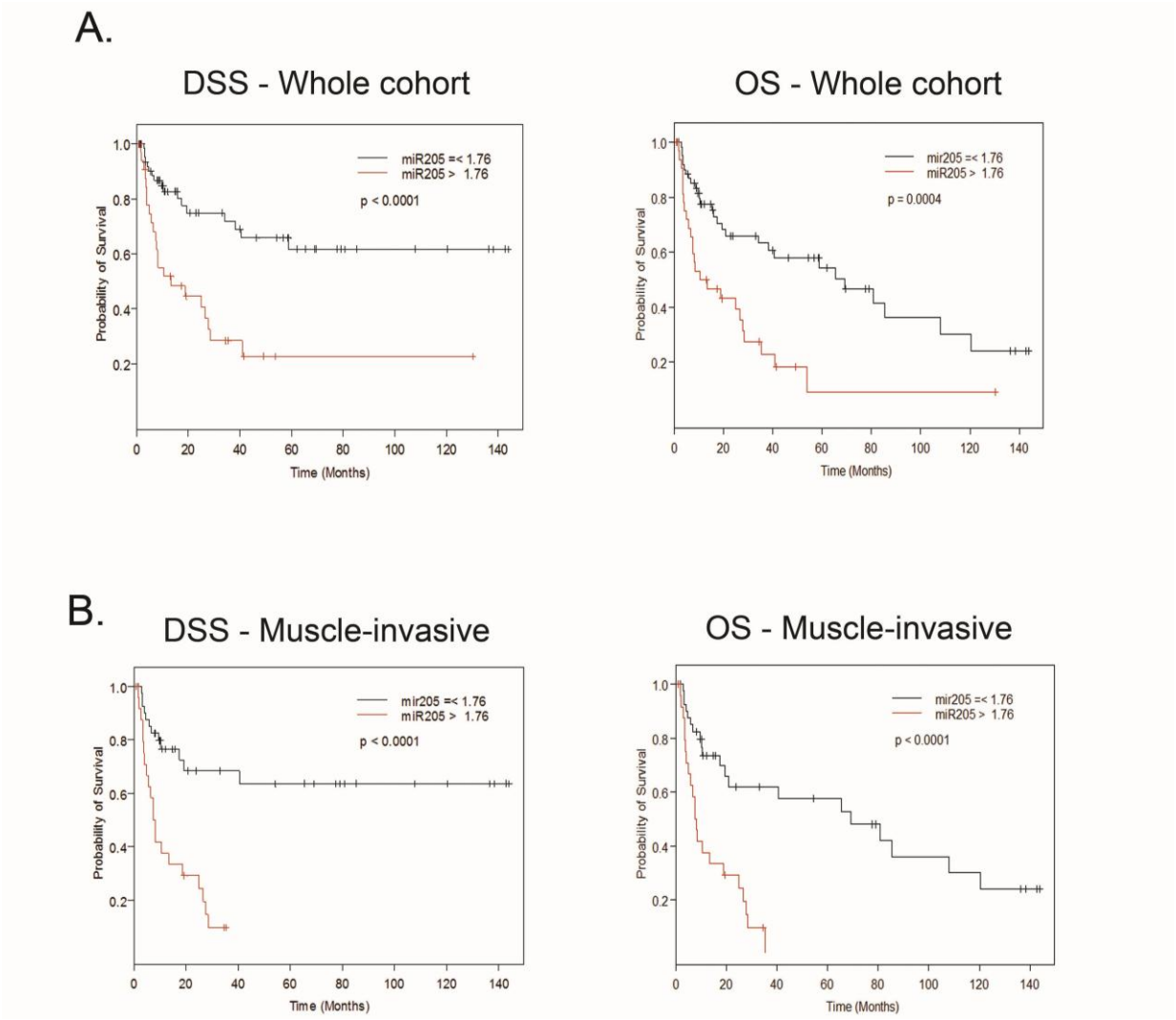

Figure 30: High miR-205 expression correlates with poor survival. "Kaplan-Meier disease specific survival (DSS) and overall survival (OS) curves generated based on the RT-PCR results of mature miR-205 expression in the primary tumors. (A) DSS and OS of the whole cohort including superficial and muscle invasive cancers (n=98). High expression of miR-205 was associated with poor probability of DSS and OS (median DSS 13.4 months, median OS 12 months), as compared to lower miR-205 (median DSS >140 months, median OS 69.1 months), log-rank p<0.0001 for DSS and p=0.0004 for OS. (B) DSS and OS for the subset of patients with muscle-invasive cancer (n=66). Patients with elevated miR-205 had worse clinical outcomes (median DSS 8.11 months, median OS 8.11 months) than patients with low miR-205 (median DSS >140 months, median OS 69.1 months)." Reprinted from (203)

CHAPTER 4:

DISCUSSION

1. Summary of the findings

In summary, our data demonstrate the important role of ΔNp63α in inhibiting EMT in BC. As ΔNp63α is the most abundant isoform of p63 in BC, the effect of ΔNp63α on EMT represents the effect of all p63 isoforms. One mechanism by which ΔNp63α inhibits EMT is regulating the expression of miR-205, a well established negative regulator of ZEB1 and ZEB2, because up- or down-regulation of ΔNp63α results in parallel changes in miR-205 levels and reciprocal effects on ZEB1 and ZEB2 expression, morphological alteration, and invasion. We also reveal, for the first time, that ΔNp63α binds to a highly conserved regulatory region of miR-205HG, influences the recruitment of RNA Pol II to the promoter of miR-205HG to regulate the transcription of miR-205HG as well as miR-205 which is transcribed along with its "host" gene. Interestingly, we also discovered that miR-205 expression is well correlated with poor clinical outcomes in BC patients, especially in MIBC patients. A similar (but weaker) correlation was discovered previously with p63 expression (145). These data suggest that miR-205 and p63 can be used as markers for the lethal subset of BC patient. Moreover, since miR-205 is a downstream target of p63, the p63 pathway can be a signature of this lethal BC subset.

2. ΔNp63α partially induces EMT

Interestingly, in 2011, Oh *et al.* reported that ΔNp63α promotes EMT in normal human keratinocytes (197). Their data also suggest that ΔNp63α triggers EMT in an TGFβ-dependent manner and provides keratinocytes with stem cell properties. In our BC cell lines, we also observed an induction in expression of at least one mesenchymal marker, Slug (SNAI2), in all ΔNp63α KD cell lines and a reduction in Slug expression in ΔNp63α overexpressed UC3 cells (Fig.), indicating that ΔNp63α does have some EMT-promoting effects. However, the EMT-

promoting effects of ΔNp63α-dependent Slug expression on cellular morphology and invasion appear to be overwhelmed by the anti-EMT effects of ΔNp63α in BC. This discrepancy in EMT-related effect of ΔNp63α could be due to the difference in cell type models used in the two studies, emphasizing the cell type dependent effects of ΔNp63α.

3. MiR-205 is only one explanation for EMT

The effect of ΔNp63α modulation on cell morphology, invasion and the expressions of EMT markers in BC cell lines clearly demonstrate ΔNp63α as an inhibitor of EMT. The signaling cascade ΔNp63α-miR-205-ZEB1/2 is one mechanism by which p63 regulates EMT in BC. This signaling cascade was also validated as an EMT inhibition mechanism in prostate cancer in a recent publication (204). In this paper, by using an approach similar to ours, the authors demonstrated that modulation of ΔNp63 expression by siRNA or overexpressing vector resulted in down or up-regulation of miR-205, respectively, and an inverse effect on ZEB1. They also showed that ΔNp63 overexpression inhibited cell migration and that inhibition of miR-205 in ΔNp63 overexpressed cells overcame the migration inhibition by ΔNp63. However, provided that p63 has multiple downstream targets that may involve in multiple different signaling pathways, it is possible that ΔNp63α inhibits EMT via mechanisms other than or in addition to the transcriptional regulation of miR-205. Future studies should be designed to explore those mechanisms.

4. TAp63 and Dicer

It is well established that ΔNp63 and TAp63 can share the same downstream targets but exert opposite effects by virtue of ΔNp63's ability to directly compete for TAp63 target

promoters or by sequestering TAp63, forming inactive tetramers (205,206). Using a knockout mouse model, Su *et al.* showed that *TAp63*$^{+/-}$ and *TAp63*$^{-/-}$ mice develop spontaneous carcinomas and sarcomas which were highly metastatic. Interestingly downregulation of Dicer mRNA and protein expression was observed in metastatic mouse and human tumors deficient in TAp63. Since Dicer is a crucial molecule in miRNA processing, decreased Dicer expression generates a global decrease in mature miRNA expression represented by miR-130b, miR-34a, miR-10b, miR-200b, and miR-200c. Their study strongly demonstrated that TAp63 regulates the transcription of Dicer and suppresses metastasis (171). Provided that the panp63 shRNA construct used in our study can diminish the expression of all p63 isoforms including TAp63 and ΔNp63, there was a possibility that the effects on miR-205 and EMT we observed in BC were by loss of TAp63-regulated Dicer expression. However, in our BC cell lines, the panp63 shRNA produced no changes in Dicer mRNA expression (Fig. 31A), and in fact it actually led to increased miR-200c expression in the UC14 cells (Fig. 31B). The endogenous expression level of TAp63 is very low in all of our BC cell lines, strongly suggesting that its effects are in general insignificant. In addition, modulation of ΔNp63α results in the parallel changes in miR-205HG and miR-205, strongly suggesting that DNp63 plays an important role in the generation of the pri-miR-205, not at the miRNA maturation step. In general, our data describing the role of ΔNp63α in EMT in BC do not contradict to previous findings (171).

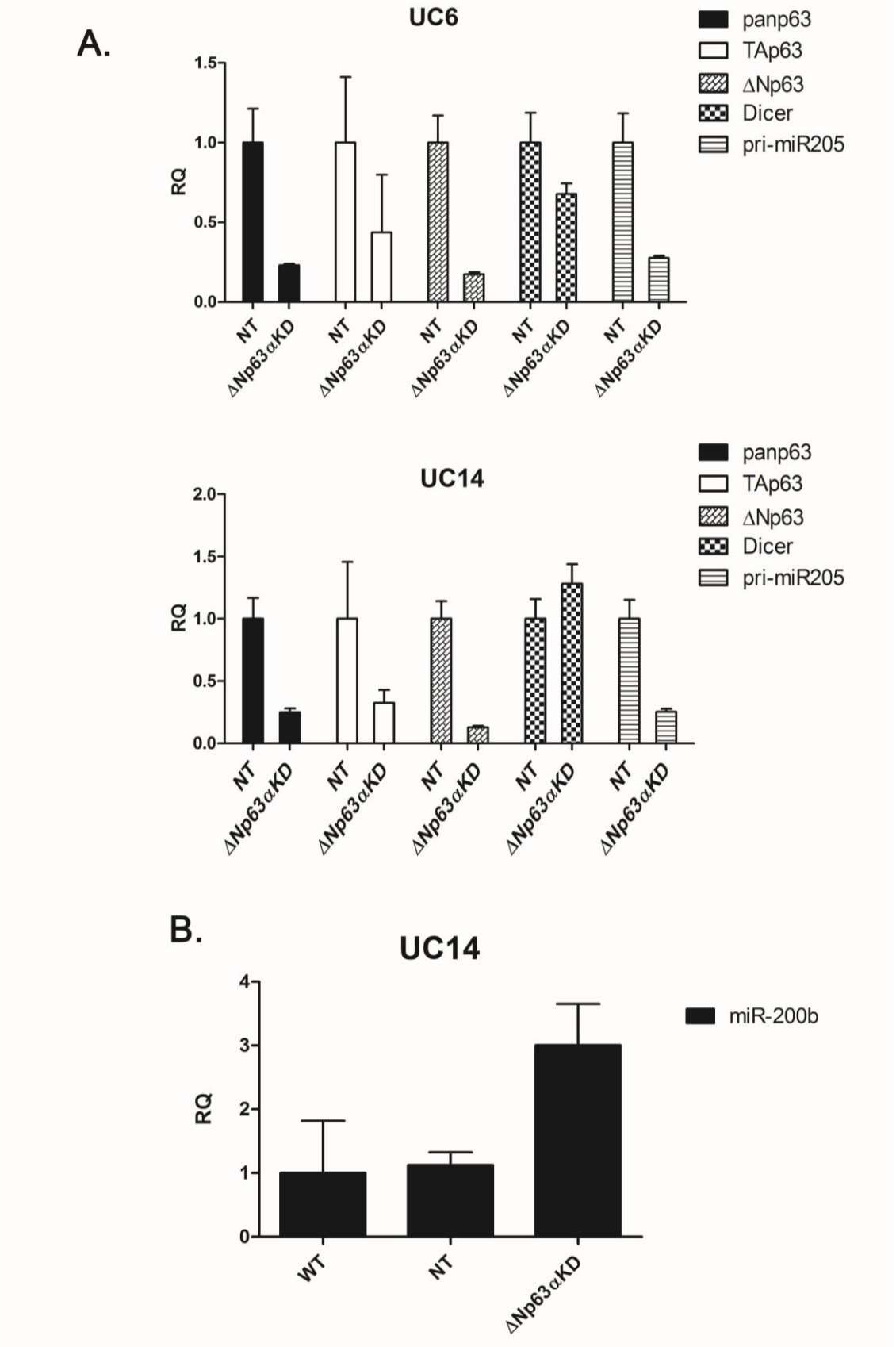
A.
UC6
panp63
TAp63
ΔNp63
Dicer
pri-miR205
RQ
1.5
1.0
0.5
0.0
NT
ΔNp63αKD
UC14
2.0
B.
miR-200b
4
3
2
1
0
WT

Figure 31: ΔNp63α does not affect *Dicer* transcription. (A) qRT-PCR results showing the changes in the expression of panp63, ΔNp63, TAp63 and pri-miR-205, but not Dicer when panp63 is knocked down in UC6 and UC14. (B) Upregulation of miR-200b in UC14 ΔNp63αKD cells. Bars show the RQ of gene expression ± RQ max and RQ min.

5. p53, p73 and p63 in the p53REs

p63, p53 and p73 belong the one transcription factor family due to the homology in their sequence and structure. This homology allows the family members share many same targets and regulate transcription together. Since the p63 binding site in Region 2 contains a p53RE, the experiments described to this point did not rule out the possibility that p53 and/or p73 could also bind to Region 2 to regulate the transcription of miR-205. Indeed, p53 was reported to directly bind to Region 2 (as determined by ChIP and Electrophoretic Mobility Shift Assay (EMSA)) and regulate the transcription of miR-205 in triple negative breast cancer cells (207). Therefore, we performed ChIP using an anti-p53 antibody in UC6, which has WT p53 (208). Primers detecting the promoter of p21, a canonical target of p53, were used as a positive control. Interestingly, we did not observe any enrichment of p53 binding in Region 2 (Fig. 32). Moreover, the mutation status of p53 did not correlate with expression of miR-205 (or for that matter, members of the miR-200 family) in our BC cell lines. For example: UC6 has WT p53 and high expression of miR-205; however, UC11 also has WT p53 but miR-205 expression in UC11 is very low. Another example is that UC14 has mutant p53 but also has high expression of miR-205 (208). The transcriptional regulation of miR-205 by ΔNp63 was confirmed in two studies in prostate cancer (204,209). In both studies, ΔNp63 was shown to bind to Region 2, similar to our finding.

Lack of p53's binding in Region 2 of miR-205 is very intriguing providing that the whole-site p53RE locates in this region. A possibility is that ΔNp63α, which is abundant in UC6, plays a major role in binding to and regulating the expression of miR-205 in normal unstimulated condition; however, in stimulated condition that triggers the activity of p53, such as DNA damage condition, p53 may target miR-205. This hypothesis needs to be proved in future experiments.

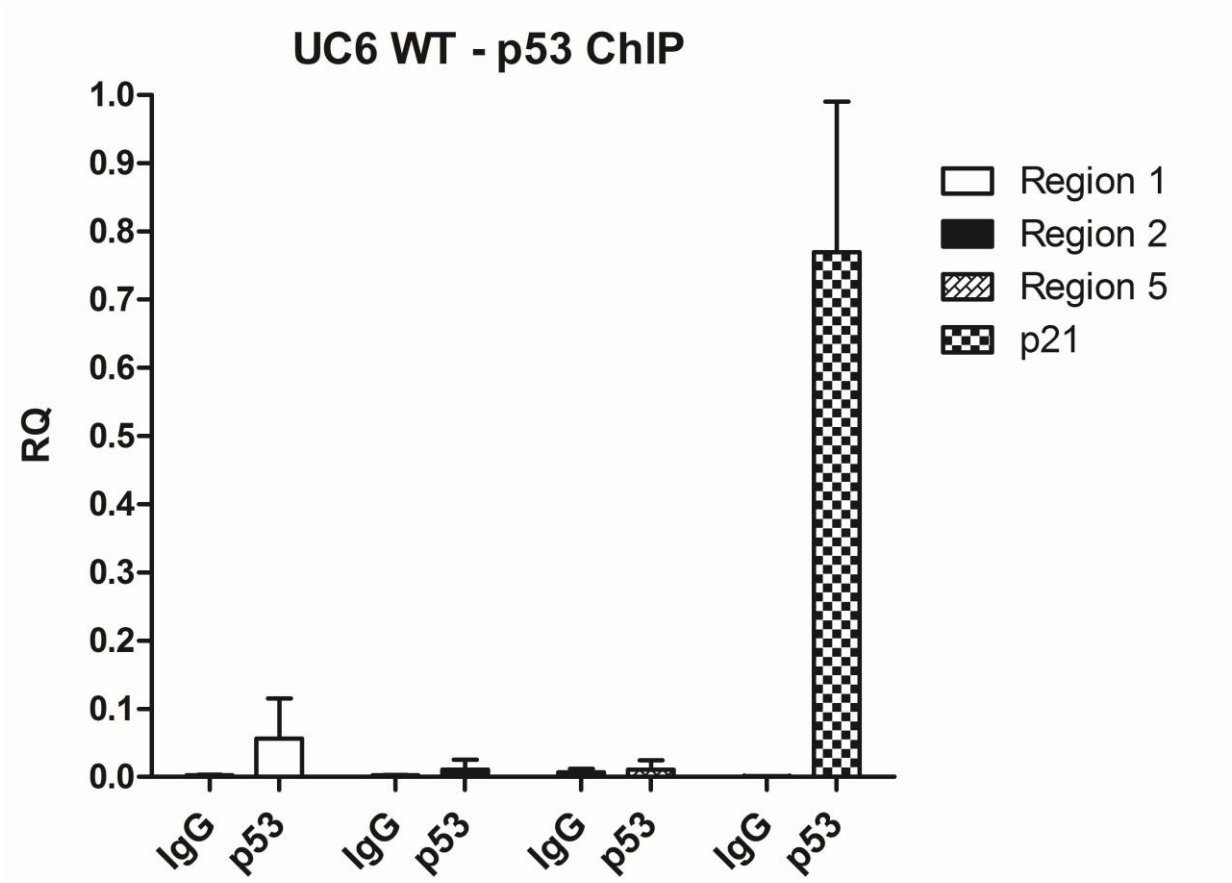

Figure 32: p53 does not bind to Region 2. Real time PCR data from ChIP experiment shows no enrichment of p53 binding to Region 2 and Region 5 compared to IgG negative control. A small enrichment of p53 binding was detected in Region 1; however, this enrichment is minimal compared to the enrichment of p53 binding to the promoter of p21, the positive control. Bars represent mean ± SD of RQ values for p53 in triplicate samples

6. ΔNp63 and clinical outcomes

Despite the association of miR-205 and poor survival in MIBC, we do not believe that miR-205 drives the biology of bladder cancer lethality. Instead, it appears that ΔNp63, the upstream regulator of miR-205, is the master regulator of this lethal phenotype and miR-205 serves as a downstream marker of ΔNp63 activity. Evidence supporting this conclusion is from an on-going study in which we are trying to classify MIBC in to subsets based on unsupervised hierarchical clustering of gene expression profiling data. The idea for this study comes from the fact that MIBC patients respond differently to therapy, indicating the difference in the original nature of MIBC in each patient. This observation is also true for many other types of cancer and a typical example is breast cancer which has been classified into five subtypes: normal-like, luminal A, luminal B, HER2-enriched and basal-like (210,211). By using the same approach with the study in breast cancer (211), we have characterized primary tumor samples from 73 MIBC patients, the majority of whom had not been exposed to any type of cancer treatment, and discovered that these samples clustered into three discrete subsets. This result has been confirmed in three other independent gene expression profiling datasets. Interestingly, the subset that correlates with the worst clinical outcomes has an enrichment of ΔNp63's downstream targets, including the urothelial basal cell markers CK-5 and CK-14 (212,213) and P-cadherin. Together with the correlation between ΔNp63, miR-205 and poor survival, these new data confirm the enhancement of the p63 signaling pathway in the lethal subset of MIBC. One interpretation for our findings is that $\Delta Np63^{hi}miR\text{-}205^{hi}$ cells in this lethal subset of MIBC display a basal-like phenotype because they originated from the basal layer of urothelium. Therefore, they potentially also possess the stem cell phenotype that support cancer progression, metastasis and drug resistant. The other two subsets associate with better clinical outcomes because, potentially, they arise from independent and more well-differentiated

progenitor cells. Our data and our interpretation are consistent with other studies in BC from different groups of researchers. They also discovered the differentiation hierarchy in BC and reported CK-5 and CK-14 as markers of the basal subtype and poor clinical outcome (110,117).

CHAPTER 5:

FUTURE DIRECTIONS

1. Determine p63 isoform/isoforms binding to region 2

Since p63 isoforms share the same DNA binding domain, they all potentially have the ability to bind to region 2. Even though ΔNp63α is the most abundant isoform in BC, other p63 isoforms still exist in BC. Therefore, we would perform ChIP to examine p63 binding to the miR-205 promoter using antibodies specific for TA-, ΔN-, α, β and γ isoforms of p63. The results of this experiment would help us to determine the specific isoforms involved in regulating miR-205 and/or miR-205HG.

2. Determine how ΔNp63α promotes the recruitment of RNA Pol II to the promoter of miR-205HG

Similar to many other miRNAs, miR-205 is transcribed along with it "host" gene and ΔNp63 is somehow involved in the recruitment of RNA Pol II to the promoter of miR-205HG to regulate the transcription of miR-205 and miR-205HG. However, in contrast to its clear binding to region 2, our ChIP results strongly suggest that ΔNp63α does not interact directly with the miR-205HG 5' proximal promoter. How p63 binding to Region 2 (located 2.5kb downstream of the transcription start site of miR-205HG) affects the binding of Pol II to Region 1 remains elusive. One possibility is that Region 2 is an enhancer for miR-205HG. The structure of chromatin in this region might bring the ΔNp63α that is bound to region 2 close to the proximal promoter of miR-205HG and affect Pol II recruitment. The sterile α motif (SAM) residue located at the C-terminus of ΔNp63α facilitates protein-protein interactions by forming both homo- and hetero-oligomers (214-216). Huang, Y. et al. demonstrated that ΔNp63α interacts with the C-terminal domain (CTD) of RNA Pol II via its SAM domain and that mutation of the SAM domain significantly hampered the interaction between ΔNp63α and

RNA Pol II CTD (217). In addition, despite lacking TA domains, the ΔNp63 isoforms are still able to transactivate downstream targets due to a second TA domain located in their N-termini (151,152). However, the transactivating efficiency and target selectivity of this additional transactivation domain is still undetermined. We hypothesize that ΔNp63α recruits RNA Pol II to the promoter of mir-205HG via its SAM domain and participates in activating the transcription of miR-205HG via its secondary TA domain. We would perform co-immunoprecipitation (Co-IP) to determine the interaction between ΔNp63α and RNA Pol II CTD. We would also overexpress WT, mutated forms ΔNp63α with truncated SAM domain at the C-terminus, and/or truncated TA domain at the N-terminus in UC3 and determine their ability to interact with RNA Pol II CTD by Co-IP, their ability to recruit RNA Pol II to the promoter of miR-205HG by ChIP, as well as their ability to activate transcription by nuclear run-on.

The three dimensional conformation of chromatin in the nucleus may bring two or more chromatin domains that appear distant in the linear structure together in close spatial proximity, facilitating functional interactions among proteins bound at regulatory sites that are far apart in term of genomic distance to mediate transcriptional control (218,219). The p63 binding site on miR-205 located about 4kb away from the promoter region of miR-205HG could be brought to the promoter of miR-205HG in the higher order chromatin structure. To prove this hypothesis, we would perform chromatin immunoprecipitation – chromosome conformation capture (ChIP-3C) using a ΔNp63-specific antibody. This technique combines the traditional ChIP and 3C assays (Fig. 33), in which chromatin is formaldehyde cross-linked, fragmented by sonication, ChIP enriched, and "proximity ligated" to capture spatially related DNA fragments, which are then detected by site-specific PCR. This technique has been used to study chromatin looping as a mechanism by which important transcription factors mediate transcription (220-222).

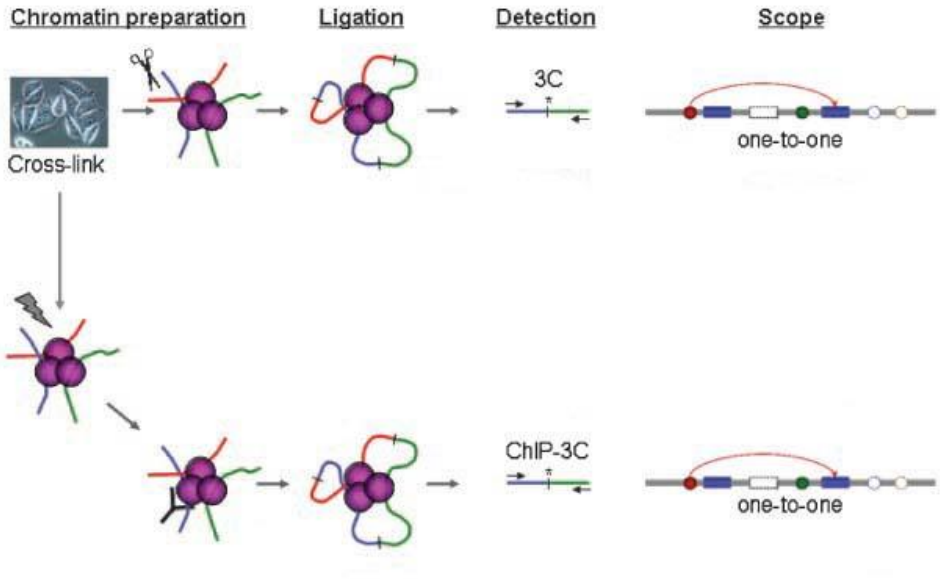

Figure 33: Schematic illustration of chromatin conformation capture (3C) (top) and chromatin immunoprecipitation-chromatin conformation capture (ChIP-3C) (bottom). *Adapted from Fullwood, M. J., and Ruan, Y. J., Cell Biochem 107, 30-39 (2009)*

3. Determine whether ΔNp63α facilitates splicing of miR-205HG

How ΔNp63α binding to region 2 promotes miR-205 expression is another question that remains unresolved. Moreover, since miR-205 is located within miR-205HG, how miR-205 is separated out of the "host" gene to go through the maturation process is also an interesting research topic. Although it is formally possible that ΔNp63α controls miR-205 transcription via an intragenic promoter that is regulated in parallel with the miR-205HG promoter, we do not favor this hypothesis, because RNA Pol II binding to region 2 appears to be much weaker than binding to region 1. Instead, we currently favor the idea that miR-205HG's promoter also serves as the promoter for miR-205 and that ΔNp63 promotes miR-205 expression via co-transcriptional splicing. A role for ΔNp63α in splicing was first proposed by Fomenkov *et al.* in 2003 (223). These authors showed that ΔNp63α bound to apobec-1-binding protein-1 (ABBP1), a member of the RNA processing machinery, via the SAM domain. This interaction

affected the mRNA processing step of FGFR-2 and resulted in an alternative splicing toward the K-SAM isoform. Mutation of the SAM domain of ΔNp63α abrogated the ΔNp63α-ABBP1 interaction and altered the FGFR-2 splicing process. In a follow up study led by the same group of researchers, they demonstrated that ΔNp63α formed a trimeric protein complex with SRA4/Scaf4, another member of the RNA splicing machinery, and the C-terminal domain (CTD) of RNA Pol II (217). Mutation of the SAM domain of ΔNp63α, again, induced aberrant splicing of the p63 mRNA transcript, resulting in a C-terminally truncated p63. In addition, accumulating studies show the coupling between transcription by RNA polymerase II with pre-messenger RNA processing reactions, such as 5'-end capping, splicing and 3'-end formation (224,225). These lines of evidence lead us to hypothesize that ΔNp63α binding to region 2 recruits the spicing factors ABBP1 and/or SRA4/Scaf4 to facilitate splicing out pri-miR-205.

To prove this hypothesis, we would first perform ChIP for ABBP1 and SRA4/Scaf4 followed by Co-IP to determine whether ABBP1 and/or SRA4/Scaf4 form a complex with ΔNp63α at region 2. It was reported that the SAM domain of ΔNp63α is critical for the interaction between ΔNp63α and ABBP1 as well as SRA4 (217,223). Therefore, we would screen our BC cell lines for expression of ABBP1 and SRA4 and then overexpress the WT ΔNp63α or a mutated form of ΔNp63α missing SAM domain together with ABBP1 and/or SRA4 in the cell line with low expression of panp63, ΔNp63α, ABBP1, SRA4, miR-205 and miR-205HG and compare the protein-protein interaction efficiency between these proteins by Co-IP to demonstrate the importance of SAM domain in these interactions. The next step would be to examine the role of ΔNp63α in miR-205HG's splicing. We would overexpress the WT and mutant forms of ΔNp63 and measure the expression of miR-205HG, pri-miR-205 and mature miR-205, comparing the results among the overexpressed samples to identify the role of ΔNp63α, ABBP1and/or SRA4 in miR-205HG's splicing. The primers for miR-205HG would

be designed to flank the junction between exon 1 and 2 (HG1-2), exon 2 and 3 (HG2-3), exon 3 and 4 (HG3-4). The primers for pri-miR-205 would be within exon 3 of miR-205HG and located around 100bp upstream of miR-205 sequence.

4. Determine whether ΔNp63α is dynamically regulated during MIBC progression and metastasis

p63 is a master regulator of epithelial development. Because of its crucial role in epithelial cells, we consider p63 to be a prototypic epithelial marker. By virtue of its ability to suppress ZEB1/2 expression, miR-205, a downstream target of ΔNp63, is also a typical epithelial marker. Our data demonstrating that ΔNp63α inhibits EMT, suppresses invasion and maintains the epithelial phenotype, in part via miR-205, would lead one to conclude that ΔNp63 would prevent tumor progression and metastasis. However, our data and our previous findings (145) also establish that there is a correlation between expression of ΔNp63 and miR-205 and adverse clinical outcomes. This finding is paradoxical with respect to multiple publications in the literature documenting the importance of EMT in tumor progression and metastasis (26) and the observation that metastasis is invariably associated with BC mortality. However, for the past few years, scientists' view regarding the importance of the "epithelial" and "mesenchymal" status of cancer cells in tumor progression and metastasis have changed dramatically. Even though EMT contributes to invasion, metastatic dissemination, and stem cell properties, it is inevitable that metastases are epithelial and in this regard resemble primary tumors. Therefore, with respect to the ability to metastasize, being "epithelial" or "mesenchymal" is not as critical as being able to flexibly transform from one state to the other under environmental selection pressure. Metastatic epithelial cancer cells can acquire

mesenchymal traits via EMT to escape from the primary tumor site, circulate in the blood stream and attach to lymph nodes and distant organ, but then they appear to undergo "mesenchymal-to-epithelial transition" (MET) to return to their original epithelial status when they colonize metastatic sites. This flexibility of metastatic cancer cells is known as cancer "plasticity" (2). An elegant study using a carcinogen-induced squamous cell carcinoma mouse model convincingly demonstrated the importance of plasticity of cancer cells *in vivo* (74). This mouse model carries a skin-specific TWIST Tet-on inducible construct that was activated locally by topical application of doxycycline (dox) or systemic dox exposure by providing the drug in the drinking water. Results from this study showed that local induction of TWIST promoted EMT which facilitated tumor dissemination into blood circulation, forming circulating tumor cells (CTC), and causing extravasation. However, metastasizing tumor cells remained dormant at distant organs unless EMT was reversed by turning off TWIST. Reversion of EMT supported metastases formation by promoting cancer cell proliferation (74). Interestingly, ΔNp63α appears to have opposite properties to those of TWIST in BC: ΔNp63α inhibits EMT and promotes proliferation (189) Moreover, ΔNp63α appears to sustain "stemness" in epithelial cancer cells (179), and these effects probably also contribute to ΔNp63α's role in supporting the colonization step of the metastasis cascade. As a result, it is possible that ΔNp63α is dynamically regulated during the whole metastasis process in metastatic cancer cells. If it is the case, the cancer cells that successfully escape from the primary tumor site to enter the blood circulation (CTCs) should have lower ΔNp63α expression than do cells in the primary tumors or cells in metastatic lesion.

Our future studies are designed to test this hypothesis in preclinical mouse models and in BC patients. Since deletion of both p53 and PTEN promotes MIBC (129), we will generate transgenic mice carrying the transgenes with LoxP flanking *p53* and *PTEN*

(*p53*$^{flox/flox}$;*PTEN*$^{flox/flox}$). These transgenic mice will have deletion of *p53* and *PTEN* in the urothelium of the bladder when we surgically delivered an adenovirus expressing Cre recombinase into the bladder lumen. We will also generate ΔNp63α Tet-off inducible mice that show inhibition of ΔNp63α expression upon doxycycline (dox) treatment. ΔNp63α Tet-off mice will be crossed with *p53*$^{flox/flox}$;*PTEN*$^{flox/flox}$ mice to create the transgenic mouse model in which the expression of ΔNp63α, p53 and PTEN can be modulated. By delivering Cre Adenovirus into the bladder lumen, we induce the formation of MIBC. After the tumors are formed, mice will be separated into three groups. One control group that does not receive dox will have unmodulated ΔNp63α expression. One group which receives dox by injection into the bladder lumen will have ΔNp63α inhibition in tumor cells restricted in the bladder. The other group which receives dox in drinking water will continuously have ΔNp63α inhibition in tumor cells even when tumor cells migrate out of the bladder and disseminate throughout the body. Comparing the metastasis incidence and the rate of metastasis formation among these two experimental groups and the control group will demonstrate the importance of ΔNp63α in metastasis as well as the regulation of this protein throughout the metastasis process.

REFERENCES

1. Kalluri, R., and Weinberg, R. A. (2009) The basics of epithelial-mesenchymal transition. *J Clin Invest* **119**, 1420-1428
2. Polyak, K., and Weinberg, R. A. (2009) Transitions between epithelial and mesenchymal states: acquisition of malignant and stem cell traits. *Nat Rev Cancer* **9**, 265-273
3. Urban, A. E., Zhou, X., Ungos, J. M., Raible, D. W., Altmann, C. R., and Vize, P. D. (2006) FGF is essential for both condensation and mesenchymal-epithelial transition stages of pronephric kidney tubule development. *Dev Biol* **297**, 103-117
4. Schmidt-Ott, K. M., Lan, D., Hirsh, B. J., and Barasch, J. (2006) Dissecting stages of mesenchymal-to-epithelial conversion during kidney development. *Nephron Physiol* **104**, p56-60
5. Li, B., Zheng, Y. W., Sano, Y., and Taniguchi, H. (2011) Evidence for mesenchymal-epithelial transition associated with mouse hepatic stem cell differentiation. *PLoS One* **6**, e17092
6. Bischof, P., Aplin, J. D., Bentin-Ley, U., Brannstrom, M., Casslen, B., Castrillo, J. L., Classen-Linke, I., Critchley, H. O., Devoto, L., D'Hooghe, T., Horcajadas, J. A., Groothuis, P., Ivell, R., Pongrantz, I., Macklon, N. S., Sharkey, A., Vicovac, L., White, J. O., Winterhager, E., von Wolff, M., Simon, C., and Stavreus-Evers, A. (2006) Implantation of the human embryo: research lines and models. From the implantation research network 'Fruitful'. *Gynecol Obstet Invest* **62**, 206-216
7. Aplin, J. D., Haigh, T., Vicovac, L., Church, H. J., and Jones, C. J. (1998) Anchorage in the developing placenta: an overlooked determinant of pregnancy outcome? *Hum Fertil (Camb)* **1**, 75-79

8. Hay, E. D. (1990) Role of cell-matrix contacts in cell migration and epithelial-mesenchymal transformation. *Cell Differ Dev* **32**, 367-375

9. Thiery, J. P., and Sleeman, J. P. (2006) Complex networks orchestrate epithelial-mesenchymal transitions. *Nat Rev Mol Cell Biol* **7**, 131-142

10. Hay, E. D. (1995) An overview of epithelio-mesenchymal transformation. *Acta Anat (Basel)* **154**, 8-20

11. Jaskoll, T., Greenberg, G., and Melnick, M. (1991) Neural tube and neural crest: a new view with time-lapse high-definition photomicroscopy. *Am J Med Genet* **41**, 333-345

12. Sauka-Spengler, T., and Bronner-Fraser, M. (2008) A gene regulatory network orchestrates neural crest formation. *Nat Rev Mol Cell Biol* **9**, 557-568

13. Knecht, A. K., and Bronner-Fraser, M. (2002) Induction of the neural crest: a multigene process. *Nat Rev Genet* **3**, 453-461

14. Diegelmann, R. F., and Evans, M. C. (2004) Wound healing: an overview of acute, fibrotic and delayed healing. *Front Biosci* **9**, 283-289

15. Kisseleva, T., and Brenner, D. A. (2008) Mechanisms of fibrogenesis. *Exp Biol Med (Maywood)* **233**, 109-122

16. Midwood, K. S., Williams, L. V., and Schwarzbauer, J. E. (2004) Tissue repair and the dynamics of the extracellular matrix. *Int J Biochem Cell Biol* **36**, 1031-1037

17. Savagner, P., Kusewitt, D. F., Carver, E. A., Magnino, F., Choi, C., Gridley, T., and Hudson, L. G. (2005) Developmental transcription factor slug is required for effective re-epithelialization by adult keratinocytes. *J Cell Physiol* **202**, 858-866

18. Zeisberg, M., Yang, C., Martino, M., Duncan, M. B., Rieder, F., Tanjore, H., and Kalluri, R. (2007) Fibroblasts derive from hepatocytes in liver fibrosis via epithelial to mesenchymal transition. *J Biol Chem* **282**, 23337-23347

19. Kim, K. K., Kugler, M. C., Wolters, P. J., Robillard, L., Galvez, M. G., Brumwell, A. N., Sheppard, D., and Chapman, H. A. (2006) Alveolar epithelial cell mesenchymal transition develops in vivo during pulmonary fibrosis and is regulated by the extracellular matrix. *Proc Natl Acad Sci U S A* **103**, 13180-13185

20. Rastaldi, M. P., Ferrario, F., Giardino, L., Dell'Antonio, G., Grillo, C., Grillo, P., Strutz, F., Muller, G. A., Colasanti, G., and D'Amico, G. (2002) Epithelial-mesenchymal transition of tubular epithelial cells in human renal biopsies. *Kidney Int* **62**, 137-146

21. Kalluri, R., and Neilson, E. G. (2003) Epithelial-mesenchymal transition and its implications for fibrosis. *J Clin Invest* **112**, 1776-1784

22. Strutz, F., Zeisberg, M., Ziyadeh, F. N., Yang, C. Q., Kalluri, R., Muller, G. A., and Neilson, E. G. (2002) Role of basic fibroblast growth factor-2 in epithelial-mesenchymal transformation. *Kidney Int* **61**, 1714-1728

23. Okada, H., Strutz, F., Danoff, T. M., Kalluri, R., and Neilson, E. G. (1996) Possible mechanisms of renal fibrosis. *Contrib Nephrol* **118**, 147-154

24. Hanahan, D., and Weinberg, R. A. (2000) The hallmarks of cancer. *Cell* **100**, 57-70

25. Fidler, I. J. (2003) The pathogenesis of cancer metastasis: the 'seed and soil' hypothesis revisited. *Nat Rev Cancer* **3**, 453-458

26. McConkey, D. J., Choi, W., Marquis, L., Martin, F., Williams, M. B., Shah, J., Svatek, R., Das, A., Adam, L., Kamat, A., Siefker-Radtke, A., and Dinney, C. (2009) Role of epithelial-to-mesenchymal transition (EMT) in drug sensitivity and metastasis in bladder cancer. *Cancer Metastasis Rev* **28**, 335-344

27. Birchmeier, W., and Birchmeier, C. (1995) Epithelial-mesenchymal transitions in development and tumor progression. *EXS* **74**, 1-15

28. Jechlinger, M., Grunert, S., and Beug, H. (2002) Mechanisms in epithelial plasticity and metastasis: insights from 3D cultures and expression profiling. *J Mammary Gland Biol Neoplasia* **7**, 415-432

29. Bissell, M. J., Radisky, D. C., Rizki, A., Weaver, V. M., and Petersen, O. W. (2002) The organizing principle: microenvironmental influences in the normal and malignant breast. *Differentiation* **70**, 537-546

30. Willipinski-Stapelfeldt, B., Riethdorf, S., Assmann, V., Woelfle, U., Rau, T., Sauter, G., Heukeshoven, J., and Pantel, K. (2005) Changes in cytoskeletal protein composition indicative of an epithelial-mesenchymal transition in human micrometastatic and primary breast carcinoma cells. *Clin Cancer Res* **11**, 8006-8014

31. Ozdamar, B., Bose, R., Barrios-Rodiles, M., Wang, H. R., Zhang, Y., and Wrana, J. L. (2005) Regulation of the polarity protein Par6 by TGFbeta receptors controls epithelial cell plasticity. *Science* **307**, 1603-1609

32. Peinado, H., Olmeda, D., and Cano, A. (2007) Snail, Zeb and bHLH factors in tumour progression: an alliance against the epithelial phenotype? *Nat Rev Cancer* **7**, 415-428

33. Gregory, P. A., Bert, A. G., Paterson, E. L., Barry, S. C., Tsykin, A., Farshid, G., Vadas, M. A., Khew-Goodall, Y., and Goodall, G. J. (2008) The miR-200 family and miR-205 regulate epithelial to mesenchymal transition by targeting ZEB1 and SIP1. *Nat Cell Biol* **10**, 593-601

34. Korpal, M., and Kang, Y. (2008) The emerging role of miR-200 family of microRNAs in epithelial-mesenchymal transition and cancer metastasis. *RNA Biol* **5**, 115-119

35. Gregory, P. A., Bracken, C. P., Bert, A. G., and Goodall, G. J. (2008) MicroRNAs as regulators of epithelial-mesenchymal transition. *Cell Cycle* **7**, 3112-3118

36. Adam, L., Zhong, M., Choi, W., Qi, W., Nicoloso, M., Arora, A., Calin, G., Wang, H., Siefker-Radtke, A., McConkey, D., Bar-Eli, M., and Dinney, C. (2009) miR-200 expression regulates epithelial-to-mesenchymal transition in bladder cancer cells and reverses resistance to epidermal growth factor receptor therapy. *Clin Cancer Res* **15**, 5060-5072

37. Xu, J., Lamouille, S., and Derynck, R. (2009) TGF-beta-induced epithelial to mesenchymal transition. *Cell Res* **19**, 156-172

38. Zavadil, J., and Bottinger, E. P. (2005) TGF-beta and epithelial-to-mesenchymal transitions. *Oncogene* **24**, 5764-5774

39. Conacci-Sorrell, M., Zhurinsky, J., and Ben-Ze'ev, A. (2002) The cadherin-catenin adhesion system in signaling and cancer. *J Clin Invest* **109**, 987-991

40. Nelson, W. J., and Nusse, R. (2004) Convergence of Wnt, beta-catenin, and cadherin pathways. *Science* **303**, 1483-1487

41. Sanchez-Tillo, E., de Barrios, O., Siles, L., Cuatrecasas, M., Castells, A., and Postigo, A. (2011) beta-catenin/TCF4 complex induces the epithelial-to-mesenchymal transition (EMT)-activator ZEB1 to regulate tumor invasiveness. *Proc Natl Acad Sci U S A* **108**, 19204-19209

42. Yook, J. I., Li, X. Y., Ota, I., Fearon, E. R., and Weiss, S. J. (2005) Wnt-dependent regulation of the E-cadherin repressor snail. *J Biol Chem* **280**, 11740-11748

43. Wu, Z. Q., Li, X. Y., Hu, C. Y., Ford, M., Kleer, C. G., and Weiss, S. J. (2012) Canonical Wnt signaling regulates Slug activity and links epithelial-mesenchymal transition with epigenetic Breast Cancer 1, Early Onset (BRCA1) repression. *Proc Natl Acad Sci U S A* **109**, 16654-16659

44. Medici, D., Hay, E. D., and Olsen, B. R. (2008) Snail and Slug promote epithelial-mesenchymal transition through beta-catenin-T-cell factor-4-dependent expression of transforming growth factor-beta3. *Mol Biol Cell* **19**, 4875-4887

45. Bailey, J. M., Singh, P. K., and Hollingsworth, M. A. (2007) Cancer metastasis facilitated by developmental pathways: Sonic hedgehog, Notch, and bone morphogenic proteins. *J Cell Biochem* **102**, 829-839

46. Guruharsha, K. G., Kankel, M. W., and Artavanis-Tsakonas, S. (2012) The Notch signalling system: recent insights into the complexity of a conserved pathway. *Nat Rev Genet* **13**, 654-666

47. Wang, Z., Li, Y., Kong, D., and Sarkar, F. H. (2010) The role of Notch signaling pathway in epithelial-mesenchymal transition (EMT) during development and tumor aggressiveness. *Curr Drug Targets* **11**, 745-751

48. Matsuno, Y., Coelho, A. L., Jarai, G., Westwick, J., and Hogaboam, C. M. (2012) Notch signaling mediates TGF-beta1-induced epithelial-mesenchymal transition through the induction of Snai1. *Int J Biochem Cell Biol* **44**, 776-789

49. Katoh, Y., and Katoh, M. (2008) Hedgehog signaling, epithelial-to-mesenchymal transition and miRNA (review). *Int J Mol Med* **22**, 271-275

50. Baum, B., Settleman, J., and Quinlan, M. P. (2008) Transitions between epithelial and mesenchymal states in development and disease. *Semin Cell Dev Biol* **19**, 294-308

51. Larue, L., and Bellacosa, A. (2005) Epithelial-mesenchymal transition in development and cancer: role of phosphatidylinositol 3' kinase/AKT pathways. *Oncogene* **24**, 7443-7454

52. Jiang, J., Tang, Y. L., and Liang, X. H. (2011) EMT: a new vision of hypoxia promoting cancer progression. *Cancer Biol Ther* **11**, 714-723

53. Brabletz, T., Jung, A., Reu, S., Porzner, M., Hlubek, F., Kunz-Schughart, L. A., Knuechel, R., and Kirchner, T. (2001) Variable beta-catenin expression in colorectal cancers indicates tumor progression driven by the tumor environment. *Proc Natl Acad Sci U S A* **98**, 10356-10361

54. Franci, C., Takkunen, M., Dave, N., Alameda, F., Gomez, S., Rodriguez, R., Escriva, M., Montserrat-Sentis, B., Baro, T., Garrido, M., Bonilla, F., Virtanen, I., and Garcia de Herreros, A. (2006) Expression of Snail protein in tumor-stroma interface. *Oncogene* **25**, 5134-5144

55. Sheehan, K. M., Gulmann, C., Eichler, G. S., Weinstein, J. N., Barrett, H. L., Kay, E. W., Conroy, R. M., Liotta, L. A., and Petricoin, E. F., 3rd. (2008) Signal pathway profiling of epithelial and stromal compartments of colonic carcinoma reveals epithelial-mesenchymal transition. *Oncogene* **27**, 323-331

56. Strathdee, G. (2002) Epigenetic versus genetic alterations in the inactivation of E-cadherin. *Semin Cancer Biol* **12**, 373-379

57. Brooks-Wilson, A. R., Kaurah, P., Suriano, G., Leach, S., Senz, J., Grehan, N., Butterfield, Y. S., Jeyes, J., Schinas, J., Bacani, J., Kelsey, M., Ferreira, P., MacGillivray, B., MacLeod, P., Micek, M., Ford, J., Foulkes, W., Australie, K., Greenberg, C., LaPointe, M., Gilpin, C., Nikkel, S., Gilchrist, D., Hughes, R., Jackson, C. E., Monaghan, K. G., Oliveira, M. J., Seruca, R., Gallinger, S., Caldas, C., and Huntsman, D. (2004) Germline E-cadherin mutations in hereditary diffuse gastric cancer: assessment of 42 new families and review of genetic screening criteria. *J Med Genet* **41**, 508-517

58. Azarschab, P., Stembalska, A., Loncar, M. B., Pfister, M., Sasiadek, M. M., and Blin, N. (2003) Epigenetic control of E-cadherin (CDH1) by CpG methylation in metastasising laryngeal cancer. *Oncol Rep* **10**, 501-503

59. Tellez, C. S., Juri, D. E., Do, K., Bernauer, A. M., Thomas, C. L., Damiani, L. A., Tessema, M., Leng, S., and Belinsky, S. A. EMT and stem cell-like properties associated with miR-205 and miR-200 epigenetic silencing are early manifestations during carcinogen-induced transformation of human lung epithelial cells. *Cancer Res* **71**, 3087-3097

60. Vrba, L., Jensen, T. J., Garbe, J. C., Heimark, R. L., Cress, A. E., Dickinson, S., Stampfer, M. R., and Futscher, B. W. Role for DNA methylation in the regulation of miR-200c and miR-141 expression in normal and cancer cells. *PLoS One* **5**, e8697

61. Yu, F., Jiao, Y., Zhu, Y., Wang, Y., Zhu, J., Cui, X., Liu, Y., He, Y., Park, E. Y., Zhang, H., Lv, X., Ma, K., Su, F., Park, J. H., and Song, E. MicroRNA 34c gene down-regulation via DNA methylation promotes self-renewal and epithelial-mesenchymal transition in breast tumor-initiating cells. *J Biol Chem* **287**, 465-473

62. Bloushtain-Qimron, N., Yao, J., Snyder, E. L., Shipitsin, M., Campbell, L. L., Mani, S. A., Hu, M., Chen, H., Ustyansky, V., Antosiewicz, J. E., Argani, P., Halushka, M. K., Thomson, J. A., Pharoah, P., Porgador, A., Sukumar, S., Parsons, R., Richardson, A. L., Stampfer, M. R., Gelman, R. S., Nikolskaya, T., Nikolsky, Y., and Polyak, K. (2008) Cell type-specific DNA methylation patterns in the human breast. *Proc Natl Acad Sci U S A* **105**, 14076-14081

63. Grooteclaes, M. L., and Frisch, S. M. (2000) Evidence for a function of CtBP in epithelial gene regulation and anoikis. *Oncogene* **19**, 3823-3828

64. Eger, A., Aigner, K., Sonderegger, S., Dampier, B., Oehler, S., Schreiber, M., Berx, G., Cano, A., Beug, H., and Foisner, R. (2005) DeltaEF1 is a transcriptional repressor of E-cadherin and regulates epithelial plasticity in breast cancer cells. *Oncogene* **24**, 2375-2385

65. Sanchez-Tillo, E., Lazaro, A., Torrent, R., Cuatrecasas, M., Vaquero, E. C., Castells, A., Engel, P., and Postigo, A. ZEB1 represses E-cadherin and induces an EMT by recruiting the SWI/SNF chromatin-remodeling protein BRG1. *Oncogene* **29**, 3490-3500

66. Shirakihara, T., Saitoh, M., and Miyazono, K. (2007) Differential regulation of epithelial and mesenchymal markers by deltaEF1 proteins in epithelial mesenchymal transition induced by TGF-beta. *Mol Biol Cell* **18**, 3533-3544

67. Park, S. M., Gaur, A. B., Lengyel, E., and Peter, M. E. (2008) The miR-200 family determines the epithelial phenotype of cancer cells by targeting the E-cadherin repressors ZEB1 and ZEB2. *Genes Dev* **22**, 894-907

68. Chang, C. J., Chao, C. H., Xia, W., Yang, J. Y., Xiong, Y., Li, C. W., Yu, W. H., Rehman, S. K., Hsu, J. L., Lee, H. H., Liu, M., Chen, C. T., Yu, D., and Hung, M. C. (2011) p53 regulates epithelial-mesenchymal transition and stem cell properties through modulating miRNAs. *Nat Cell Biol* **13**, 317-323

69. Ma, L., Teruya-Feldstein, J., and Weinberg, R. A. (2007) Tumour invasion and metastasis initiated by microRNA-10b in breast cancer. *Nature* **449**, 682-688

70. Reya, T., Morrison, S. J., Clarke, M. F., and Weissman, I. L. (2001) Stem cells, cancer, and cancer stem cells. *Nature* **414**, 105-111

71. Singh, A., and Settleman, J. EMT, cancer stem cells and drug resistance: an emerging axis of evil in the war on cancer. *Oncogene* **29**, 4741-4751

72. Mani, S. A., Guo, W., Liao, M. J., Eaton, E. N., Ayyanan, A., Zhou, A. Y., Brooks, M., Reinhard, F., Zhang, C. C., Shipitsin, M., Campbell, L. L., Polyak, K., Brisken, C., Yang, J., and Weinberg, R. A. (2008) The epithelial-mesenchymal transition generates cells with properties of stem cells. *Cell* **133**, 704-715

73. Ben-Porath, I., Thomson, M. W., Carey, V. J., Ge, R., Bell, G. W., Regev, A., and Weinberg, R. A. (2008) An embryonic stem cell-like gene expression signature in poorly differentiated aggressive human tumors. *Nat Genet* **40**, 499-507

74. Tsai, J. H., Donaher, J. L., Murphy, D. A., Chau, S., and Yang, J. Spatiotemporal regulation of epithelial-mesenchymal transition is essential for squamous cell carcinoma metastasis. *Cancer Cell* **22**, 725-736

75. Hou, J. M., Krebs, M., Ward, T., Sloane, R., Priest, L., Hughes, A., Clack, G., Ranson, M., Blackhall, F., and Dive, C. Circulating tumor cells as a window on metastasis biology in lung cancer. *Am J Pathol* **178**, 989-996

76. Kallergi, G., Papadaki, M. A., Politaki, E., Mavroudis, D., Georgoulias, V., and Agelaki, S. Epithelial to mesenchymal transition markers expressed in circulating tumour cells of early and metastatic breast cancer patients. *Breast Cancer Res* **13**, R59

77. Bartel, D. P. (2004) MicroRNAs: genomics, biogenesis, mechanism, and function. *Cell* **116**, 281-297

78. Deng, S., Calin, G. A., Croce, C. M., Coukos, G., and Zhang, L. (2008) Mechanisms of microRNA deregulation in human cancer. *Cell Cycle* **7**, 2643-2646

79. Stahlhut Espinosa, C. E., and Slack, F. J. (2006) The role of microRNAs in cancer. *Yale J Biol Med* **79**, 131-140

80. Winter, J., Jung, S., Keller, S., Gregory, R. I., and Diederichs, S. (2009) Many roads to maturity: microRNA biogenesis pathways and their regulation. *Nat Cell Biol* **11**, 228-234

81. Baskerville, S., and Bartel, D. P. (2005) Microarray profiling of microRNAs reveals frequent coexpression with neighboring miRNAs and host genes. *RNA* **11**, 241-247

82. Ozsolak, F., Poling, L. L., Wang, Z., Liu, H., Liu, X. S., Roeder, R. G., Zhang, X., Song, J. S., and Fisher, D. E. (2008) Chromatin structure analyses identify miRNA promoters. *Genes Dev* **22**, 3172-3183

83. Corcoran, D. L., Pandit, K. V., Gordon, B., Bhattacharjee, A., Kaminski, N., and Benos, P. V. (2009) Features of mammalian microRNA promoters emerge from polymerase II chromatin immunoprecipitation data. *PLoS One* **4**, e5279

84. Morlando, M., Ballarino, M., Gromak, N., Pagano, F., Bozzoni, I., and Proudfoot, N. J. (2008) Primary microRNA transcripts are processed co-transcriptionally. *Nat Struct Mol Biol* **15**, 902-909

85. MacRae, I. J., Ma, E., Zhou, M., Robinson, C. V., and Doudna, J. A. (2008) In vitro reconstitution of the human RISC-loading complex. *Proc Natl Acad Sci U S A* **105**, 512-517

86. Gregory, R. I., Chendrimada, T. P., Cooch, N., and Shiekhattar, R. (2005) Human RISC couples microRNA biogenesis and posttranscriptional gene silencing. *Cell* **123**, 631-640

87. Diederichs, S., and Haber, D. A. (2007) Dual role for argonautes in microRNA processing and posttranscriptional regulation of microRNA expression. *Cell* **131**, 1097-1108

88. Eulalio, A., Huntzinger, E., and Izaurralde, E. (2008) Getting to the root of miRNA-mediated gene silencing. *Cell* **132**, 9-14

89. Westholm, J. O., and Lai, E. C. Mirtrons: microRNA biogenesis via splicing. *Biochimie* **93**, 1897-1904

90. Gantier, M. P., McCoy, C. E., Rusinova, I., Saulep, D., Wang, D., Xu, D., Irving, A. T., Behlke, M. A., Hertzog, P. J., Mackay, F., and Williams, B. R. Analysis of microRNA turnover in mammalian cells following Dicer1 ablation. *Nucleic Acids Res* **39**, 5692-5703

91. Zhang, Z., Qin, Y. W., Brewer, G., and Jing, Q. MicroRNA degradation and turnover: regulating the regulators. *Wiley Interdiscip Rev RNA* **3**, 593-600

92. Ho, P. L., Kurtova, A., and Chan, K. S. Normal and neoplastic urothelial stem cells: getting to the root of the problem. *Nat Rev Urol* **9**, 583-594

93. Tran, M. N., Goodwin Jinesh, G., McConkey, D. J., and Kamat, A. M. Bladder cancer stem cells. *Curr Stem Cell Res Ther* **5**, 387-395

94. Thomson, J. A., and Odorico, J. S. (2000) Human embryonic stem cell and embryonic germ cell lines. *Trends Biotechnol* **18**, 53-57

95. Takahashi, K., and Yamanaka, S. (2006) Induction of pluripotent stem cells from mouse embryonic and adult fibroblast cultures by defined factors. *Cell* **126**, 663-676

96. Galli, R., Borello, U., Gritti, A., Minasi, M. G., Bjornson, C., Coletta, M., Mora, M., De Angelis, M. G., Fiocco, R., Cossu, G., and Vescovi, A. L. (2000) Skeletal myogenic potential of human and mouse neural stem cells. *Nat Neurosci* **3**, 986-991

97. Lantz, C. S., and Huff, T. F. (1995) Differential responsiveness of purified mouse c-kit+ mast cells and their progenitors to IL-3 and stem cell factor. *J Immunol* **155**, 4024-4029

98. Jost, S. P., Gosling, J. A., and Dixon, J. S. (1989) The morphology of normal human bladder urothelium. *J Anat* **167**, 103-115

99. Khandelwal, P., Abraham, S. N., and Apodaca, G. (2009) Cell biology and physiology of the uroepithelium. *Am J Physiol Renal Physiol* **297**, F1477-1501

100. Lavelle, J., Meyers, S., Ramage, R., Bastacky, S., Doty, D., Apodaca, G., and Zeidel, M. L. (2002) Bladder permeability barrier: recovery from selective injury of surface epithelial cells. *Am J Physiol Renal Physiol* **283**, F242-253

101. Kreft, M. E., Sterle, M., Veranic, P., and Jezernik, K. (2005) Urothelial injuries and the early wound healing response: tight junctions and urothelial cytodifferentiation. *Histochem Cell Biol* **123**, 529-539

102. Cotsarelis, G., Cheng, S. Z., Dong, G., Sun, T. T., and Lavker, R. M. (1989) Existence of slow-cycling limbal epithelial basal cells that can be preferentially stimulated to proliferate: implications on epithelial stem cells. *Cell* **57**, 201-209

103. Tsujimura, A., Koikawa, Y., Salm, S., Takao, T., Coetzee, S., Moscatelli, D., Shapiro, E., Lepor, H., Sun, T. T., and Wilson, E. L. (2002) Proximal location of mouse prostate epithelial stem cells: a model of prostatic homeostasis. *J Cell Biol* **157**, 1257-1265

104. Morris, R. J., and Potten, C. S. (1994) Slowly cycling (label-retaining) epidermal cells behave like clonogenic stem cells in vitro. *Cell Prolif* **27**, 279-289

105. Kurzrock, E. A., Lieu, D. K., Degraffenried, L. A., Chan, C. W., and Isseroff, R. R. (2008) Label-retaining cells of the bladder: candidate urothelial stem cells. *Am J Physiol Renal Physiol* **294**, F1415-1421

106. Shin, K., Lee, J., Guo, N., Kim, J., Lim, A., Qu, L., Mysorekar, I. U., and Beachy, P. A. Hedgehog/Wnt feedback supports regenerative proliferation of epithelial stem cells in bladder. *Nature* **472**, 110-114

107. Karni-Schmidt, O., Castillo-Martin, M., Shen, T. H., Gladoun, N., Domingo-Domenech, J., Sanchez-Carbayo, M., Li, Y., Lowe, S., Prives, C., and Cordon-Cardo,

C. Distinct expression profiles of p63 variants during urothelial development and bladder cancer progression. *Am J Pathol* **178**, 1350-1360

108. Signoretti, S., Pires, M. M., Lindauer, M., Horner, J. W., Grisanzio, C., Dhar, S., Majumder, P., McKeon, F., Kantoff, P. W., Sellers, W. R., and Loda, M. (2005) p63 regulates commitment to the prostate cell lineage. *Proc Natl Acad Sci U S A* **102**, 11355-11360

109. Tran, M. N., Goodwin Jinesh, G., McConkey, D. J., and Kamat, A. M. (2010) Bladder cancer stem cells. *Curr Stem Cell Res Ther* **5**, 387-395

110. Chan, K. S., Espinosa, I., Chao, M., Wong, D., Ailles, L., Diehn, M., Gill, H., Presti, J., Jr., Chang, H. Y., van de Rijn, M., Shortliffe, L., and Weissman, I. L. (2009) Identification, molecular characterization, clinical prognosis, and therapeutic targeting of human bladder tumor-initiating cells. *Proc Natl Acad Sci U S A* **106**, 14016-14021

111. Yang, Y. M., and Chang, J. W. (2008) Bladder cancer initiating cells (BCICs) are among EMA-CD44v6+ subset: novel methods for isolating undetermined cancer stem (initiating) cells. *Cancer Invest* **26**, 725-733

112. He, X., Marchionni, L., Hansel, D. E., Yu, W., Sood, A., Yang, J., Parmigiani, G., Matsui, W., and Berman, D. M. (2009) Differentiation of a highly tumorigenic basal cell compartment in urothelial carcinoma. *Stem Cells* **27**, 1487-1495

113. She, J. J., Zhang, P. G., Wang, Z. M., Gan, W. M., and Che, X. M. (2008) Identification of side population cells from bladder cancer cells by DyeCycle Violet staining. *Cancer Biol Ther* **7**, 1663-1668

114. Ning, Z. F., Huang, Y. J., Lin, T. X., Zhou, Y. X., Jiang, C., Xu, K. W., Huang, H., Yin, X. B., and Huang, J. (2009) Subpopulations of stem-like cells in side population cells from the human bladder transitional cell cancer cell line T24. *J Int Med Res* **37**, 621-630

115. Su, Y., Qiu, Q., Zhang, X., Jiang, Z., Leng, Q., Liu, Z., Stass, S. A., and Jiang, F. (2010) Aldehyde dehydrogenase 1 A1-positive cell population is enriched in tumor-initiating cells and associated with progression of bladder cancer. *Cancer Epidemiol Biomarkers Prev* **19**, 327-337

116. Volkmer, J. P., Sahoo, D., Chin, R. K., Ho, P. L., Tang, C., Kurtova, A. V., Willingham, S. B., Pazhanisamy, S. K., Contreras-Trujillo, H., Storm, T. A., Lotan, Y., Beck, A. H., Chung, B. I., Alizadeh, A. A., Godoy, G., Lerner, S. P., van de Rijn, M., Shortliffe, L. D., Weissman, I. L., and Chan, K. S. (2012) Three differentiation states risk-stratify bladder cancer into distinct subtypes. *Proc Natl Acad Sci U S A* **109**, 2078-2083

117. Volkmer, J. P., Sahoo, D., Chin, R. K., Ho, P. L., Tang, C., Kurtova, A. V., Willingham, S. B., Pazhanisamy, S. K., Contreras-Trujillo, H., Storm, T. A., Lotan, Y., Beck, A. H., Chung, B. I., Alizadeh, A. A., Godoy, G., Lerner, S. P., van de Rijn, M., Shortliffe, L. D., Weissman, I. L., and Chan, K. S. Three differentiation states risk-stratify bladder cancer into distinct subtypes. *Proc Natl Acad Sci U S A* **109**, 2078-2083

118. Siegel, R., Naishadham, D., and Jemal, A. Cancer statistics, 2012. *CA Cancer J Clin* **62**, 10-29

119. Dinney, C. P., McConkey, D. J., Millikan, R. E., Wu, X., Bar-Eli, M., Adam, L., Kamat, A. M., Siefker-Radtke, A. O., Tuziak, T., Sabichi, A. L., Grossman, H. B., Benedict, W. F., and Czerniak, B. (2004) Focus on bladder cancer. *Cancer Cell* **6**, 111-116

120. Mitra, N., and Indurkhya, A. (2005) A propensity score approach to estimating the cost-effectiveness of medical therapies from observational data. *Health Econ* **14**, 805-815

121. Castillo-Martin, M., Domingo-Domenech, J., Karni-Schmidt, O., Matos, T., and Cordon-Cardo, C. Molecular pathways of urothelial development and bladder tumorigenesis. *Urol Oncol* **28**, 401-408

122. McConkey, D. J., Lee, S., Choi, W., Tran, M., Majewski, T., Siefker-Radtke, A., Dinney, C., and Czerniak, B. Molecular genetics of bladder cancer: Emerging mechanisms of tumor initiation and progression. *Urol Oncol* **28**, 429-440

123. Cohen, S. M. (1998) Urinary bladder carcinogenesis. *Toxicol Pathol* **26**, 121-127

124. Zhang, Z. T., Pak, J., Shapiro, E., Sun, T. T., and Wu, X. R. (1999) Urothelium-specific expression of an oncogene in transgenic mice induced the formation of carcinoma in situ and invasive transitional cell carcinoma. *Cancer Res* **59**, 3512-3517

125. Zhang, Z. T., Pak, J., Huang, H. Y., Shapiro, E., Sun, T. T., Pellicer, A., and Wu, X. R. (2001) Role of Ha-ras activation in superficial papillary pathway of urothelial tumor formation. *Oncogene* **20**, 1973-1980

126. Sun, T. T., Zhao, H., Provet, J., Aebi, U., and Wu, X. R. (1996) Formation of asymmetric unit membrane during urothelial differentiation. *Mol Biol Rep* **23**, 3-11

127. Lobban, E. D., Smith, B. A., Hall, G. D., Harnden, P., Roberts, P., Selby, P. J., Trejdosiewicz, L. K., and Southgate, J. (1998) Uroplakin gene expression by normal and neoplastic human urothelium. *Am J Pathol* **153**, 1957-1967

128. Cheng, J., Huang, H., Pak, J., Shapiro, E., Sun, T. T., Cordon-Cardo, C., Waldman, F. M., and Wu, X. R. (2003) Allelic loss of p53 gene is associated with genesis and maintenance, but not invasion, of mouse carcinoma in situ of the bladder. *Cancer Res* **63**, 179-185

129. Puzio-Kuter, A. M., Castillo-Martin, M., Kinkade, C. W., Wang, X., Shen, T. H., Matos, T., Shen, M. M., Cordon-Cardo, C., and Abate-Shen, C. (2009) Inactivation of p53 and Pten promotes invasive bladder cancer. *Genes Dev* **23**, 675-680

130. Yoo, L. I., Liu, D. W., Le Vu, S., Bronson, R. T., Wu, H., and Yuan, J. (2006) Pten deficiency activates distinct downstream signaling pathways in a tissue-specific manner. *Cancer Res* **66**, 1929-1939

131. Czerniak, B., Cohen, G. L., Etkind, P., Deitch, D., Simmons, H., Herz, F., and Koss, L. G. (1992) Concurrent mutations of coding and regulatory sequences of the Ha-ras gene in urinary bladder carcinomas. *Hum Pathol* **23**, 1199-1204

132. Knowles, M. A., and Williamson, M. (1993) Mutation of H-ras is infrequent in bladder cancer: confirmation by single-strand conformation polymorphism analysis, designed restriction fragment length polymorphisms, and direct sequencing. *Cancer Res* **53**, 133-139

133. Karimianpour, N., Mousavi-Shafaei, P., Ziaee, A. A., Akbari, M. T., Pourmand, G., Abedi, A., Ahmadi, A., and Afshin Alavi, H. (2008) Mutations of RAS gene family in specimens of bladder cancer. *Urol J* **5**, 237-242

134. Sibley, K., Cuthbert-Heavens, D., and Knowles, M. A. (2001) Loss of heterozygosity at 4p16.3 and mutation of FGFR3 in transitional cell carcinoma. *Oncogene* **20**, 686-691

135. Knowles, M. A. (2007) Role of FGFR3 in urothelial cell carcinoma: biomarker and potential therapeutic target. *World J Urol* **25**, 581-593

136. Chatterjee, S. J., Datar, R., Youssefzadeh, D., George, B., Goebell, P. J., Stein, J. P., Young, L., Shi, S. R., Gee, C., Groshen, S., Skinner, D. G., and Cote, R. J. (2004) Combined effects of p53, p21, and pRb expression in the progression of bladder transitional cell carcinoma. *J Clin Oncol* **22**, 1007-1013

137. Esrig, D., Elmajian, D., Groshen, S., Freeman, J. A., Stein, J. P., Chen, S. C., Nichols, P. W., Skinner, D. G., Jones, P. A., and Cote, R. J. (1994) Accumulation of nuclear p53 and tumor progression in bladder cancer. *N Engl J Med* **331**, 1259-1264

138. Cote, R. J., Dunn, M. D., Chatterjee, S. J., Stein, J. P., Shi, S. R., Tran, Q. C., Hu, S. X., Xu, H. J., Groshen, S., Taylor, C. R., Skinner, D. G., and Benedict, W. F. (1998) Elevated and absent pRb expression is associated with bladder cancer progression and has cooperative effects with p53. *Cancer Res* **58**, 1090-1094

139. Xu, H. J., Cairns, P., Hu, S. X., Knowles, M. A., and Benedict, W. F. (1993) Loss of RB protein expression in primary bladder cancer correlates with loss of heterozygosity at the RB locus and tumor progression. *Int J Cancer* **53**, 781-784

140. Aveyard, J. S., Skilleter, A., Habuchi, T., and Knowles, M. A. (1999) Somatic mutation of PTEN in bladder carcinoma. *Br J Cancer* **80**, 904-908

141. Wang, D. S., Rieger-Christ, K., Latini, J. M., Moinzadeh, A., Stoffel, J., Pezza, J. A., Saini, K., Libertino, J. A., and Summerhayes, I. C. (2000) Molecular analysis of PTEN and MXI1 in primary bladder carcinoma. *Int J Cancer* **88**, 620-625

142. Koga, F., Kawakami, S., Fujii, Y., Saito, K., Ohtsuka, Y., Iwai, A., Ando, N., Takizawa, T., Kageyama, Y., and Kihara, K. (2003) Impaired p63 expression associates with poor prognosis and uroplakin III expression in invasive urothelial carcinoma of the bladder. *Clin Cancer Res* **9**, 5501-5507

143. Koga, F., Kawakami, S., Kumagai, J., Takizawa, T., Ando, N., Arai, G., Kageyama, Y., and Kihara, K. (2003) Impaired Delta Np63 expression associates with reduced beta-catenin and aggressive phenotypes of urothelial neoplasms. *Br J Cancer* **88**, 740-747

144. Urist, M. J., Di Como, C. J., Lu, M. L., Charytonowicz, E., Verbel, D., Crum, C. P., Ince, T. A., McKeon, F. D., and Cordon-Cardo, C. (2002) Loss of p63 expression is associated with tumor progression in bladder cancer. *Am J Pathol* **161**, 1199-1206

145. Choi, W., Shah, J. B., Tran, M., Svatek, R., Marquis, L., Lee, I. L., Yu, D., Adam, L., Wen, S., Shen, Y., Dinney, C., McConkey, D. J., and Siefker-Radtke, A. (2012) p63 expression defines a lethal subset of muscle-invasive bladder cancers. *PLoS One* **7**, e30206

146. Karni-Schmidt, O., Castillo-Martin, M., Shen, T. H., Gladoun, N., Domingo-Domenech, J., Sanchez-Carbayo, M., Li, Y., Lowe, S., Prives, C., and Cordon-Cardo, C. (2011) Distinct expression profiles of p63 variants during urothelial development and bladder cancer progression. *Am J Pathol* **178**, 1350-1360

147. Westfall, M. D., and Pietenpol, J. A. (2004) p63: Molecular complexity in development and cancer. *Carcinogenesis* **25**, 857-864

148. Lin, Y. L., Sengupta, S., Gurdziel, K., Bell, G. W., Jacks, T., and Flores, E. R. (2009) p63 and p73 transcriptionally regulate genes involved in DNA repair. *PLoS Genet* **5**, e1000680

149. Pozzi, S., Zambelli, F., Merico, D., Pavesi, G., Robert, A., Maltere, P., Gidrol, X., Mantovani, R., and Vigano, M. A. (2009) Transcriptional network of p63 in human keratinocytes. *PLoS One* **4**, e5008

150. Yang, A., Kaghad, M., Wang, Y., Gillett, E., Fleming, M. D., Dotsch, V., Andrews, N. C., Caput, D., and McKeon, F. (1998) p63, a p53 homolog at 3q27-29, encodes multiple products with transactivating, death-inducing, and dominant-negative activities. *Mol Cell* **2**, 305-316

151. Helton, E. S., Zhu, J., and Chen, X. (2006) The unique NH2-terminally deleted (DeltaN) residues, the PXXP motif, and the PPXY motif are required for the transcriptional activity of the DeltaN variant of p63. *J Biol Chem* **281**, 2533-2542

152. Dohn, M., Zhang, S., and Chen, X. (2001) p63alpha and DeltaNp63alpha can induce cell cycle arrest and apoptosis and differentially regulate p53 target genes. *Oncogene* **20**, 3193-3205

153. Wu, G., Nomoto, S., Hoque, M. O., Dracheva, T., Osada, M., Lee, C. C., Dong, S. M., Guo, Z., Benoit, N., Cohen, Y., Rechthand, P., Califano, J., Moon, C. S., Ratovitski, E., Jen, J., Sidransky, D., and Trink, B. (2003) DeltaNp63alpha and TAp63alpha regulate transcription of genes with distinct biological functions in cancer and development. *Cancer Res* **63**, 2351-2357

154. Donehower, L. A., Harvey, M., Slagle, B. L., McArthur, M. J., Montgomery, C. A., Jr., Butel, J. S., and Bradley, A. (1992) Mice deficient for p53 are developmentally normal but susceptible to spontaneous tumours. *Nature* **356**, 215-221

155. Mills, A. A., Zheng, B., Wang, X. J., Vogel, H., Roop, D. R., and Bradley, A. (1999) p63 is a p53 homologue required for limb and epidermal morphogenesis. *Nature* **398**, 708-713

156. Yang, A., Schweitzer, R., Sun, D., Kaghad, M., Walker, N., Bronson, R. T., Tabin, C., Sharpe, A., Caput, D., Crum, C., and McKeon, F. (1999) p63 is essential for regenerative proliferation in limb, craniofacial and epithelial development. *Nature* **398**, 714-718

157. Candi, E., Rufini, A., Terrinoni, A., Dinsdale, D., Ranalli, M., Paradisi, A., De Laurenzi, V., Spagnoli, L. G., Catani, M. V., Ramadan, S., Knight, R. A., and Melino,

G. (2006) Differential roles of p63 isoforms in epidermal development: selective genetic complementation in p63 null mice. *Cell Death Differ* **13**, 1037-1047

158. Laurikkala, J., Mikkola, M. L., James, M., Tummers, M., Mills, A. A., and Thesleff, I. (2006) p63 regulates multiple signalling pathways required for ectodermal organogenesis and differentiation. *Development* **133**, 1553-1563

159. Romano, R. A., Smalley, K., Magraw, C., Serna, V. A., Kurita, T., Raghavan, S., and Sinha, S. DeltaNp63 knockout mice reveal its indispensable role as a master regulator of epithelial development and differentiation. *Development* **139**, 772-782

160. Su, X., Paris, M., Gi, Y. J., Tsai, K. Y., Cho, M. S., Lin, Y. L., Biernaskie, J. A., Sinha, S., Prives, C., Pevny, L. H., Miller, F. D., and Flores, E. R. (2009) TAp63 prevents premature aging by promoting adult stem cell maintenance. *Cell Stem Cell* **5**, 64-75

161. Cheng, W., Jacobs, W. B., Zhang, J. J., Moro, A., Park, J. H., Kushida, M., Qiu, W., Mills, A. A., and Kim, P. C. (2006) DeltaNp63 plays an anti-apoptotic role in ventral bladder development. *Development* **133**, 4783-4792

162. Nylander, K., Vojtesek, B., Nenutil, R., Lindgren, B., Roos, G., Zhanxiang, W., Sjostrom, B., Dahlqvist, A., and Coates, P. J. (2002) Differential expression of p63 isoforms in normal tissues and neoplastic cells. *J Pathol* **198**, 417-427

163. Reis-Filho, J. S., Torio, B., Albergaria, A., and Schmitt, F. C. (2002) p63 expression in normal skin and usual cutaneous carcinomas. *J Cutan Pathol* **29**, 517-523

164. Mills, A. A. (2006) p63: oncogene or tumor suppressor? *Curr Opin Genet Dev* **16**, 38-44

165. Flores, E. R., Sengupta, S., Miller, J. B., Newman, J. J., Bronson, R., Crowley, D., Yang, A., McKeon, F., and Jacks, T. (2005) Tumor predisposition in mice mutant for

p63 and p73: evidence for broader tumor suppressor functions for the p53 family. *Cancer Cell* **7**, 363-373

166. Keyes, W. M., Vogel, H., Koster, M. I., Guo, X., Qi, Y., Petherbridge, K. M., Roop, D. R., Bradley, A., and Mills, A. A. (2006) p63 heterozygous mutant mice are not prone to spontaneous or chemically induced tumors. *Proc Natl Acad Sci U S A* **103**, 8435-8440

167. Talos, F., Wolff, S., Beyer, U., Dobbelstein, M., and Moll, U. M. Brdm2 - an aberrant hypomorphic p63 allele. *Cell Death Differ* **17**, 184-186

168. Su, X., Chakravarti, D., and Flores, E. R. p63 steps into the limelight: crucial roles in the suppression of tumorigenesis and metastasis. *Nat Rev Cancer* **13**, 136-143

169. Moll, U. M., and Slade, N. (2004) p63 and p73: roles in development and tumor formation. *Mol Cancer Res* **2**, 371-386

170. Flores, E. R. (2007) The roles of p63 in cancer. *Cell Cycle* **6**, 300-304

171. Su, X., Chakravarti, D., Cho, M. S., Liu, L., Gi, Y. J., Lin, Y. L., Leung, M. L., El-Naggar, A., Creighton, C. J., Suraokar, M. B., Wistuba, I., and Flores, E. R. (2010) TAp63 suppresses metastasis through coordinate regulation of Dicer and miRNAs. *Nature* **467**, 986-990

172. Guo, X., Keyes, W. M., Papazoglu, C., Zuber, J., Li, W., Lowe, S. W., Vogel, H., and Mills, A. A. (2009) TAp63 induces senescence and suppresses tumorigenesis in vivo. *Nat Cell Biol* **11**, 1451-1457

173. Crook, T., Nicholls, J. M., Brooks, L., O'Nions, J., and Allday, M. J. (2000) High level expression of deltaN-p63: a mechanism for the inactivation of p53 in undifferentiated nasopharyngeal carcinoma (NPC)? *Oncogene* **19**, 3439-3444

174. Senoo, M., Tsuchiya, I., Matsumura, Y., Mori, T., Saito, Y., Kato, H., Okamoto, T., and Habu, S. (2001) Transcriptional dysregulation of the p73L / p63 / p51 / p40 / KET gene

in human squamous cell carcinomas: expression of Delta Np73L, a novel dominant-negative isoform, and loss of expression of the potential tumour suppressor p51. *Br J Cancer* **84**, 1235-1241

175. Hibi, K., Trink, B., Patturajan, M., Westra, W. H., Caballero, O. L., Hill, D. E., Ratovitski, E. A., Jen, J., and Sidransky, D. (2000) AIS is an oncogene amplified in squamous cell carcinoma. *Proc Natl Acad Sci U S A* **97**, 5462-5467

176. Liefer, K. M., Koster, M. I., Wang, X. J., Yang, A., McKeon, F., and Roop, D. R. (2000) Down-regulation of p63 is required for epidermal UV-B-induced apoptosis. *Cancer Res* **60**, 4016-4020

177. Ratovitski, E. A., Patturajan, M., Hibi, K., Trink, B., Yamaguchi, K., and Sidransky, D. (2001) p53 associates with and targets Delta Np63 into a protein degradation pathway. *Proc Natl Acad Sci U S A* **98**, 1817-1822

178. Yugawa, T., Narisawa-Saito, M., Yoshimatsu, Y., Haga, K., Ohno, S., Egawa, N., Fujita, M., and Kiyono, T. (2010) DeltaNp63alpha repression of the Notch1 gene supports the proliferative capacity of normal human keratinocytes and cervical cancer cells. *Cancer Res* **70**, 4034-4044

179. Keyes, W. M., Pecoraro, M., Aranda, V., Vernersson-Lindahl, E., Li, W., Vogel, H., Guo, X., Garcia, E. L., Michurina, T. V., Enikolopov, G., Muthuswamy, S. K., and Mills, A. A. (2011) DeltaNp63alpha is an oncogene that targets chromatin remodeler Lsh to drive skin stem cell proliferation and tumorigenesis. *Cell Stem Cell* **8**, 164-176

180. Rocco, J. W., Leong, C. O., Kuperwasser, N., DeYoung, M. P., and Ellisen, L. W. (2006) p63 mediates survival in squamous cell carcinoma by suppression of p73-dependent apoptosis. *Cancer Cell* **9**, 45-56

181. Siegel, R., Naishadham, D., and Jemal, A. (2013) Cancer statistics, 2013. *CA Cancer J Clin* **63**, 11-30

182. Fukushima, H., Koga, F., Kawakami, S., Fujii, Y., Yoshida, S., Ratovitski, E., Trink, B., and Kihara, K. (2009) Loss of DeltaNp63alpha promotes invasion of urothelial carcinomas via N-cadherin/Src homology and collagen/extracellular signal-regulated kinase pathway. *Cancer Res* **69**, 9263-9270

183. Dinney, C. P., Fishbeck, R., Singh, R. K., Eve, B., Pathak, S., Brown, N., Xie, B., Fan, D., Bucana, C. D., Fidler, I. J., and et al. (1995) Isolation and characterization of metastatic variants from human transitional cell carcinoma passaged by orthotopic implantation in athymic nude mice. *J Urol* **154**, 1532-1538

184. Boyden, S. (1962) The chemotactic effect of mixtures of antibody and antigen on polymorphonuclear leucocytes. *J Exp Med* **115**, 453-466

185. Kleinman, H. K., and Martin, G. R. (2005) Matrigel: basement membrane matrix with biological activity. *Semin Cancer Biol* **15**, 378-386

186. Chow, S. E., Chang, Y. L., Chuang, S. F., and Wang, J. S. (2011) Wogonin induced apoptosis in human nasopharyngeal carcinoma cells by targeting GSK-3beta and DeltaNp63. *Cancer Chemother Pharmacol* **68**, 835-845

187. Patrone, G., Puppo, F., Cusano, R., Scaranari, M., Ceccherini, I., Puliti, A., and Ravazzolo, R. (2000) Nuclear run-on assay using biotin labeling, magnetic bead capture and analysis by fluorescence-based RT-PCR. *Biotechniques* **29**, 1012-1014, 1016-1017

188. Roman, S., Petre, A., Thepot, A., Hautefeuille, A., Scoazec, J. Y., Mion, F., and Hainaut, P. (2007) Downregulation of p63 upon exposure to bile salts and acid in normal and cancer esophageal cells in culture. *Am J Physiol Gastrointest Liver Physiol* **293**, G45-53

189. Marquis, L., Tran, M., Choi, W., Lee, I. L., Huszar, D., Siefker-Radtke, A., Dinney, C., and McConkey, D. J. (2012) p63 expression correlates with sensitivity to the Eg5 inhibitor ZD4877 in bladder cancer cells. *Cancer Biol Ther* **13**

190. Blanpain, C., and Fuchs, E. (2007) p63: revving up epithelial stem-cell potential. *Nat Cell Biol* **9**, 731-733

191. Senoo, M., Pinto, F., Crum, C. P., and McKeon, F. (2007) p63 Is essential for the proliferative potential of stem cells in stratified epithelia. *Cell* **129**, 523-536

192. Stemmler, M. P. (2008) Cadherins in development and cancer. *Mol Biosyst* **4**, 835-850

193. Rieger-Christ, K. M., Cain, J. W., Braasch, J. W., Dugan, J. M., Silverman, M. L., Bouyounes, B., Libertino, J. A., and Summerhayes, I. C. (2001) Expression of classic cadherins type I in urothelial neoplastic progression. *Hum Pathol* **32**, 18-23

194. Jarrard, D. F., Paul, R., van Bokhoven, A., Nguyen, S. H., Bova, G. S., Wheelock, M. J., Johnson, K. R., Schalken, J., Bussemakers, M., and Isaacs, W. B. (1997) P-Cadherin is a basal cell-specific epithelial marker that is not expressed in prostate cancer. *Clin Cancer Res* **3**, 2121-2128

195. Lee, J. M., Dedhar, S., Kalluri, R., and Thompson, E. W. (2006) The epithelial-mesenchymal transition: new insights in signaling, development, and disease. *J Cell Biol* **172**, 973-981

196. Tsai, J. H., Donaher, J. L., Murphy, D. A., Chau, S., and Yang, J. (2012) Spatiotemporal regulation of epithelial-mesenchymal transition is essential for squamous cell carcinoma metastasis. *Cancer Cell* **22**, 725-736

197. Oh, J. E., Kim, R. H., Shin, K. H., Park, N. H., and Kang, M. K. DeltaNp63alpha protein triggers epithelial-mesenchymal transition and confers stem cell properties in normal human keratinocytes. *J Biol Chem* **286**, 38757-38767

198. Lee, R. C., Feinbaum, R. L., and Ambros, V. (1993) The C. elegans heterochronic gene lin-4 encodes small RNAs with antisense complementarity to lin-14. *Cell* **75**, 843-854

199. Saini, H. K., Griffiths-Jones, S., and Enright, A. J. (2007) Genomic analysis of human microRNA transcripts. *Proc Natl Acad Sci U S A* **104**, 17719-17724

200. Rodriguez, A., Griffiths-Jones, S., Ashurst, J. L., and Bradley, A. (2004) Identification of mammalian microRNA host genes and transcription units. *Genome Res* **14**, 1902-1910

201. Borchert, G. M., Lanier, W., and Davidson, B. L. (2006) RNA polymerase III transcribes human microRNAs. *Nat Struct Mol Biol* **13**, 1097-1101

202. el-Deiry, W. S., Kern, S. E., Pietenpol, J. A., Kinzler, K. W., and Vogelstein, B. (1992) Definition of a consensus binding site for p53. *Nat Genet* **1**, 45-49

203. Tran, M. N., Choi, W., Wszolek, M. F., Navai, N., Lee, I. L., Nitti, G., Wen, S., Flores, E. R., Siefker-Radtke, A., Czerniak, B., Dinney, C., Barton, M., and McConkey, D. J. The p63 isoform DeltaNp63alpha inhibits epithelial-mesenchymal transition in human bladder cancer cells: Role of miR205. *J Biol Chem*

204. Tucci, P., Agostini, M., Grespi, F., Markert, E. K., Terrinoni, A., Vousden, K. H., Muller, P. A., Dotsch, V., Kehrloesser, S., Sayan, B. S., Giaccone, G., Lowe, S. W., Takahashi, N., Vandenabeele, P., Knight, R. A., Levine, A. J., and Melino, G. (2012) Loss of p63 and its microRNA-205 target results in enhanced cell migration and metastasis in prostate cancer. *Proc Natl Acad Sci U S A* **109**, 15312-15317

205. Candi, E., Dinsdale, D., Rufini, A., Salomoni, P., Knight, R. A., Mueller, M., Krammer, P. H., and Melino, G. (2007) TAp63 and DeltaNp63 in cancer and epidermal development. *Cell Cycle* **6**, 274-285

206. Senoo, M., Matsumura, Y., and Habu, S. (2002) TAp63gamma (p51A) and dNp63alpha (p73L), two major isoforms of the p63 gene, exert opposite effects on the vascular endothelial growth factor (VEGF) gene expression. *Oncogene* **21**, 2455-2465

207. Piovan, C., Palmieri, D., Di Leva, G., Braccioli, L., Casalini, P., Nuovo, G., Tortoreto, M., Sasso, M., Plantamura, I., Triulzi, T., Taccioli, C., Tagliabue, E., Iorio, M. V., and Croce, C. M. (2012) Oncosuppressive role of p53-induced miR-205 in triple negative breast cancer. *Mol Oncol*

208. Sabichi, A., Keyhani, A., Tanaka, N., Delacerda, J., Lee, I. L., Zou, C., Zhou, J. H., Benedict, W. F., and Grossman, H. B. (2006) Characterization of a panel of cell lines derived from urothelial neoplasms: genetic alterations, growth in vivo and the relationship of adenoviral mediated gene transfer to coxsackie adenovirus receptor expression. *J Urol* **175**, 1133-1137

209. Gandellini, P., Profumo, V., Casamichele, A., Fenderico, N., Borrelli, S., Petrovich, G., Santilli, G., Callari, M., Colecchia, M., Pozzi, S., De Cesare, M., Folini, M., Valdagni, R., Mantovani, R., and Zaffaroni, N. (2012) miR-205 regulates basement membrane deposition in human prostate: implications for cancer development. *Cell Death Differ*

210. Sorlie, T., Perou, C. M., Tibshirani, R., Aas, T., Geisler, S., Johnsen, H., Hastie, T., Eisen, M. B., van de Rijn, M., Jeffrey, S. S., Thorsen, T., Quist, H., Matese, J. C., Brown, P. O., Botstein, D., Lonning, P. E., and Borresen-Dale, A. L. (2001) Gene expression patterns of breast carcinomas distinguish tumor subclasses with clinical implications. *Proc Natl Acad Sci U S A* **98**, 10869-10874

211. Perou, C. M., Sorlie, T., Eisen, M. B., van de Rijn, M., Jeffrey, S. S., Rees, C. A., Pollack, J. R., Ross, D. T., Johnsen, H., Akslen, L. A., Fluge, O., Pergamenschikov, A.,

Williams, C., Zhu, S. X., Lonning, P. E., Borresen-Dale, A. L., Brown, P. O., and Botstein, D. (2000) Molecular portraits of human breast tumours. *Nature* **406**, 747-752

212. Romano, R. A., Ortt, K., Birkaya, B., Smalley, K., and Sinha, S. (2009) An active role of the DeltaN isoform of p63 in regulating basal keratin genes K5 and K14 and directing epidermal cell fate. *PLoS One* **4**, e5623

213. Romano, R. A., Birkaya, B., and Sinha, S. (2007) A functional enhancer of keratin14 is a direct transcriptional target of deltaNp63. *J Invest Dermatol* **127**, 1175-1186

214. Chi, S. W., Ayed, A., and Arrowsmith, C. H. (1999) Solution structure of a conserved C-terminal domain of p73 with structural homology to the SAM domain. *EMBO J* **18**, 4438-4445

215. Kim, C. A., Phillips, M. L., Kim, W., Gingery, M., Tran, H. H., Robinson, M. A., Faham, S., and Bowie, J. U. (2001) Polymerization of the SAM domain of TEL in leukemogenesis and transcriptional repression. *EMBO J* **20**, 4173-4182

216. Schultz, J., Ponting, C. P., Hofmann, K., and Bork, P. (1997) SAM as a protein interaction domain involved in developmental regulation. *Protein Sci* **6**, 249-253

217. Huang, Y. P., Kim, Y., Li, Z., Fomenkov, T., Fomenkov, A., and Ratovitski, E. A. (2005) AEC-associated p63 mutations lead to alternative splicing/protein stabilization of p63 and modulation of Notch signaling. *Cell Cycle* **4**, 1440-1447

218. Woodcock, C. L. (2006) Chromatin architecture. *Curr Opin Struct Biol* **16**, 213-220

219. West, A. G., and Fraser, P. (2005) Remote control of gene transcription. *Hum Mol Genet* **14 Spec No 1**, R101-111

220. Cai, S., Lee, C. C., and Kohwi-Shigematsu, T. (2006) SATB1 packages densely looped, transcriptionally active chromatin for coordinated expression of cytokine genes. *Nat Genet* **38**, 1278-1288

221. Horike, S., Cai, S., Miyano, M., Cheng, J. F., and Kohwi-Shigematsu, T. (2005) Loss of silent-chromatin looping and impaired imprinting of DLX5 in Rett syndrome. *Nat Genet* **37**, 31-40

222. Fullwood, M. J., and Ruan, Y. (2009) ChIP-based methods for the identification of long-range chromatin interactions. *J Cell Biochem* **107**, 30-39

223. Fomenkov, A., Huang, Y. P., Topaloglu, O., Brechman, A., Osada, M., Fomenkova, T., Yuriditsky, E., Trink, B., Sidransky, D., and Ratovitski, E. (2003) P63 alpha mutations lead to aberrant splicing of keratinocyte growth factor receptor in the Hay-Wells syndrome. *J Biol Chem* **278**, 23906-23914

224. Kornblihtt, A. R., de la Mata, M., Fededa, J. P., Munoz, M. J., and Nogues, G. (2004) Multiple links between transcription and splicing. *RNA* **10**, 1489-1498

225. Pawlicki, J. M., and Steitz, J. A. (2010) Nuclear networking fashions pre-messenger RNA and primary microRNA transcripts for function. *Trends Cell Biol* **20**, 52-61

VITAE

Mai Ngoc-Anh Tran was born in Ho Chi Minh City (HCMC), Vietnam on August 15, 1983, daughter of Truong Phat Tran and Anh Ngoc Nguyen. Mai is the third child in her family. Upon graduating from Le Quy Don high school, HCMC, Vietnam, Mai enrolled at The University of Agriculture and Forestry, HCMC, Vietnam for her bachelor degree in Biotechnology from 2001 to 2005. After receiving her B.S. degree, Mai worked as a quality control for Tan Hiep Phat group, a beverage company in HCMC, for a year and then joined in the Open University as a lab manager and instructor for a year. In 2007, Mai received the fellowship from Vietnam Education Foudation and persued her PhD study in the United State of America at the University of Texas Health Science Center at Houston – School of Biomedical Sciences. In May 2008, Mai joined the lab of Dr. David McConkey at the University of Texas – M.D. Anderson Cancer Center, where she examined the role of p63 in bladder cancer.